Faculty of Engineering and Science

Optimizing Hybrid Fermentation Process: From Dark, Photo and Hybrid Fermentation Parametric Study to Mechanism Proposal and Kinetic Modelling

ELDON CHUA CHUNG HAN

0000-0002-4154-6013

This thesis is presented for the Degree of

Doctor of Philosophy

of

Curtin University

October 2023

DECLARATION

To the best of my knowledge and belief, this report contains no material previously published by any other person except where due acknowledgement has been made. This report contains no material which has been accepted for the award of any other degree or diploma in any university.

Signature   :

Name   : Eldon Chung Han Chua

Date   : 25th October 2023

ACKNOWLEDGMENT

LIST OF PUBLICATIONS

Conference papers:

1. Chua, E. C. H., Wee, S. K., Kansedo, J., Lau, S. Y., Lim, K. H., Doi, S. S., & Lipton, A. N. (2023). Growth Study and Biological Hydrogen Production by novel strain Bacillus paramycoides. *MATEC Web of Conferences*, *377*, 01004. https://doi.org/10.1051/MATECCONF/202337701004

Journal papers:

1. Chung Han Chua, E., Wee, S. K., Kansedo, J., Lau, S. Y., Lim, K. H., Dol, S. S., & Lipton, A. N. (2023). Biological Hydrogen Energy Production by Novel Strains Bacillus paramycoides and Cereibacter azotoformans through Dark and Photo Fermentation. *Energies*, *16*(9), 3807. https://doi.org/10.3390/EN16093807

2. E. Chung Han Chua *et al.*, "NOVEL STRAINS BACILLUS PARAMYCOIDES & CEREIBACTER AZOTOFORMANS FOR BIOLOGICAL HYDROGEN PRODUCTION: A PARAMETRIC STUDY," *Eur. Chem. Bull*, vol. 2023, pp. 7999–8012. 10.48047/ecb/2023.12.si7.6932023.22/08/2023

EXECUTIVE SUMMARY

The need for sustainable energy sources is imperative due to the environmental consequences of fossil fuel use, including the release of greenhouse gases from the combustion of oil and gas, leading to climate change, global warming, and rising sea levels. Among various alternatives, green hydrogen is considered promising due to its clean energy properties, with the distinct advantage of producing only water when reacting with oxygen to produce electricity. Consequently, researchers are investigating the potential of using abundant biomass to produce biological green hydrogen through the anaerobic degradation of organic substrates. The study began by employing 16S ribosomal RNA (rRNA) gene polymerase chain reaction (PCR) and gram staining to identify microorganisms. The analysis categorized them as gram-positive *Bacillus paramycoides* and gram-negative *Cereibacter azotoformans*. Growth behaviour studies were conducted using 1g/L and 10g/L inoculum concentrations to analyse bacterial strains. The study initially using a 1g/L inoculum concentration was incomplete, prompting a repetition with a 10g/L inoculum, resulting in both *Bacillus paramycoides* and *Cereibacter azotoformans* displaying all three growth phases. The inoculum from the 24-hour log phase will be employed in subsequent dark, light, and co-culture fermentations. In the subsequent phase, a preliminary parametric study was carried out, focusing separately on dark and photo fermentation. In dark fermentation, the research determined that the optimal carbon feedstocks for biological hydrogen production were 17.5g/L xylose and 20g/L glucose, with the highest hydrogen yield achieved using a 2g/L inoculum concentration and the addition of 50μM of Co^{2+}. For photo fermentation, the study found that 10g/L xylose and 17.5g/L glucose served as the best carbon source concentrations, with an optimal condition of 50μM Mn^{2+} as a micronutrient and a 4g/L inoculum concentration for *Cereibacter sp*. Subsequently, the results from the preliminary phase were input into Design-Expert v13 software, utilizing Response Surface Methodology (RSM) to perform a systematic step-by-step optimization for co-culture fermentation. Ultimately, optimal operating conditions were determined, including a carbon feedstock of 17.5g/L xylose, a dark/photo fermentative bacteria ratio of 1:2, pH 9, 20μM of Co^{2+} and an operating temperature of 50°C. From the optimization process, hybrid fermentation increased the biological hydrogen yield by 658% and 1199% compared to dark and photo fermentation, respectively. Finally, hybrid fermentation was performed in a 2L continuous stirred

tank reactor, and the biological hydrogen yield was 3.92 L H_2/ L medium. In addition, a proposed mechanism is illustrated to demonstrate the conversion of xylose to hydrogen and VFAs through a series of enzymes in dark fermentation. The VFAs are subsequently utilized in the TCA cycle of photo fermentation to produce excess hydrogen. Furthermore, a sequential dark/photo fermentation is conducted under optimized conditions, and the experimental results are validated using kinetic modelling with the 4th order Runge-Kutta method. The obtained R-squared value (>0.99) indicates that the kinetic modelling effectively represents the experimental results. The production of hybrid fermentative green hydrogen from lignocellulosic biomass, achieved through step-by-step co-culture fermentation optimization using novel strains, offers a sustainable solution to address environmental challenges.

TABLE OF CONTENTS

LIST OF FIGURES

LIST OF TABLES

LIST OF ABBREVIATIONS

Abbreviation	Designation
GHG	Greenhouse gas
VFAs	Volatile fatty acids
PNSB	purple non-sulfur bacteria
RSM	Respond Surface Methodology
TCA	Tricarboxylic Acids Cycle
FVW	Vegetable waste
CWP	Cheese whey powder
COD	Chemical oxygen demand
VSS	Volatile suspended solid
TS	Total solid
PPM	Part per million
SEM	Scanning electron microscope
PNS	Purple non-sulfer
UV-VIS spectroscopy	Ultraviolet–visible spectroscopy
PCR	Polymerase chain reaction
ATP	Adenosine triphosphate
ORP	Oxidation reduction potential
NADPH	Nicotinamide adenine dinucleotide phosphate
CSTR	Continuous stirred tank bioreactor
RPM	Rotation per minute
PHA	Polyhydroxyalkanoate
NADH	Nicotinamide adenine dinucleotide (NADH)
Acetyl-CoA	Acetylcoenzyme A
PS	Photosystem
ODE	Ordinary Differential Equation

LIST OF SYMBOLS

Symbol	Designation
O_2	Oxygen
H_2	Hydrogen
°C	Degree Celcius
m^3	Metre cube
mL	Millilitre
Zn	Zinc
Mn	Manganese
Ca	Calcium
Co	Cobalt
Ni	Nickel
Fe	Iron
Cu	Copper
µM	Micromolar
D/L	Dark/light
mV	Millivolt
R^2	R-squared value

CHAPTER 1: INTRODUCTION

1.1 Background

In the burgeoning epoch of science and technology, energy plays a vital role. The oil crisis that occurred in the 1970s indicated that the current energy management system is not sustainable over a long period of time. The utilization of a myriad quantity of fossil fuels after the industrial revolution has led to excessive greenhouse gas (GHG) emissions. The combustion of fossil fuels creates GHG that has caused climate change and global warming, resulting in increasing sea levels [1], [2]. To reduce the world's dependence on fossil fuels for energy generation and address these issues, alternative technology for energy conversion is essential. Renewable energy has been proposed as a solution to alleviate environmental pollution issues, particularly hydrogen energy exploration, as a promising alternative to replace fossil fuels. The high calorific value (140 kJ/g), carbon-neutral, and environmentally friendly features of hydrogen make hydrogen economy a vital role in the near future [3], [4].

The element hydrogen is widely available in the universe, although it cannot be found in its pure form on Earth. To obtain gaseous hydrogen from various molecules, including hydrocarbons, water, hydrides, and acids, further isolation is required [5]. The production of hydrogen energy can be categorized as either grey, blue, or green hydrogen (Figure 1.1), depending on the feedstocks and production method used [6]. Grey hydrogen is produced from hydrocarbons using high-energy thermochemical conversion technology. Blue hydrogen follows the same production method but involves carbon capture and storage [7]. In contrast, green hydrogen is derived from renewable resources such as biomass and water. One of the production technologies for green hydrogen is metabolic engineering, which is used to establish a sustainable pathway for converting biomass waste into valuable biochemicals or biohydrogen fuel [8].
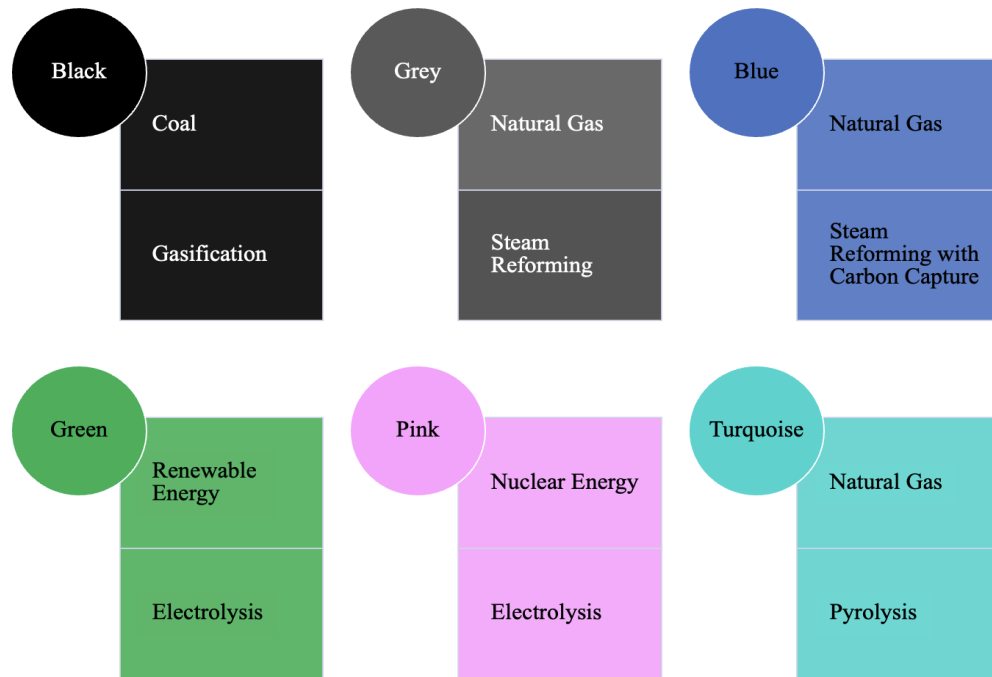
Figure 1.1: Differentiation of hydrogen production pathways into various colour codes.

The traditional processes of producing hydrogen, namely electrolysis and thermochemical reactions, are currently utilized for creating hydrogen energy. The technology of electrolysis splits water to isolate hydrogen, while thermochemical reactions such as reforming, gasification, and pyrolysis mainly use fossil fuels for hydrogen production [9]–[11]. Nevertheless, energy-intensive methods are associated with operational obstacles and harmful environmental impacts such as the production of a large amount of greenhouse gases (GHG) [12]. Commercial hydrogen production techniques rely on finite feedstocks like natural gas (76g/L) and coal (23g/L), which results in the emission of 830 megatons of GHG annually [6]. To overcome the issues associated with traditional hydrogen production, dark fermentation is utilized for hydrogen production due to its energy-efficient and environmentally friendly features [13]. Dark fermentation is an effective pathway for the degradation of organic substrates by anaerobic bacteria like *Clostridium, Enterobacter, Escherichia* [14]. Moreover, the abundant generation of lignocellulosic and biomass wastes such as palm oil mill effluent, winery wastewater, paper waste, post-harvest agricultural waste, and woody biomass have significantly contributed to the economic viability of sustainable biopathway hydrogen formation [15]–[17]. Therefore, the process of dark

13

fermentation by anaerobic microorganisms presents a promising solution for contributing to green energy in the near future.

The low yield of hydrogen production to fulfill the global energy demand is one of the major factors that has restricted dark fermentation for commercialization. During the fermentation process, the buildup of liquid metabolites such as butyric acid, formic acid, lactic acid, acetic acid, and propionic acid may lead to a reduction in pH, which inhibits microbial activity and the production of hydrogen element [18]. To avoid releasing these volatile fatty acids (VFAs) into the environment, they must be captured and treated. Fortunately, purple non-sulfur bacteria (PNSB) can be used to address this issue arising from dark fermentation. These photosynthetic bacteria can utilize the liquid metabolites built up during dark fermentation to produce additional biological hydrogen through photo fermentation. PNSBs such as *Rhodopseudomonas faecalis*, *Rhodopseudomonas rutila* and *Rhodobacter sphaeroides* can transform VFAs into hydrogen element using sunlight as a source of energy [19], [20]. Therefore, the dark-photo hybrid fermentation has gained increasing attention for further development.

The fermentation process is sensitive to various operating conditions such as the type and amount of carbon sources used, bacterial concentration, operating temperature, pH, and micronutrients in the fermentation broth. Proper consideration of these operating parameters can enhance biological hydrogen formation from the fermentation process. In addition, the potential for biological hydrogen yield may vary depending on the strain of microorganism used. Therefore, in this project, the symbiotic effect of the novel strains *Bacillus paramycoides* and *Cereibacter azotoformans* in a hybrid fermentation process will be investigated for biological hydrogen formation. The growth behaviour of these bacteria strains will be examined prior to the biological hydrogen fermentation, followed by a parametric study of dark and photo fermentation individually. Finally, Respond Surface Methodology (RSM) under Design-Expert software will be employed to optimize the hybrid fermentation for enhanced biological hydrogen production. After the experimental work, the Fourth Order Runge-Kutta method will be used to perform kinetic modelling and validate the fermentation results. A proposed mechanism for hydrogen evolution in the hybrid fermentation will be demonstrated.

1.2 Research Problem Statement

During the industrial revolution, global energy consumption increased exponentially, raising concerns among scientists about how to become more environmentally sustainable. The enormous quantity of fossil fuels combusted to create energy has emitted GHG, causing environmental pollution and global warming. To address these issues, renewable energy sources such as wind, solar, and geothermal energy have been proposed. Among these sources, hydrogen energy has attracted researchers due to its environmentally friendly feature of only producing water when reacting with oxygen. However, current commercialized electrolysis or thermochemical processes for hydrogen production utilize high energy or finite fossil fuels. Therefore, this research project focuses on fermentation technology, which uses significantly lower energy for biological hydrogen generation. Nonetheless, the fermentation process produces a low hydrogen yield due to the complex and time-consuming metabolic pathways. This may affect the reliability of fermentation technology as a primary way to fulfill the world's hydrogen energy demand. Also, recognizing the limitation of low hydrogen production in single fermentation systems, the introduction of a hybrid approach has been pivotal in addressing this issue. Prior to scaling up the hybrid process, a comprehensive understanding of kinetic modelling is essential. It is worth noting that there is a scarcity of existing records on the kinetic modelling of hybrid processes utilizing this particular strain of bacteria, underscoring the innovative nature of our research. Consequently, this project aims to enhance biological hydrogen production from the fermentation process by manipulating variables such as types and amounts of carbon feedstocks, bacteria concentration, operating temperature, pH, and micronutrients in the fermentation broth. The ideal operating parameters need to be formulated to maximize the biological hydrogen yield. Additionally, novel bacteria strains will be explored, as different strains have different potential to create biological hydrogen. The goal of this research project is to improve biological hydrogen production through variable manipulation and exploring the biological interactions between novel strains.

1.3 Aims and Objectives

The aim of this research project is to improve bacteria selectivity by manipulating variables and formulating substrates-bacteria to increase biological hydrogen yield. The specific research objectives are as follows:

1. To identify bacteria strains and determine the relationship between growth dynamics and biological hydrogen production of mono-culture *Bacillus paramycoides* and *Cereibacter azotoformans*.

2. To evaluate mono-culture parametric study of *Bacillus paramycoides* and *Cereibacter azotoformans* through dark and light fermentation: A preliminary study for co-culture hybrid fermentation.

3. To optimize co-culture hybrid fermentation by *Bacillus paramycoides* and *Cereibacter azotoformans* with Response Surface Methodology.

4. To propose co-culture fermentation metabolic pathway for xylose conversion and perform 4th order Runge Kutta method for data validation.

1.4 Gap of Knowledge

The research under consideration addresses a notable knowledge gap concerning the comprehensive understanding and optimization of the hybrid fermentation process, involving the combination of dark and photo fermentation methods. Although dark and photo fermentation have been subjects of independent research efforts, their co-culture relationship to enhance hydrogen production remains an emerging and relatively unexplored domain. Moreover, the proposal of a mechanistic model and the application of kinetic modelling techniques to this hybrid process represent a novel and ground-breaking aspect of the research. The primary objective of this study is to bridge these knowledge gaps by not only streamlining the hybrid fermentation process but also by providing profound insights into the intricate mechanisms at play. As a result, this research is poised to yield substantial contributions to the progress of sustainable bioenergy production, while simultaneously advancing the comprehension of the multifaceted interactions within hybrid fermentation systems.

1.5 Significances

Renewable energy to replace environmentally damaging fossil fuels is crucial. The development and advancement of hydrogen technology is certainly significant, especially in terms of reducing environmental problems. Utilizing hydrogen to fulfill energy demand will significantly reduce gas pollution, creating cleaner air. This research study's contributions include minimizing biomass waste, exploring fermentative hydrogen production, enhancing hydrogen yield, and understanding the biological activity of *Cereibacter azotoformans* and *Bacillus paramycoides*. The fermentation process could utilize lignocellulosic biomass, wastewater, and food waste as substrates to produce useful by-products such as biohydrogen energy, thereby reducing biomass waste in the environment. Additionally, hydrogen yield from the fermentation process can be enhanced by experimental studies based on types of substrates, percentage of substrates, inoculum concentration, and types of metal ion addition. This could contribute to the hydrogen industrial sector's ability to supply hydrogen for energy generation purposes. Moreover, to optimize biological hydrogen yield, the activities of fermentative bacteria, such as *Cereibacter azotoformans* and *Bacillus paramycoides*, should be well studied to increase metabolism for production purposes. This may contribute to the study of the biological activity of these two bacterial strains for future bioproduction. In summary, the aim of this project is to increase fermentative biological hydrogen yield by manipulating variables and formulating substrates-bacteria for future commercialization.

1.6 Scope

The scope of this research project includes investigation of bacterial activities during the fermentation process and optimize the production of biological hydrogen through parametric studies of mono-culture dark and photo fermentation, and co-culture hybrid fermentation. Bacterial growth curve studies were conducted in 200mL conical flasks using 1g/L and 10g/L inoculum concentration for up to 96 hours. Liquid samples and biological hydrogen production were analyzed periodically. Parametric studies were performed using different types and percentages of substrates, such as xylose and glucose, with concentrations ranging from 0g/L to 20g/L in 2.5g/L intervals. After identifying the best-performing substrates, parametric studies based on inoculum

concentration and metal ion types were carried out. For metal ions, 50µmol of iron, calcium, manganese, zinc, cobalt, copper, and nickel were added to the culture medium to obtain the highest biological hydrogen yield from single strain dark and light fermentation. Furthermore, the effect of inoculum concentration on biological hydrogen yield was studied by dark and light fermentation using concentrations ranging from 2g/L to 10g/L in 2g/L intervals. In the next step of the experiment, *Cereibacter azotoformans* and *Bacillus paramycoides* were combined for co-culture hybrid fermentation. Respond Surface Methodology (RSM) under Design-Expert software was employed to optimize the biological hydrogen production from co-culture hybrid fermentation. The optimal parameters from preliminary dark and light fermentation experiments were used as positive controls in hybrid fermentation. For substrate type and concentration, the optimal concentrations were found to be 17.5g/L xylose for dark and 10g/L xylose for light fermentation. Therefore, concentrations ranging from 0g/L to 17.5g/L of xylose were investigated for hybrid biological hydrogen fermentation. In addition, the optimal inoculum concentrations were found to be 2g/L for dark and 4g/L for photo fermentation. Therefore, concentrations ranging from 0.1g/L to 2g/L of *Bacillus paramycoides* and from 0.1g/L to 4g/L of *Cereibacter azotoformans* were investigated in RSM to find the optimal bacteria ratio for co-culture fermentation. After determining the optimal xylose concentration and bacteria ratio, the operating temperature was investigated at 30-55°C and pH at 5-9 to optimize biological hydrogen yield. Furthermore, it was found that manganese and cobalt metal ions were suitable for photo and dark fermentation, respectively, to produce biological hydrogen. Therefore, concentrations ranging from 0µmol to 100µmol of Co^{2+} and Mn^{2+} ions were investigated for hybrid biological hydrogen fermentation. The optimal concentration for Co^{2+} and Mn^{2+} ions was 20µmol. Hence, concentrations ranging from 0µmol to 20µmol of Co^{2+} and Mn^{2+} ions were investigated in RSM to find the optimal micronutrient ratio for co-culture fermentation. Lastly, all the optimized operating conditions were utilized in a scaled-up 200mL conical flask and 2L bioreactor for co-culture hybrid fermentation to produce biological hydrogen. A Fourth Order-Runge Kutta method was utilized for kinetic modelling and validated with the fermentation results. Finally, a proposed mechanism for hydrogen evolution in hybrid fermentation was demonstrated.

1.7 Report Layout

Chapter 1 highlights the importance of green energy, specifically hydrogen energy which can be categorized as grey, blue, or green. This chapter also covers the methods used to produce hydrogen and emphasizes the importance of green hydrogen energy formation. In addition, it introduces the concepts of dark and photo fermentation, as well as the use of hybrid fermentation to address the low hydrogen yield from mono-culture fermentation. Chapter 1 also discusses the research problems, aims and objectives, significance, and scope of the study. Chapter 2 provides a literature review, highlighting gaps in previous research and adding novelty to the project. Chapter 3 describes the experimental methodologies, including the preparation of microorganism strains and culture medium, the setup and operating parameters for mono-culture and co-culture fermentation, and the analytical methods used to obtain results. Chapters 4 to 8 present the results and discussions of the research project, covering topics such as strains identification, growth behaviour, substrate types and concentration, inoculum concentration, metal ions, and biological hydrogen production optimization by hybrid fermentation. Chapter 7 includes the results of the upscaled fermentation process. The proposed mechanisms and data validation with simulation are demonstrated in Chapter 8. Chapter 9 provides the overall research findings and conclusions, including future study and recommendations.

CHAPTER 2: LITERATURE REVIEW

2.1 Overview

Bioenergy signifies a sustainable yet futuristic alternative to replace fossil fuels. Compared to the commercialized hydrogen formation techniques, biological hydrogen formation does not rely on fossil fuels for energy conversion. Biological hydrogen is a significant energy source that alleviates the issue of limited resources and promotes sustainability. It is deemed as fuel with a bright prospect arising from its high energy density and sustainable features [21]. Bioenergy not only fulfils the growth of energy demand but also simultaneously resolves the issue of depleting fossil fuel reserves and the increasing pollutants resulting from fossil fuels combustion [22]. It is estimated that fossil fuels may be consumed in 35, 37, and 107 years for oil, gas, and coal, respectively, if the latest trend of fossil fuels utilization continues to surge [23]. The climate change due to the high amount of fossil fuel combustion has attracted significant attention among researchers, policymakers, and environmental scientists to explore the best alternative to replace fossil fuels [24], [25]. Moreover, approximately 1.3 billion tons of biomass food waste are produced annually. Hence, biomass food waste conversion to bioenergy will be an enormous environment enhancement due to the sustainable feedstock utilization [26]. To produce bioenergy from environment-friendly, low cost and renewable resources, biological hydrogen production by fermentation can be an alternative approach [7]. Biological hydrogen production was introduced in the 19th century [27]. It is a metabolic process that involves microorganisms such as cyanobacteria, dark fermentative bacteria, purple nonsulfer and microalgae during the process. Furthermore, biological hydrogen production requires only a little energy for operation and produces near zero pollutants [5]. Nonetheless, the operating parameters such as pH, light intensity, operating temperature, feedstock concentration, and microbial concentration of the fermentation process may vary depending on fermentation feedstocks and microorganisms strains [28]. Therefore, it is worth investigating the optimal operating conditions to enhance biological hydrogen yield from fermentation technology. The following section reviews hydrogen production from electrolysis, thermochemical pathways, dark fermentation, photo fermentation, and hybrid fermentation. The reviews also include

how operating conditions may affect the biological hydrogen yield from the fermentation process.

2.2 Hydrogen Production from Electrolysis and Thermochemical Pathways

Numerous research projects are underway for renewable energy production, including hydrogen energy formation from electrolysis and thermochemical reactions such as pyrolysis, gasification, and steam reforming. Among these technologies, electrolysis and steam reforming are the most common pathways for producing grey and blue hydrogen. Electrolysis (Figure 2.1) involves water splitting mechanism to split water and form hydrogen molecule [5]. The technology takes place in an electrolyzer using water as the substrate, which is then dissociated into O_2 and H_2 by electric current [29]. Moreover, steam reforming is another commercialized pathway for hydrogen production. The endothermic reaction takes place when heat is supplied to generate syngas. The chemical reaction between water and hydrocarbon occurs through steam reforming for syngas production, which contains hydrogen atoms [30]. Furthermore, pyrolysis is another thermochemical reaction that transforms hydrogen-containing compounds into hydrogen elements through thermal decomposition process with high temperatures of 540-1000°C without oxygen [31]. Lastly, gasification utilizes thermochemical reaction to create syngas from biomass or fossil fuels. The thermochemical process uses heat from oxygen and/or steam to maintain. A temperature of >700°C to transform fossil fuels or biomass into syngas.
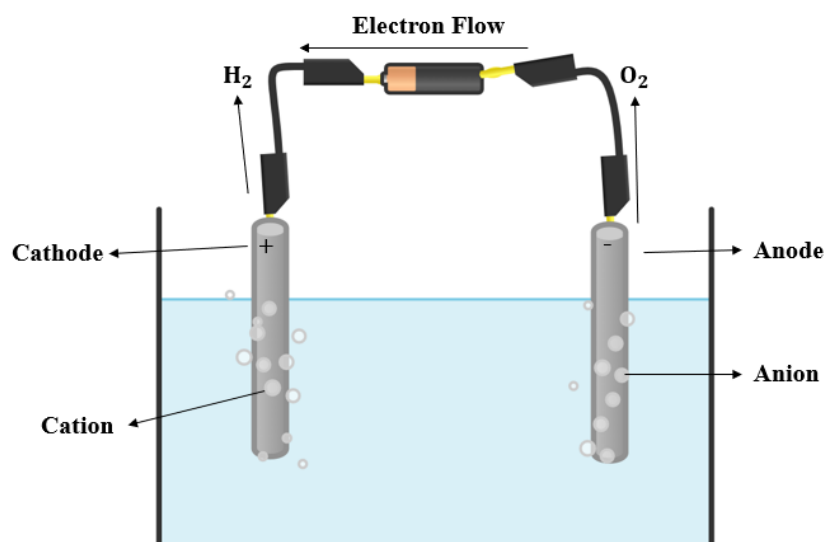
Figure 2.1: Basic electrolysis set up.

Electrolysis and thermochemical pathways are well-known methods for hydrogen production, but they suffer from several disadvantages. For instance, their operational costs are high, which can increase the price of hydrogen production, and they may not be economically feasible compared to fossil fuels [12]. In addition, electrolysis and thermochemical reactions require significant energy input with low energy conversion efficiency to produce hydrogen, which can result in a negative net energy output [5]. Nevertheless, some of these technologies can cause environmental damage by emitting GHG during the production process [29]. Therefore, researchers are exploring greener methods such as biological hydrogen production pathways due to their environmentally friendly features. The mild operating conditions, low energy requirements, and utilization of biomass waste feedstock have attracted significant research interest for the generation of green hydrogen [32].

2.3 Dark Fermentation

Anaerobic degradation or anaerobic fermentation is a well-known and commercialized technology for waste management. The mild operation conditions, quick installation, budget investment cost, and positive profitability indicator have made anaerobic digestion a preferable pathway compared to other technologies [33]. Biological hydrogen production through organic wastes has immense potential to sustain the energy demand for future globe. However, in the current understanding, most of the

hydrogen production through biological pathways are still in lab scale. There were only a few pilot-scale studies such as $11m^3$ production by Zhang et al. and 100,000 litres production by Vatsala et al. [34], [35]. More exploration on biological pathway for green hydrogen generation are required to commercialize anaerobic degradation technology. For dark fermentation, it adapts anaerobic bacteria to transform organic material into hydrogen element. Figure 2.2 illustrates the basic set-up of dark fermentation for hydrogen production:
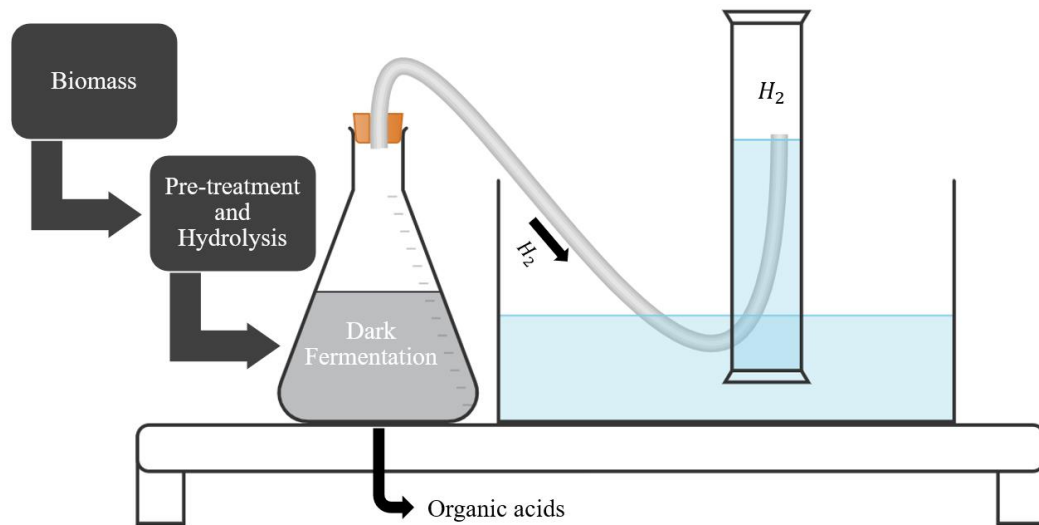
Figure 2.2: Demonstration of dark fermentation and hydrogen production.

Organic substrates, such as lignocellulosic wastes from the agriculture industry, biomass wastes from the food industry, and wastewater from the manufacturing industry, can serve as substrates for dark fermentation process [36]. The acetate-mediated pathway is the dominant mechanism in dark fermentation for hydrogen gas production [7]. The stoichiometry can be demonstrated as:

$$C_6H_{12}O_6 + 2H_2O \rightarrow 2CH_3COOH + 4H_2 + 2CO_2 \qquad (2.1)$$
$$C_6H_{12}O_6 + 2H_2O \rightarrow CH_3CH_2CH_2COOH + 4H_2 + 2CO_2 \qquad (2.2)$$
$$3C_6H_{12}O_6 \rightarrow 4CH_3CH_2COOH + 2H_2O + 2CO_2 + 2CH_3COOH \qquad (2.3)$$
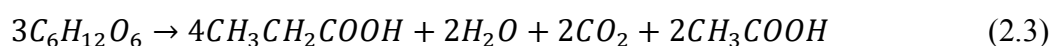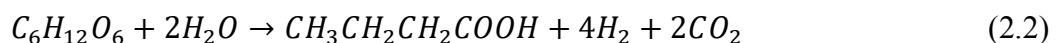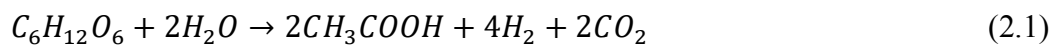
In studies, it has been observed that the theoretical hydrogen yield is higher than the actual yield due to the consumption of carbon sources by microbes for their growth [37]. Additionally, volatile fatty acids formation in dark fermentation effluent can lead to a decrease in pH, resulting in a lower yield of hydrogen production [38].

Several microorganisms including *Bacillus sp.*, *Enterobacter sp.*, and *Clostridium sp.* have been tested for hydrogen production [39]. However, the most commonly used dark fermentative bacteria are the *Clostridium* species which consist of C. *pasteurianum*, C. *thermolacticum*, C. *buytricum*, and C. *bifermentants* [40]. The types and amounts of volatile fatty acids produced may vary among different species of bacteria, which can affect the yield of hydrogen from dark fermentation. Various factors such as operating temperature, carbon source concentration, pH, partial pressure, and hydraulic retention time have a significant impact on the dark fermentation process as they can affect both the yield of hydrogen and the formation of by-products [41].

Dark fermentation is a promising method to produce hydrogen without dependence of sunlight. Nevertheless, pH reduction can inhibit hydrogen generation after some time [29]. The substrates decomposition by microorganism into VFAs, such as propionic, formic, acetic, lactic, and butyric acids, may also inhibit enzyme activity and hinder the production of green hydrogen [42], [43]. To fully utilize the dark fermentative effluent, the light fermentation process is often utilized for further biological hydrogen production. Purple nonsulfer (PNS) bacteria, such as RS–DSMZ, RS–NRRL, RS–RV, along with their combinations, are commonly used for the further process after dark fermentation [42].

2.4 Photo Fermentation

Photo fermentation transforms organic acid wastes into hydrogen element by phototrophic microorganisms. It is an attractive solution to extract additional hydrogen from effluents of dark fermentation [44]. PNS bacteria are employed in photo fermentation technology for mediation [45]. For example, *Rhodobacter capsulatus, Rhodobacter sulfidophilus, Rhodopseudomonas palustris,* and *Rhodospirillum rubrum* are well known PNS bacteria that participate in the light fermentation [46]. These phototrophic microbes can grow chemo-heterotrophically, photo-heterotrophically, and photo-autotrophically depending on the light intensity, degree of anaerobiosis, and types of carbon sources [47]. Nevertheless, for PNS bacteria growth and hydrogen production, photo-heterotrophically mode is preferred. During the photo-heterotrophically operation, organic acids can be substituted as substrates for PNS

bacteria growth, while sunlight can play as a role in energy sources for hydrogen evolution [41]. The phenomenon can be discussed as:

$$CH_3COOH + Sunlight \rightarrow 4H_2 + 2CO_2 \qquad (2.4)$$

$$CH_3CH_2CH_2COOH + 3H_2O + Sunlight \rightarrow 10H_2 + 4CO_2 \qquad (2.5)$$

$$HCOOH + Sunlight \rightarrow H_2 + CO_2 \qquad (2.6)$$
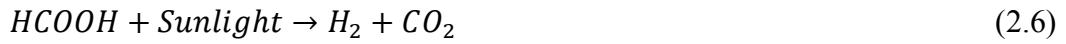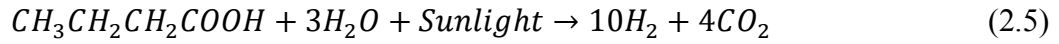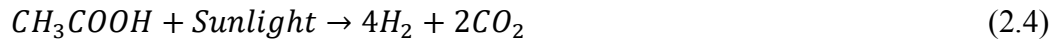
In light fermentation, hydrogenase and nitrogenase are the key enzymes for catalytic reaction. The catalytic reaction is named as citric acid cycle (TCA cycle), where hydrogen production performance strongly relies on nitrogenase activity [48]. Figure 2.3 illustrates the hydrogen production pathway by PNS bacteria.
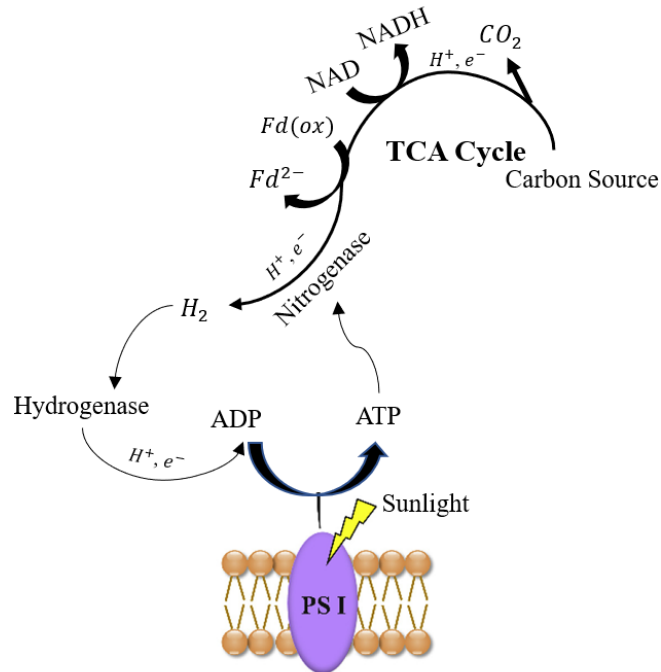
Figure 2.3: Purple Nonsulfer (PNS) bacteria photo fermentation pathway for hydrogen generation [48].

Li et al. (2019) added dark fermentative effluents as succedaneum to enhance the pH stability and biological hydrogen production yield in photo fermentation. In the research study, corn straw enzymatic hydrolysate was employed to adjust the nutrition of dark fermentation effluents. The results showed that the optimization process has successfully enhanced the biological hydrogen yield and production rate by 4 and 5 times, compared to the operating condition without enzymatic hydrolysate. To be exact,

biological hydrogen yield was improved from 312.54 to 1287.06 mL H_2 / g totally organic carbon and maximum hydrogen production rate achieved was 10.23 mL H_2/h, compared to the initial rate of 2.14 mL H_2/h. Furthermore, part of the sodium citrate buffer can be substituted with dark fermentation effluents to maintain the pH stability in fermentation broth. This resulted a reduction of buffer reagents usage, hence decrease in CO_2 GHG emission of 2.17g [49]. Moreover, Jiang et al. (2021) managed to optimize photo fermentative biological hydrogen generation from *Arundo donax* by adding glycerol in the medium. The optimization parameter ranged from 0 to 15g/L of glycerol addition, and the maximum biological hydrogen yield achieved was 79.2mL H_2/g substrate at 15g/L of glycerol addition. The biological hydrogen yield was improved by 294% compared to the mono-substrate solution. In addition, by Pearson's correlation analysis, they realized that *Arundo donax* L./glycerol ratio played an important role in photo fermentation process [50]. Moreover, Yue et al. (2021) generated biological hydrogen from eight kinds of shrub landscaping wastes by PNS microorganism. The shrub types were *Buxus megistophylla, Photinia fraseri, Buxus sinica, Sabina Chinensis, Berberis thunbergii, Ligustrum quihoui, Pittosporum tobira,* and *Ligustrum vicaryi*. After the research work, *Buxus megistophylla* was found to be the optimal for biological hydrogen formation. The hydrogen yield was 73.82mL H_2/g substrate. They also found that operating parameters such as shrubs feedstock concentration, fermentation temperature, and medium initial pH had a significant influence on hydrogen production from *Buxus megistophylla* [51]. Nonetheless, sunlight is essential for light fermentative chemical reaction to occur. Environment without sunlight can be an obstacle to scale-up photo fermentation technology [29]. Thus, hybrid dark-photo fermentation is demonstrated to enhance substrate-hydrogen conversion efficiency [52].

2.5 Hybrid Fermentation

Hybrid fermentation can be performed in two ways: co-culture hybrid fermentation or sequential dark-light fermentation [19], [44], [53]. Figure 2.4 illustrates simultaneous and two-stage dark/photo fermentation. In this process, carbon sources are consumed by dark fermentative bacteria to produce biological hydrogen and VFAs. On the other hand, photo fermentative bacteria then utilize these VFAs to produce additional

biological hydrogen, reducing fermentation time and increasing hydrogen productivity [54].
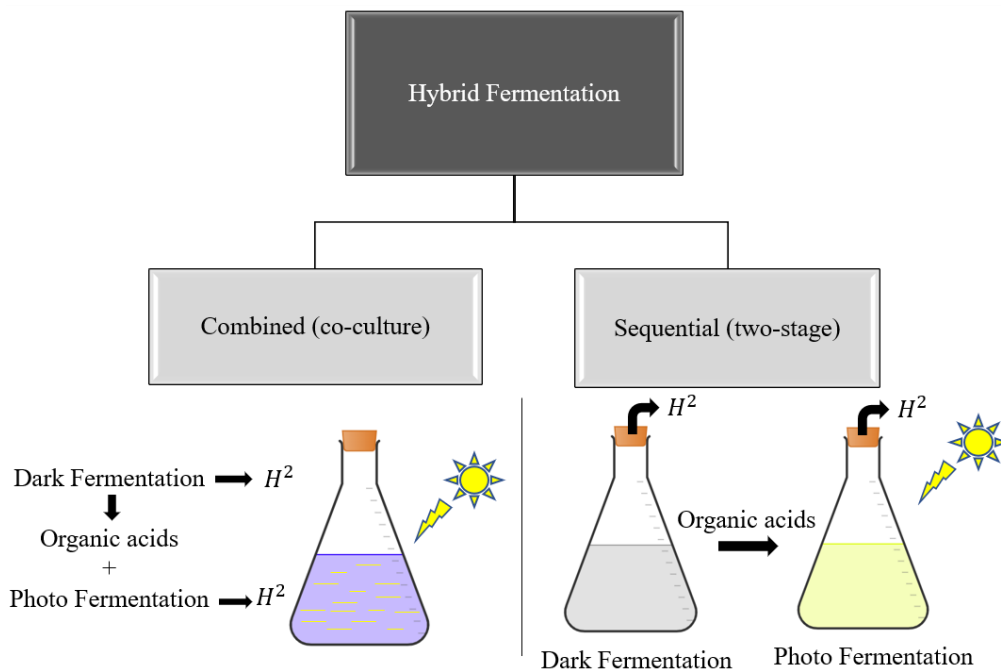
Figure 2.4: Illustration of combined and sequential hybrid fermentation [55], [56].

Zagrodnik (2015) performed co-culture hybrid fermentation for biological hydrogen production. The microbe strains utilized were dark-fermentative *C. acetobutylicum* and photo-fermentative *Rhodobacter sp.* during the research study. With the proper pH employed, they achieved an optimized production rate and yield of 2.533 L H_2/L medium and 6.22mol H_2/mol glucose, respectively [56]. Furthermore, Dinesh et al. (2020) produced biological hydrogen by subsequent dark and photo fermentation technology. By utilizing *Bacillus cereus* for dark fermentation and *Rhodopseudomonas rutila* for photo fermentation, they were able to decompose 100g/L of rice straw hydrolysate and achieve a hydrogen yield of 1.82mol H_2/mol glucose [19]. In addition, a pilot test of sequential dark-photo fermentation was carried out by Zhang et al. (2018) in an $11 m^3$ bioreactor. They carried out dark fermentation in a $3 m^3$ reactor and photo fermentation an $8 m^3$ reactor. The operating conditions were pH 4.5 and 35 °C for dark fermentation, and pH 7.0 and 30 °C for photo fermentation. Utilizing corn stover as the substrate, they achieved an overall biogas production rate of $87.8 m^3$/day with 68g/L of hydrogen content, resulting in an average hydrogen production rate of $59.7 m^3$/day [34]. Nevertheless, fermentative bacteria

require proper nutrients and operating conditions to survive and produce green hydrogen. The enzymes produced by different bacterial strains are responsible for breaking down complex substrates into hydrogen element or essential living elements for the bacteria. Thus, proper cultural procedures are necessary beforehand for fermentative microbes to grow and reproduce. Investigation of fermentation operating parameters is crucial to maximizing biological hydrogen production. The following sections review the effect of different operating conditions.

2.6 Operating Conditions Affecting Fermentation Process

Microbes' activities are sensitive to different operational conditions depending on the strains used. These operating conditions include the types and concentrations of feedstocks provided, operating pH and temperature, micronutrients supplied, and microbe inoculum concentration, all which have a significant impact on the biological hydrogen yield from the fermentation process. Optimal operating conditions should be examined to maximize the biological hydrogen formation depending on the bacterial strains used. The following section reviews various operating conditions that may affect the biological hydrogen yield from anaerobic degradation by different microbes.

2.6.1 Effect of Feedstock Types and Concentration on Fermentation Process

Organic matter is available in simple or complex forms, produced from animals, plants, or microbial cell communities. Well-known organic matters such as wheat, rice, corn, sweet potatoes, or cassava have been the source of glucose or starch-based substrates. These include D-glucose sugar molecules that are widely available after hydrolysis and are ready to be fermented [57]. The traditional substrate utilized for fermentation is sugar or sugar-based by-products. Nevertheless, with the wide variety of sugar available such as polysaccharides, disaccharides, and monosaccharides, the results of fermentation can vary depending on the type of sugar utilized [58]. For instance, Ren et al. (2008) investigated the types of sugars utilized during the dark fermentation process. Different sugars, sucrose, glucose, lactose, fructose, and xylose were added for the fermentation study. The comparison study found that hydrogen production was the highest when xylose was utilized as the substrate for fermentation. The hydrogen yield were 240mL H_2 /g sucrose, 270 mL H_2 /g glucose, 150 mL H_2 /g lactose, 140

mL H_2 /g fructose, and 280 mL H_2 /g xylose with different carbon sources at 10 g/L concentration [59]. Moreover, the amount of substrate added may affect the biological hydrogen yield from fermentation technology. For instance, Pu et al. (2019) investigated the effect of substrate concentration on biological hydrogen production by anaerobic seed sludge. The substrate concentrations studied were 0, 7.5, 15, 22.5, 30, and 37.5 g volatile solid/L fermentation medium. The maximum hydrogen yield obtained was 75.3 mL H_2 with 15 g volatile solid/L fermentation medium [60]. Furthermore, Navarro et al. (2020) investigated the ratio of fruit and vegetable waste (FVW) and cheese whey powder (CWP) on sequential dark-photo fermentation for hydrogen production. From the research work, they studied that the type and ratio of substrates had a significant impact on the total biological hydrogen yield and intermediate products from the dark fermentation process. For the initial dark fermentation process, the higher the amount of FVW as the feedstock, the higher the concentration of lactate as the by-product, which favors photo-fermentation for biological hydrogen formation. For two-stage dark/light fermentation, the optimum biological hydrogen yield obtained 793.7 mL H_2 /g COD (chemical oxygen demand) when the FVW:CWP ratio was 1:1. The study proved that the optimal substrate ratio not only regulates the hydrogen production from the dark fermentation process but also controls the concentration and distribution of organic acids, which in turn results in higher biological hydrogen production from photo-fermentation [61]. In addition, Zagrodnik Roman (2022) fermented mixed carbon components of lignocellulosic hydrolysates to produce continuous hydrogen. He investigated the conversion efficiency of individual sugar in lignocellulosic hydrolysate between pH 4 to 7.5. Among all sugars, cellobiose was fully decomposed in dark fermentation for the entire pH range. For other substrates such as xylose and arabinose, highest decomposition rate occurred in dark fermentation when operating pH of 6 and 7 were utilized, respectively [62]. In a conclusion, microorganisms' growth rate, feedstock conversion efficiency, and hydrogen yield strongly alter with the type and concentration of chosen carbon substrate. Types and concentration of substrate are worth investigating to maximise the hydrogen formation from dark, light or hybrid fermentation. The comparisons of biological hydrogen yield from various feedstocks are tabulated in Table 2.1:

Table 2.1: Summary of Feedstock Types and Concentration on Biological Hydrogen Generation from Fermentation Process.

Substrates	Microbes	Hydrogen Yield	Ref
Sucrose, glucose, lactose, fructose, and xylose	*Thermoanaerobacterium thermosaccharolyticum*	280 mL H_2 /g xylose	[59]
0, 7.5, 15, 22.5, 30, and 37.5g volatile solid	Anaerobic seed sludge	75.3mL H_2 with 15g volatile solid/L fermentation medium	[60]
Fruit and vegetable waste (FVW) and cheese whey power (CWP)	DF + PF mixed culture	793.7 mL H_2 /g COD when FVW:CWP ratio was 1:1	[61]
Mixture of cellobiose, arabinose and xylose	*Clostridium* and *Bacillus* mixed culture	1.74mol H_2/ mol consumed	[62]

2.6.2 Effect of Operating pH on Fermentation Process

pH quantitatively measures the acidity or basicity of liquid solutions that ranged from 0 to 14. It has significant influence towards microbe's environmental conditions that are strongly related to microbial growth and survival. Moreover, microbial metabolisms, interactions and community structures are dependent on operating pH during fermentation process. Microorganisms can be categorized into three types based on their adaptability to different environmental pH levels. For instance, acidophiles have best growth rate at pH < 5, neutrophiles that grow optimally at pH 5 to 9, and alkaliphiles that have highest growth performance at pH>9 [63]. Thus, effect of operating pH towards bacteria metabolism to produce biological hydrogen should be investigated. A research work studied the effect of controlled and uncontrolled pH towards hydrogen yield from hybrid fermentation. Dark fermentative strain *Clostridium acetobutylicum* and light fermentative strain *Rhodobacter sphaeroides* were utilized in the fermentation study. The results demonstrated that with a fixed operating pH, biological hydrogen yield had increased compared to uncontrolled pH condition. Highest production rate and yield achieved were 2.533 L H_2/L medium and 6.22mol H_2/mol glucose with fixed pH value of 7 [53]. Another investigation of pH on hybrid fermentation (subsequent dark/photo fermentation) to produce biological hydrogen was performed by Dinesh et al. (2020). The rice straw hydrolysate was

decomposed fully through their fermentation process where hydrogen yield achieved was 1.82mol H_2/mol glucose. The operating initial pH was 7.0. In their hybrid fermentation process, bacteria strains utilized were *Bacillus cereus* for dark fermentation and *Rhodopseudomonas rutila* for photo fermentation [19]. Li et al. (2020) experimented biological hydrogen yield with different pH value and salinity of swine wastewater during dark fermentation. The swine wastewater was pretreated with thermophilic bacteria beforehand. The results demonstrated that fermentation medium with pH 6.0 and 1.5g/L salinity were optimal to generate biological hydrogen. Besides, the results also demonstrated that biological hydrogen yield was unsatisfactory due to the accumulation of soluble chemical oxygen demand during alkaline condition and high salinity solution at 3-3.5g/L [43]. Additionally, for PNSB, operating pH has considerable influence towards their biological hydrogen production. Guo et al. (2020) utilized photo fermentative consortium which consist of *Rhodospirillum rubrum*, *Rhodobacter sphaeroides, Rhodobacter capsulatus*, *R.capsulata,* and *R.pulastris* to produce hydrogen. The initial pH value of phosphate buffer at 6.0 have the maximum the cumulative hydrogen production, which was 569.6 mL H_2 [64]. To conclude, pH as the operating parameter will enhance biological hydrogen generation from dark, photo and hybrid fermentation. It should be evaluated in fermentation study to improve the concentration of targeted by-products. The comparisons of biological hydrogen yield from various operating pH are tabulated in Table 2.2:

Table 2.2: Summary of pH Effect on Biological Hydrogen Generation from Fermentation Process.

pH	Microbes	Hydrogen Yield	Ref
Fixed pH 7	*Clostridium acetobutylicum* & *Rhodobacter sphaeroides*	6.22mol H_2/mol glucose	[53]
Initial pH 7	*Bacillus cereus* & *Rhodopseudomonas rutila*	1.82mol H_2/mol glucose	[19]
Initial pH 6	*Bacillus sp.* AT07-1	7ml H_2/g VSS	[43]
Initial pH 6	Photo fermentative consortium	569.6 mL H_2	[64]

2.6.3 Effect of Micronutrients on Fermentation Process

Micronutrients are low-concentration chemical substances that are essential for bacteria's growth and metabolism. These chemical substances include zinc,

manganese, calcium, nickel, iron, and copper, which have significant influence on the growth and hydrogen production of PNSB and dark fermentative microbes. Enzymes, such as nitrogenase and hydrogenase, produced from fermentative microbes, may be enhanced or inhibited by the addition of heavy metal ions. Metal ions are essential for enzymes maturation; hence they regulate the activity of hydrogenase or nitrogenase enzymes for hydrogen production. However, the inappropriate type or concentration of micronutrients may cause the inhibition of membrane enzymes [65]–[70]. Trchounian et al. (2016) introduced various heavy metals and formulated different micronutrients formula for batch *Escherichia coli* culture. They studied that the growth and biological hydrogen formation by *Escherichia coli* were significantly affected by the introduction of different metal ions. The results showed that the combination of Ni^{2+} and Fe^{2+} (0.05mM) had stimulated the bacterial biomass yield by 1.5-fold. Furthermore, for biological hydrogen yield, it increased by 2.93-fold when the combination of Fe^{3+} and Mo^{6+} (0.05 mM and 0.02 mM respectively) was introduced. The stimulated hydrogen yield was 2.20 mmol/L with glycerol as the substrate. However, the addition of 0.1mM Cu^{2+} and Cu^{+} had inhibited biological hydrogen evolution from *Escherichia coli* strain [71]. Additionally, Zhang et al. (2021) revealed that the introduction of cobalt ferrate nanoparticles had improved the hydrogen evolution from dark fermentation. The mesophilic *Clostridium* anaerobic sludge was utilized in their dark fermentation work. The introduction of 0.4g/L of $CoFe_2O_4$ released Fe^{3+} and Co^{3+} into the fermentation broth upon corrosion, hence stimulated the biological hydrogen evolution by roughly 32%. The hydrogen yield was 206.03mL H_2 /g glucose. The authors also reported that increasing in $CoFe_2O_4$ concentration may inhibit enzyme activity to produce biological hydrogen [72]. Another fermentation study by seed sludge was performed by Sun et al. (2021) to investigate the effect of $MnFe_2O_4$ on biological hydrogen evolution. The addition of 400mg/L $MnFe_2O_4$ nanoparticles had a compelling effect on mesophilic and thermophilic types of dark fermentation. Roughly 40% and 133% of biological hydrogen increment were observed from mesophilic and thermophilic dark fermentation when $MnFe_2O_4$ was introduced. The release of Fe^{3+} and Mn^{2+} were essential for key enzyme synthesis and signal transduction. The results showed that biological hydrogen generated was 272.7mL H_2 /g glucose and 183.4mL H_2 /g glucose from 37°C and 50°C operating conditions [73]. As a consequence, the types and concentration of micronutrients are

worth exploring to enhance the yield of biological hydrogen from fermentation process. Table 2.3 summarizes the hydrogen yield and types of metal ions utilized for stimulation:

Table 2.3: Summary of Various Micronutrients Effect on Biological Hydrogen Yield from Fermentation Process.

Metal ions & concentration	Microbes	Hydrogen Yield	Ref
Fe^{3+} & Mo^{6+} (0.05 mM + 0.02 mM)	*Escherichia coli*	2.20 mmol/L	[71]
0.4g/L of $CoFe_2O_4$ (Fe^{3+} + Co^{3+})	*Clostridium* anaerobic sludge	206.03mL H_2 /g glucose	[72]
400mg/L of $MnFe_2O_4$ (Fe^{3+}+ Mn^{2+})	Seed Sludge (mesophilic condition)	272.7mL H_2 /g glucose	[73]
	Seed Sludge (thermophilic condition)	183.4mL H_2 /g glucose	

2.6.4 Effect of Initial Microbes Concentration on Fermentation Process

In the fermentation process, the initial bacteria concentration has significant effect on the rate of by-products formation [74]. A research work investigated the influence of initial biomass concentration on biological hydrogen production from a hybrid fermentation process. With a dark/light bacteria ratio of 1:7, the initial cell concentration investigated was 0.5 to 5g/L. The feedstock utilized was wheat powder, with a substrate concentration of 5g/L. Besides, the experimental work utilized dark fermentative anaerobic sludge and light fermentative mixed *Rhodobacter* culture. The parametric fermentation study revealed that the 1.1g/L of initial cell concentration was the optimal for biological hydrogen generation. The cumulative hydrogen concentration and yield were 118mL H_2 and 156.8mL H_2 /g starch produced, respectively [75]. Furthermore, Eker and Sarp (2017) studied the influence of initial anaerobic sludge concentration on dark fermentation technology. Ground wastepaper was acid hydrolysed beforehand and used as the feedstock in their fermentation process. The initial biomass concentrations studied were 0.25, 0.50, 1.00, 1.50, and 2.00 g/L, where the total biological hydrogen accumulated was 105.18, 105.76, 69.72, 64.81, and 50.52 mL H_2, respectively. The optimal biomass concentration to produce biological hydrogen was 0.5g/L [76]. Additionally, Giang et al. (2019) explored the

effect of initial *Chlorella sp.* concentration on biological hydrogen yield in a fermentation study. In their research study, cell concentrations were varied from 10 to 50 g/L. The paper showed that the optimal initial cell concentration for hydrogen evolution was 20g/L, with 170mL H_2/g volatile solid produced. However, a further increase in initial bacteria concentration resulted in an unsatisfactory hydrogen yield [77]. Depending on the strains utilized for the fermentation process, the initial cell concentration is vital to be studied for hydrogen yield improvement. Table 2.4 summarizes the biological hydrogen yield by various strains and concentrations of bacteria:

Table 2.4: Summary of Initial Cell Concentration on Biological Hydrogen Yield from Fermentation Process.

Initial Biomass Concentration	Microbes	Hydrogen Yield	Ref
1.1g/L	Anaerobic sludge + mixed *Rhodobacter* culture	156.8mL H_2/g starch	[75]
0.5g/L	Anaerobic sludge	206.03mL H_2 /g glucose	[76]
20g/L	*Chlorella sp.*	170mL H_2/g VS	[77]

2.6.5 Effect of Operating Temperature on Fermentation Process

An increase in temperature accelerates the metabolism of microorganisms, leading to a higher yield of by-products in the fermentation process. Nonetheless, at extremely high temperature, enzyme activity may diminish, and the protein may denature. In fermentation technology, operating temperature can be classified into mesophilic (20-40°C), thermophilic (40-65°C), and extreme thermophilic (65-80°C) conditions, depending on the type of microorganisms utilized [78]. For instance, Infantes et al. (2011) investigated biological hydrogen production under mesophilic and thermophilic conditions of 26-45℃. In their research study, 9g/L of glucose was introduced as the fermentation feedstock to convert into hydrogen energy. The results demonstrated that dark acidogenic fermentative bacteria produced optimal hydrogen yield when operating at 26℃ mesophilic condition [79]. Additionally, Ziara et al. (2019) carried out the dark fermentation process on lactate wastewater and studied the

effect of temperature on biological hydrogen formation. The dark fermentation process was operated by anaerobic sludge. The study found that biological hydrogen evolution from fermentation was successful under mesophilic condition. The results demonstrated that 45 ℃ was the optimum condition for generating maximum biological hydrogen yield of 0.91 mol H_2 / mol lactate wastewater. Furthermore, they observed that the medium with a temperature of 45°C was the maximum for lactate degradation, with an efficiency of 99.8%. In addition, 16S rRNA sequencing revealed that bacteria from the *Clostridium* genus were the most abundant during the 35 ℃ operating condition, while *Sporanaerobacter, Clostridium* and *Pseudomonas* were maximum during the 45 ℃ operation [80]. Moreover, Mazareli et al. (2021) investigated the variation of temperature on biological hydrogen yield from banana waste fermentation processes. The operating temperature investigated was 27°C to 47°C. The results from the study revealed that 37°C was the optimum for autochthonous bacteria to generate biological hydrogen from banana waste. Biological hydrogen accumulated was 70.19mL H_2 [81]. Other than that, Yue et al. (2021) carried out light fermentation to convert shrub landscaping waste into biological hydrogen energy. By utilizing *Buxus megistophylla* as the substrate and HAU-M1 photosynthetic bacteria as the fermenting cell, the final optimized cumulated hydrogen yield was 73.82mL H_2/g TS. The optimal operating temperature for biodegradation in the light fermentation was 29.78°C [51]. In summary, biological hydrogen production from fermentation technology strongly depends on the operating temperature. The fermentation temperature must be explored if different types of microbes are utilized, whether they are mesophilic, thermophilic, or extreme thermophilic bacteria. Table 2.5 summarizes the various biological hydrogen yields when different temperatures are operated.

Table 2.5: Summary of Operating Temperature Effect on Biological Hydrogen Yield from Fermentation Process.

Temperature	Microbes	Hydrogen Yield	Ref
26℃	Dark acidogenic bacteria	3186.45 mL H_2	[79]
45℃	Anaerobic sludge	0.91 mol H_2 / mol lactate wastewater	[80]
37℃	Autochthonous bacteria	70.19mL H_2	[81]
29.78 ℃	HAU-M1 photosynthetic bacteria	73.82mL H_2/g TS	[51]

2.6.6 Effect of Bioreactor Design on Fermentation Process

The bioreactor has a crucial role in the fermentation process, particularly in photo fermentation where the entry of light into the photobioreactor is essential. It offers high productivity due to reduced water evaporation and extended culture maintenance in comparison to open-air culture systems [82], [83]. The effective distribution, sources, quality, and intensity of light are vital for both biomass growth and the by-products formation by photosynthetic bacteria (PNSB) [84]. Designing a photobioreactor with a high surface-to-volume ratio is key for accelerating biochemical reactions in the photo fermentation process [85]. Whether employing artificial or natural light, or a combination of both, within the photobioreactor, selecting the right materials is crucial to maximize light capture. There are various materials available for constructing photobioreactors, including polyvinyl chloride (PVC), polyethylene, acrylic PVC, plexiglass, and glass. Glass, despite being the most transparent, comes with the drawback of costliness for large-scale photobioreactors and its inherent brittleness [86]. Continuous mixing is also a necessary step in photo fermentation to mitigate nutrient gradients, enhance mass transfer, and facilitate the separation of gas and liquid cultures. This helps prevent cell sedimentation and ensures uniform light exposure to the cells. To achieve maximum efficiency in photo biological processes, it is imperative to either evenly distribute the light throughout the reactor (dispersing light), reduce light concentration in any specific area by spreading it over a larger volume (diluting light), or ensure frequent exposure of cells to areas with higher light intensity through agitation [87]. Thus, to maximize photo fermentation efficiency, a photobioreactor should excel in light transport and distribution, enable precise operational parameter control to aid bacterial cells in efficient growth and light energy utilization, reduce both capital and operational costs, and minimize energy consumption throughout the process [86].

In conclusion, the types and concentration of substrates, operating pH, fermentation temperature, micronutrient types and mixture, and initial microorganism concentration are key operating parameters that influence the by-products formed during the biodegradation process. It is therefore crucial to study these conditions in relation to microorganisms' metabolism to produce biological hydrogen. Furthermore, the utilization of newly isolated microbial strains, *Bacillus paramycoides* and

Cereibacter azotoformans, in this research is underpinned by several justifications that set them apart from available strains. First and foremost, the use of novel strains promotes biodiversity in bioprocessing and contributes to the exploration of untapped microbial resources, aligning with sustainable and environmentally responsible practices. The research community can benefit from a broader spectrum of microbial options for various biotechnological applications, and the investigation of these newly isolated strains represents a step forward in harnessing their untapped potential. In addition, the distinctive metabolic pathways characteristic of these novel strains may offer a promising advantage in enhancing hydrogen yields, a pivotal factor in the optimization of biological hydrogen production. This outcome has far-reaching implications, as higher hydrogen yields not only signify increased energy efficiency but also translate into reduced production costs. This also signifies that less carbon source is required to achieve the same energy output, ultimately promoting resource efficiency and cost-effectiveness. The following section outlines the methodology for conducting experimental studies based on the novel strains to generate biological hydrogen energy.

CHAPTER 3: METHODOLOGY

3.1 Overview

The research project will be conducted in mainly 4 stages (Figure 3.1), namely (a) DNA sequencing and phylogenetic tree, morphology study, and growth behaviour of *Cereibacter azotoformans* and *Bacillus paramycoides*, (b) Preliminary stage of parametric study for dark and photo fermentation, (c) Optimization of co-culture hybrid fermentation by *Cereibacter azotoformans* and *Bacillus paramycoides*, (d) Kinetic modelling and proposed mechanisms for hybrid fermentation to generate biological hydrogen.
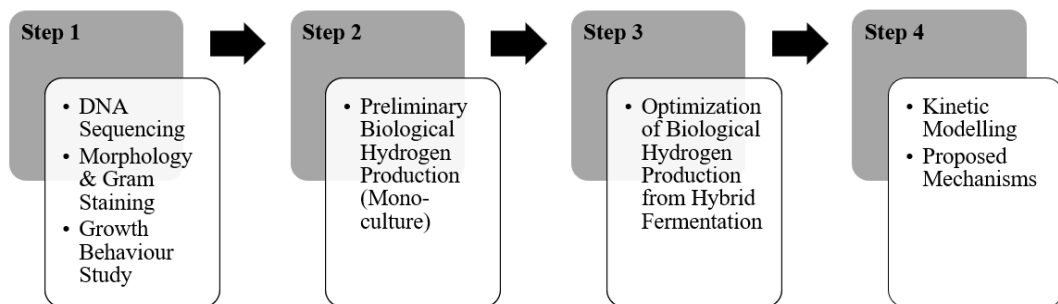
Figure 3.1: Flow Chart of Experimental Procedure.

3.2 Microorganisms and Culture Medium

Cereibacter azotoformans (JCM 9340) and *Bacillus paramycoides* (MCCC 1A04098) are the strains utilized in this research project for biological hydrogen production study (Figure 3.2). The freeze-dried form of *Cereibacter azotoformans* and *Bacillus paramycoides* were being activated in Pyrex borosilicate conical flasks for 48 hours prior to the experimental study.
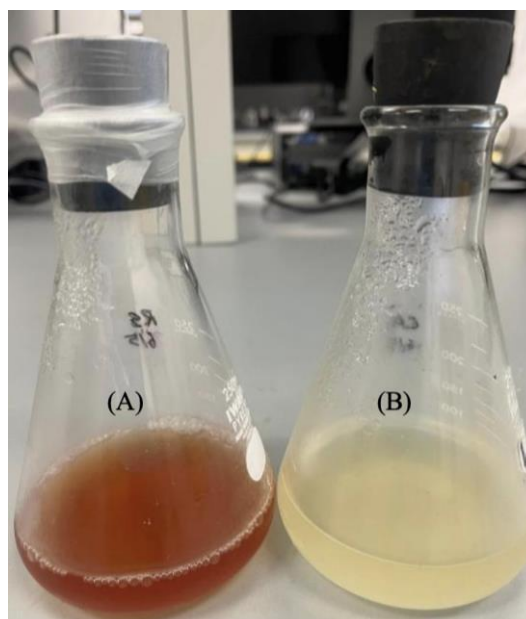
Figure 3.2: (A) *Cereibacter sp.* and (B) *Bacillus sp.* after activation from freeze dried form.

Photo fermentative PNS microbes, *Cereibacter azotoformans* JCM 9340 was cultivated in 8g of nutrient broth filled up with 1L of deionized water. The initial pH of activation broth was recorded as 6.61. Moreover, dark fermentative microbes, *Bacillus paramycoides* MCCC 1A04098 was cultivated in a culture media (1L) that contain 10g of glucose, 3g of peptone, 1g of yeast extract, 2.8g of K_2HPO_4, 3.9g of KH_2PO_4, 0.2g of $MgSO_47H_2O$, 0.1g of NaCl, 0.01g of $CaCl_26H_2O$, 0.05 g of $FeSO_47H_2O$, 0.2g of L-cysteine, and 1mL of microelements. The initial pH value of activation broth was recorded as 6.68. Microelements solution (1L) contains 0.07g of $ZnCl_2$, 0.1g of $MnCl_24H_2O$, 0.06g of H_3BO_3, 0.2g of $CoCl_26H_2O$, 0.02g of $CuCl_22H_2O$, 0.02g of $NiCl_26H_2O$, and 0.04g of $NaMoO_42H_2O$.

3.3 Experimental Set Up

Bioreactors and conical flasks, as well as cultivating media, were autoclaved at 121°C for 20 minutes before each experimental study. Carbon sources were also autoclaved separately at 110°C for 20 minutes before being introduced into the cultivating media. The growth behaviour of both bacteria was periodically analysed up to 96 hours. To reduce the cost for fermentation, 1g/L of inoculum at 24th hours was utilized during the growth behaviour study, compared to 10 g/L at 24th hours. Thus, the growth study was analysed based on 1g/L and 10g/L bacteria concentration in 250mL Pyrex conical

flasks. The growth behaviour study was performed at 33°C. After conducting the growth behaviour study for both bacteria, a preliminary stage of mono-culture and hybrid fermentation were carried out to produce biological hydrogen. Inoculation was performed in a biological safety cabinet, and the biodegradation process by *Cereibacter azotoformans* (JCM 9340) and *Bacillus paramycoides* (MCCC 1A04098) to generate hydrogen compound requires anaerobic condition. To create this anaerobic condition for the experimental study, the conical flask was flushed with argon gas to remove oxygen and closed with a rubber stopper. Furthermore, bacteria culturing was carried out in a closed desiccator with lit candles to eliminate excess oxygen from the environment. The experimental set up is illustrated in Figure 3.3:
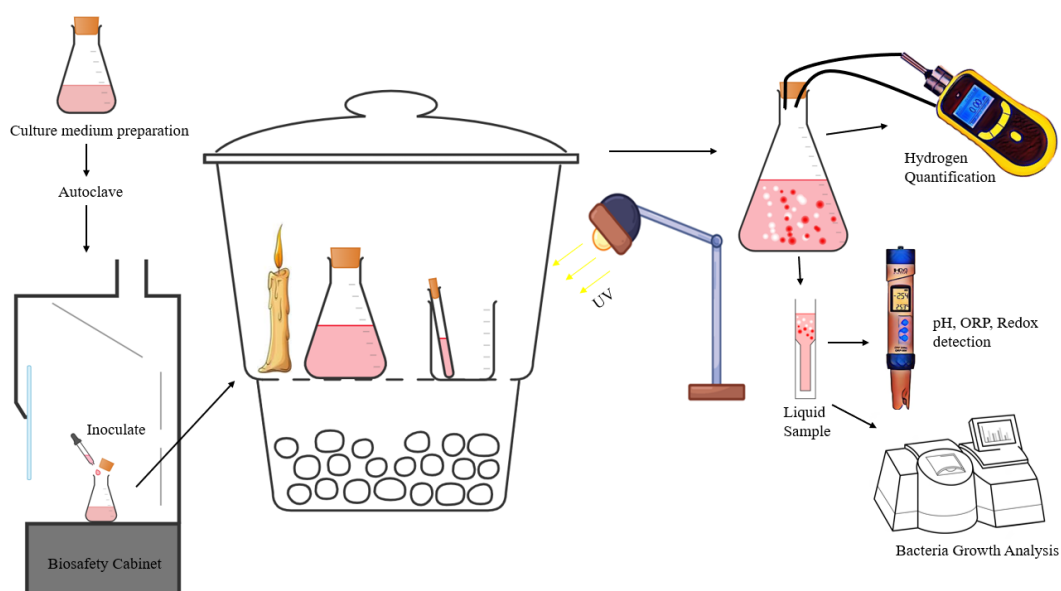
Figure 3.3: Experimental set-up for biological hydrogen fermentation.

For the preliminary stage of the mono-culture and co-culture hybrid fermentation parametric study, they were carried out in 50 mL Duran borosilicate test tubes. The optimized conditions were then performed in a 250 mL Pyrex conical flask. The parametric study included different types and concentrations of carbon sources, different types and concentrations of micronutrients, operating pH and temperature, and inoculum concentration. The activation, cultivation, and parametric study were carried out in a refrigerated static incubator. For light fermentation by *Cereibacter azotoformans*, it was constantly supplied with illumination by a 300W Ultra-Vitalux lamp. Table 3.1 shows the equipment list for experimental research study:

Table 3.1: List of equipment for experimental set up

Equipment	Brand	Purpose
Borosilicate conical flasks	Pyrex	Bacteria activation, cultivation and up-scale fermentation for *Cereibacter azotoformans* and *Bacillus paramycoides*
Borosilicate test tube	Duran	Parametric study for mono-culture dark or photo fermentation, and co-culture hybrid fermentation
Upright autoclave	HV-110 Hirayama	Sterilization for glassware, culture medium, and carbon sources
Ultra-Vitalux lamp	Osram	Illumination for photo fermentation
Refrigerated static incubator	Binder	Incubate bacteria during fermentation process at desired temperature
Class II biological safety cabinet	Esco Scientific	To perform inoculating process for safely working with materials contaminated with pathogens

Desiccator		To carry out fermentation with anaerobic condition
	Eppendorf Bioflo 320	For up-scale fermentation to produce biological hydrogen

The operating parameters for dark, light, and co-culture hybrid fermentations are listed in Table 3.2. The preliminary stage will be carried out based on mono-culture dark and photo fermentation, and the data obtained will be processed using Response Surface Methodology (RSM) in Design-Expert v13 software for the subsequent hybrid fermentation process. The operating temperature for preliminary stage dark and light fermentation was performed in 33°C.

Table 3.2: Operating conditions for dark and photo fermentation.

Type of Fermentation	Parameters	Range
Dark Fermentation	Glucose concentration	0g/L, 2.5g/L, 5g/L, 7.5g/L, 10g/L, 12.5g/L, 15g/L, 17.5g/L, 20g/L
	Xylose concentration	0g/L, 2.5g/L, 5g/L, 7.5g/L, 10g/L, 12.5g/L, 15g/L, 17.5g/L, 20g/L
	Type of micronutrients	Zn, Mn, Ca, Co, Ni, Fe, Cu
	Inoculum amount	2g/L, 4g/L, 6g/L, 8g/L, 10g/L at 24th hours log phase
Photo Fermentation	Glucose concentration	0g/L, 2.5g/L, 5g/L, 7.5g/L, 10g/L, 12.5g/L, 15g/L, 17.5g/L, 20g/L
	Xylose concentration	0g/L, 2.5g/L, 5g/L, 7.5g/L, 10g/L, 12.5g/L, 15g/L, 17.5g/L, 20g/L
	Type of micronutrients	Zn, Mn, Ca, Co, Ni, Fe, Cu

	Inoculum amount	2g/L, 4g/L, 6g/L, 8g/L, 10g/L at 24th hours log phase
Hybrid Fermentation	Xylose concentration	20 sets RSM experimental run (0 - 17.5g/L)
	Bacteria ratio	20 sets RSM experimental run *Cereibacter sp.* 0.1 - 4g/L at 24th hours log phase *Bacillus sp.* 0.1 - 2g/L at 24th hours log phase
	pH	5, 6, 7, 8, 9
	Temperature	30°C, 35°C, 40°C, 45°C, 50°C, 55°C
	Co	0μM, 20μM, 40μM, 60μM, 100μM
	Mn	0μM, 20μM, 40μM, 60μM, 100μM
	Co:Mn ratio	30 sets RSM experimental run (0 - 20μM)

3.4 Analytical Method

In this project, biological hydrogen, pH, and growth behaviour of *Bacillus paramycoides* and *Cereibacter azotoformans* will be analysed periodically throughout the experimental study. The equipment required for analytical process are tabulated in Table 3.3:

Table 3.3: List of equipment for analytical process

Equipment	Brand	Purpose
Class II biological safety cabinet	Esco Scientific	To perform analytical process for safely working with materials contaminated with pathogens

Portable hydrogen gas detector	ATO	To analyse biological hydrogen production from fermentation process
UV-VIS spectrometer	Perkin Elmer	To analyse the growth of *Bacillus paramycoides & Cereibacter azotoformans*, and carbon source quantification throughout the experimental study
pH meter	Eutech	Culture medium pH detection
Burette	Pyrex	To perform acid titration for acid quantifying
Water bath	Stuart	Boiling bath for Benedict's reaction
ORP / Hydrogen meter	Yieryi	To measure liquid hydrogen and ORP in fermentation broth

To monitor the biological hydrogen concentration produced by dark, photo, and hybrid fermentation processes, a portable hydrogen gas detector (ATO) equipped with an electrochemical detector was utilized, with a constant pump rate of 75 mL/min. The inlet and outlet of the hydrogen detector were plugged into the conical flask, creating a loop to detect the real-time concentration in the conical flask or test tube. After recording the hydrogen reading from the detector, the outlet was unplugged, and the detector continued to pump to flush away the hydrogen gas present in the conical flask, thus resetting the hydrogen gas concentration to zero. The procedure was repeated every 4 hours to measure the hydrogen gas produced periodically. In addition, the solution pH was indicated with a Eutech pH meter. Biological hydrogen production and liquid samples were analyzed and collected periodically every 4 hours during the growth behaviour study. For the parametric study, biological hydrogen production and liquid samples were analyzed and collected periodically every 24 hours. Additionally, for the pre-culture, optical density of 0.8 (600nm) was analyzed by a UV-VIS spectrometer before the growth curve study. For the bacteria growth behaviour study, solution samples were analyzed by a UV-VIS spectrometer with OD 600 nm for *Bacillus paramycoides* and *Cereibacter azotoformans*. The cell number of *Bacillus paramycoides* and *Cereibacter azotoformans* will be converted from UV spectra reading of OD 600 nm, where 1 OD of 600 nm is equal to 1.0×10^8 cells. Moreover, Benedict's test was utilized to quantify the carbon source available in the fermentation broth. Various concentrations of carbon source standards were analyzed beforehand in a UV-VIS spectrometer at OD 740 nm. The calibration curve is generated to quantify the substrate concentration in the fermentation broth. Besides, the acid titration method was used to quantify the VFAs produced during the fermentation process. For all the inoculating preparation and analytical processes, they were performed in a class II

biological safety cabinet throughout the experiment. The results will be demonstrated in the following section.

CHAPTER 4: BACTERIA STRAINS, MORPHOLOGY, AND GROWTH DYNAMICS STUDY

4.1 Overview

Cells can perform many functions. They synthesize proteins, convert substrates to energy, and even make up the tissues and organs in human bodies. Studying cell cultures and strains could lead to a deeper understanding and create breakthroughs in genetics, bioprocess research, and biomedical science. There are various bacterial cell shapes, such as rods, spirals, branches, and star shapes [88]. In this chapter, a morphology study, a growth behaviour study, and DNA sequencing were performed on both photo and dark fermentative bacteria.

4.2 Morphology and Gram Staining

Cereibacter sp. and *Bacillus sp.* were observed under scanning electron microscope. For *Bacillus paramycoides*, it is a rod-shaped bacterium with cell length of 1.8-2.2 μm, and cell width of 0.8-1.2 μm. It is isolated from the sediment of South China Sea. For *Cereibacter azotoformans*, it is an ovoid shaped PNSB with cell length of 1.5-2 μm, and cell width of 1.2-1.5 μm. It is isolated from the photosynthetic sludge. Figure 4.1 demonstrated the 2 different types of bacteria.
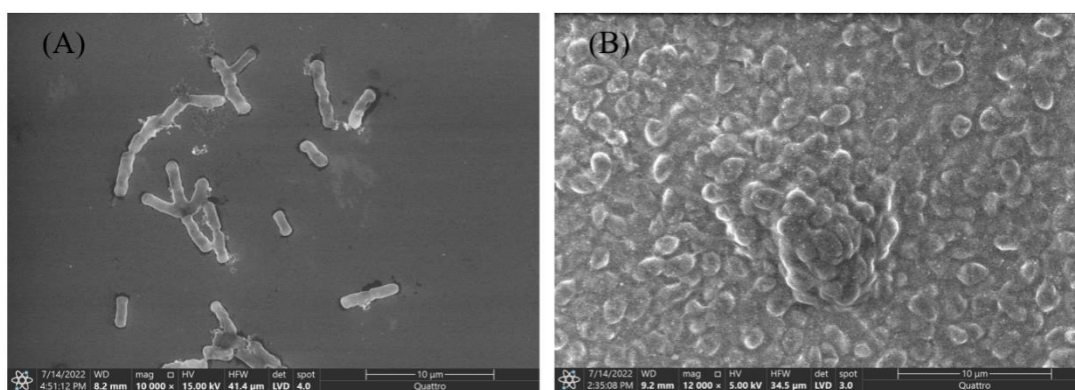
Figure 4.1: (A) *Bacillus sp.* and (B) *Cereibacter sp.* under SEM.

Gram staining procedure (Figure 4.2) was carried out to classify *Bacillus sp.* and *Cereibacter sp.* as gram-positive or gram-negative microorganisms. Firstly, cells were air-dried and heat-fixed on a microscope glass slide. The heat-fixed cells were flooded with 60 seconds crystal violet staining reagent. In the following step, glass

slide was washed with gentle stream of tap water for 2 seconds followed by gram's iodine flooding for 60 seconds. Furthermore, the glass slide was washed with ethyl alcohol for 5 to 10 seconds to remove the iodine reagent. Lastly, safranin which acted as the counterstain was flooded on the glass slide for roughly 45 seconds, followed by flushing indirect stream of tap water until no colour appeared in the effluent. The result was observed under a microscope.
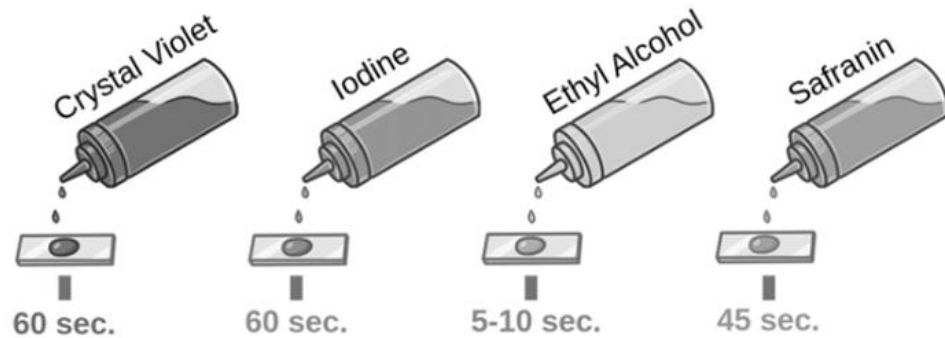
Figure 4.2: Gram Staining Procedure.

Figure 4.3 illustrated the results from gram staining process. The difference between a gram-positive and a gram-negative bacterium is that gram-positive bacteria have thick layers of peptidoglycan in the cell walls. For gram-negative bacteria, it has a thin layer of peptidoglycan in the cell walls [89]. Moreover, to differentiate a gram-positive or gram-negative bacteria, gram staining procedure can be employed. The organisms that retain the primary colour and appear purple under a microscope is gram-positive organisms, whereas organisms that appear red under a microscope are gram-negative organisms [90]. According to the literature, *Bacillus sp.* are gram-positive rods microorganisms [91]. Thus, the gram staining procedure has proved the identity of *Bacillus sp.* as gram-positive organisms and showing purple colour staining (Figure 4.3 (A)) under a microscope. For *Cereibacter sp.*, it is a gram-negative microorganism [92]. Thus, red straining (Figure 4.3 (B)) can be observed under a microscope after gram staining procedure.
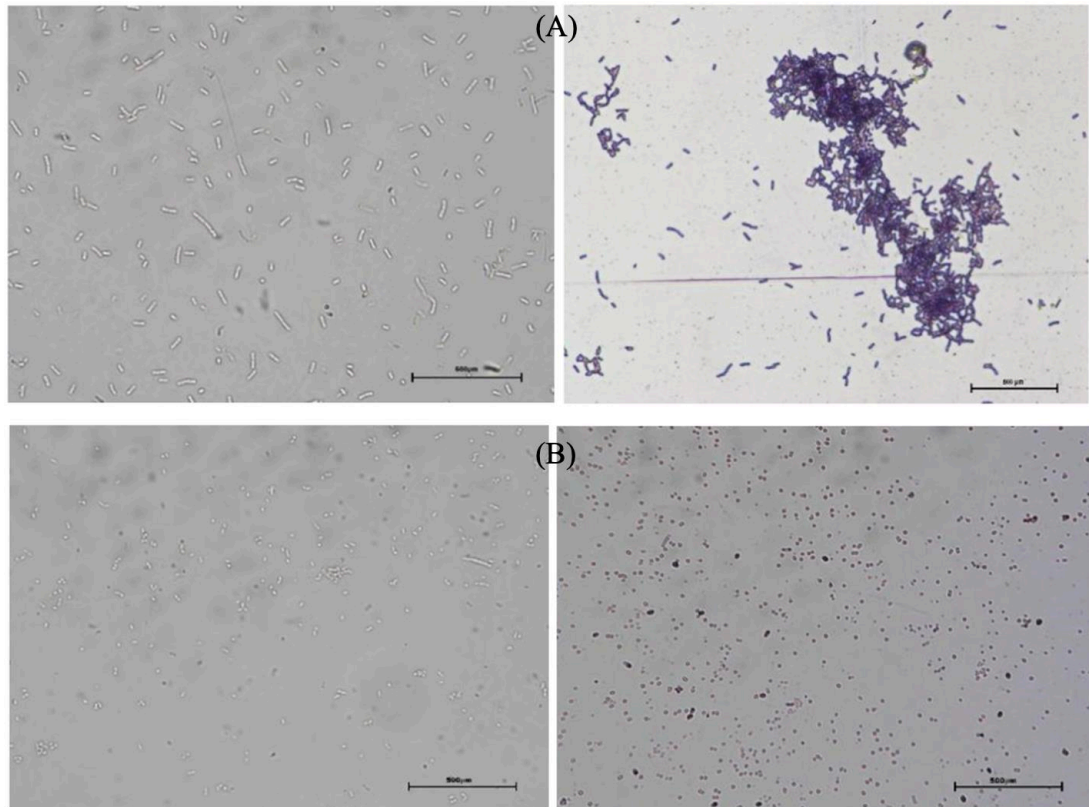
Figure 4.3: Before and after the Gram Staining procedure for (A) *Bacillus sp.* and (B) *Cereibacter sp.*.

To further identify and reconfirm the microbes' strains, DNA sequencing will be performed and demonstrated in the next section.

4.3 DNA Sequencing

The DNA was isolated and identified under the 16S ribosomal RNA (rRNA) gene polymerase chain reaction (PCR). The reaction for PCR is shown in Figure 4.4. From the total DNA, the 16S rRNA gene from the gDNA of bacterial isolates were PCR amplified using the primer 785F and 907R. The amplified product was run on to a 0.6 agarose. The agarose gel was documented and the PCR amplified product weight showed prominent DNA bandswith approximate sizes of 1500 base pairs. PCR amplified products were run on 1g/L agarose gel. Lane M indicates the DNA ladder (DNA Ladder Mix 250 to 10000 base pair, catalogue number BIO-5140). Markers with high intensity were indicated by their size. Lanes 1 and 2 indicate the PCR amplified 16S rRNA gene of the respective bacterial isolate. This analysis indicates specific amplification of the 16S rRNA gene. Sequence analysis was performed using

both forward and reverse primers and results are edited and assembled into one full-length sequence.
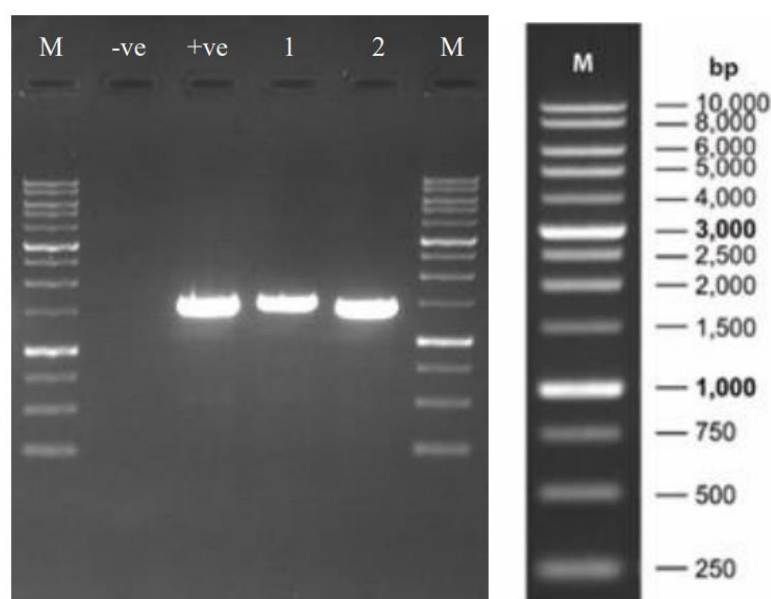
Figure 4.4: Agarose gel electrophoresis analysis of 16S rRNA genes amplified from two bacterial isolates.

The sizes of the 16S rRNA sequences obtained for each of the bacterial isolates are presented in Table 4.1. The 16S rRNA sequence of isolate 1 shows 99.93% identity to *Bacillus paramycoides*. For isolate 2, the 16S rRNA sequence is showing 100% identity to *Cereibacter azotoformans*.

Table 4.1: Bacteria isolated identified.

Sample	16S rRNA sequenced gene size (base pair)	GenBank accession number	% Identity	% Query cover	Scientific name
1	1509	NR_157734.1	99.93	100	*Bacillus paramycoides*
2	1418	NR_113300.1	100	99	*Cereibacter azotoformans*

Furthermore, phylogenetic analysis of isolates based on 16S rRNA gene sequences were compared to 16S rRNA gene sequences of hit species, highlighted the differential alignment of bacterial isolates with different species. The phylogenetic tree

(Figure 4.5) classifies the dark and photo fermentative bacteria as *Bacillus paramycoides* and *Cereibacter azotoformans*.
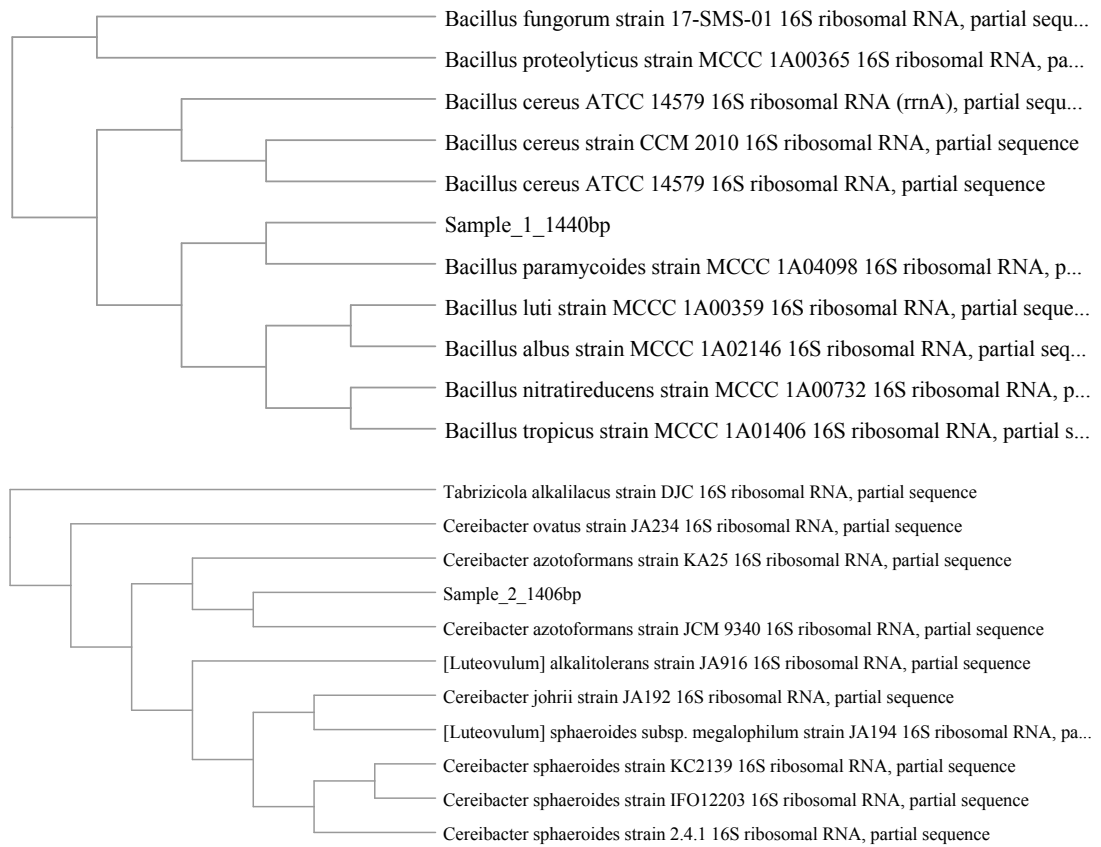
Figure 4.5: Phylogenetic tree for both isolate.

After knowing the morphology, gram staining characteristics, and identity for both bacteria, growth behaviour study was performed, and the results will be demonstrated in the following section.

4.4 Growth Behaviour Study and Biological Hydrogen Production with 1g/L Inoculum

Before conducting the parametric study on biological hydrogen production, the growth behaviour of each strain was analyzed. Figure 4.6 shows the results of the growth behaviour study on the photo-fermentative *Cereibacter azotoformans* and dark-fermentative *Bacillus paramycoides* in a 200mL fermentation medium. The growth behaviour study was performed at 33°C.
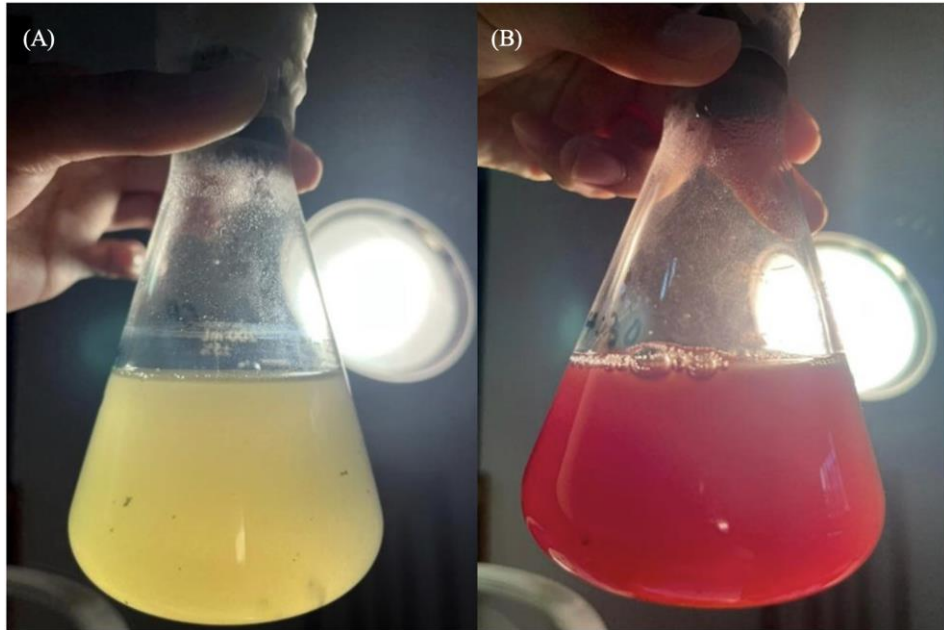
Figure 4.6: Single strain (A) dark and (B) photo fermentative bacteria growth study.

During the growth behaviour study for each strain, biological hydrogen production was analyzed simultaneously. Before the inoculation process, the initial pH of the *Cereibacter sp.* culture broth was analyzed and measured as 6.61, while the initial pH of the *Bacillus sp.* broth was measured as 6.68. Figure 4.7 presents the growth curves for both bacterial strains along with the biological hydrogen production. The biological hydrogen generation and liquid samples were collected and analyzed periodically for every 4 hours up to 4 days. Figure 4.7 illustrates that rapid biological hydrogen production occurred during the first 24 hours of dark and light biodegradation. The hydrogen production rate started to reduce and achieve a steady state from the 48th hour. The cumulative biological hydrogen production achieved was 5739 ppm and 3654 ppm, respectively, for dark fermentative *Bacillus sp.* and light fermentative *Cereibacter sp.*.

In addition, Figure 4.7 demonstrates the two growth curves for *Cereibacter azotoformans* and *Bacillus paramycoides* based on a 1g/L inoculum concentration for the growth behaviour study. The growth behaviour of *Bacillus sp.* and *Cereibacter sp.* was studied for 96 hours. During 0 to 38th hours, *Bacillus sp.*'s lag phase occurred due to the strain adapting to a new environment. After the lag phase, the exponential phase lasted for 28 hours, which appeared from the 38th to 66th hour of fermentation time. This is the stage where the maximum growth rate appeared for *Bacillus sp.*. Lastly,

from 66th to 96th hours of growth behaviour study, the stationary phase occurred where there was no net increase in cell number.

For *Cereibacter sp.*, the lag phase appeared from the 0 to 50th hours of fermentation time. During the lag phase, photo fermentative *Cereibacter sp.* tried to adapt to a new growth condition. After the individual cell matured and was ready for doubling, the exponential phase appeared from the 52nd to 96th hour of fermentation time. The doubling mechanism of *Cereibacter sp.* occurred during the log phase, thus illustrating a proportional growth curve in Figure 4.7. The results for biological hydrogen production and cell number are tabulated in Appendix 1.
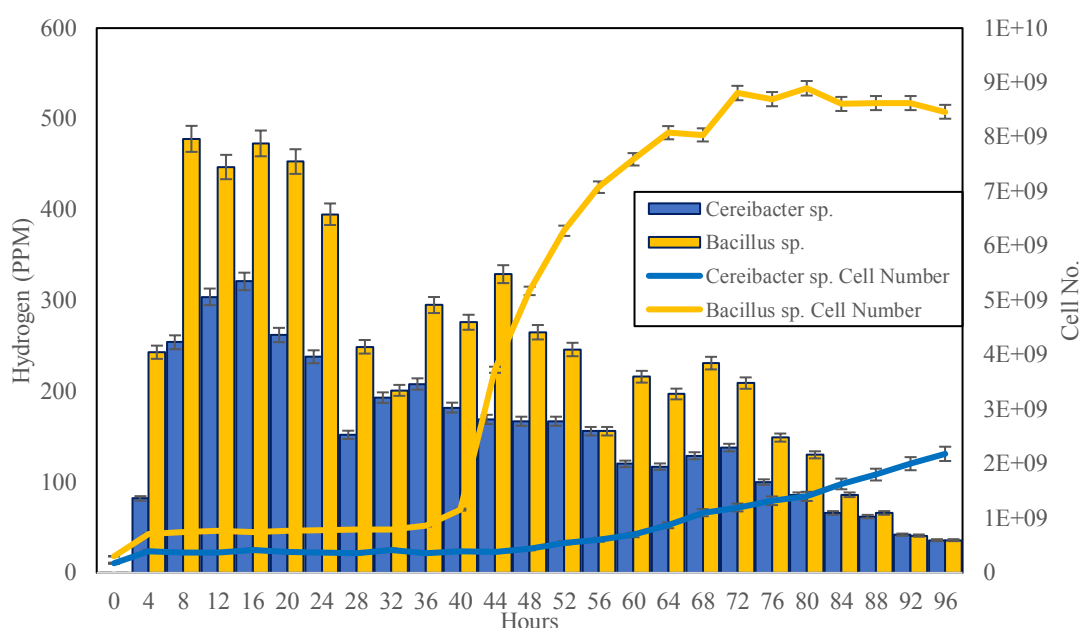
Figure 4.7: Growth curve and simultaneous biological hydrogen production by *Cereibacter azotoformans* and *Bacillus paramycoides* (1g/L inoculum).

Nonetheless, the growth curve study for *Cereibacter sp.* did not complete yet. The growth behaviour did not achieve up to stationary phase. Therefore, the growth study for both dark and light fermentative bacteria will be performed based on 10g/L inoculum concentration. The biological hydrogen production will also be analysed and interpreted in the next section.

4.5 Growth Behaviour Study and Biological Hydrogen Production with 10g/L Inoculum

During the growth behaviour study with 1g/L inoculum concentration, *Bacillus sp.* achieved lag, log, and stationary phases, while *Cereibacter sp.* only managed to reach lag and part of the exponential phase. Therefore, a new growth curve study with 10g/L inoculum concentration was conducted for both bacteria, as shown in Figure 4.8. The results for biological hydrogen production and cell number are tabulated in Appendix 2. The study lasted for 96 hours, during which biological hydrogen production was analyzed along with the growth behaviour. Liquid samples were collected every 4 hours, and the biological hydrogen generation was periodically measured. For the 10g/L inoculum concentration, both dark and light fermentation showed rapid biological hydrogen production in the first 20 hours. However, the hydrogen production rate decreased significantly from the 20th to the 44th hour of fermentation time, and steady-state biological hydrogen production began from the 44th hour until the end of the fermentation period. The cumulative biological hydrogen production after 96 hours was 4668 ppm for dark fermentative *Bacillus sp.* and 2564 ppm for photo fermentative *Cereibacter sp.* Both bacteria strains achieved up to the stationary phase in the growth curve study. *Bacillus sp.* growth curve in Figure 4.8 shows that the lag phase was from 0 to 20 hours, while the log phase lasted from the 20th to the 44th hour of fermentation time. The stationary phase for *Bacillus sp.* began at the 48th hour and continued until the 96th hour of fermentation period. For *Cereibacter sp.*, the lag phase occurred from 0 to 12 hours, followed by the exponential phase that lasted up to the 76th hour. Finally, the steady phase appeared from the 76th to the 96th hour of fermentation period.
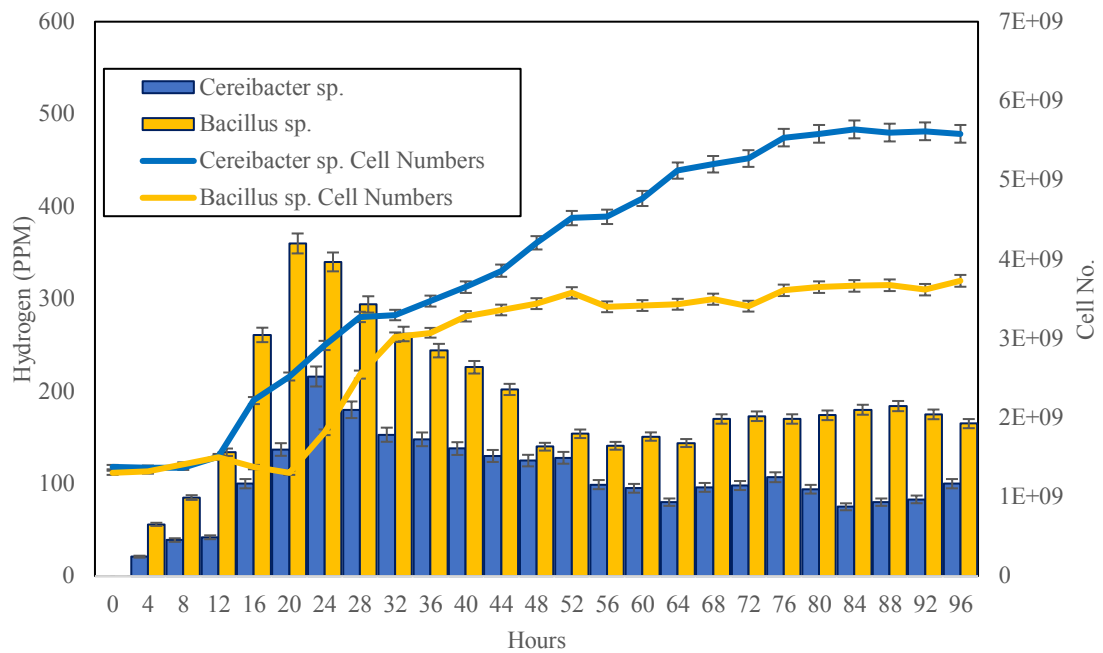
Figure 4.8: Growth curve and simultaneous biological hydrogen production by *Cereibacter azotoformans* and *Bacillus paramycoides* (10g/L inoculum).

For both the 1g/L and 10g/L inoculum growth behaviour studies, the lag phase is the initial period in the life of a bacterial population where cells adapt to a new environment. They prepare to generate proteins and cellular enzymes, which increases the size of the bacteria; thus, there is no increase in cell numbers during the lag phase. The duration of the lag phase may be influenced by the inoculum size, the physiochemical environment of both the original and new fermentation broth, and the physiological history of the bacteria [93].

In the 1g/L and 10g/L inoculum growth studies, rapid biological hydrogen production occurred during the initial lag phase of bacterial growth. This can be explained by the density-dependent communication system known as quorum sensing [94]. In quorum sensing communication system, bacteria involve cell-cell communication, which includes the production, detection, and response to extracellular signalling molecules called autoinducers. During the lag phase of bacterial growth, the cells may send autoinducer signals between the inter-species community to improve the microbial concentration. Furthermore, quorum sensing is involved in regulating enzyme production for microbial growth purposes [95]. The quorum sensing system between bacteria may improve hydrogenase or nitrogenase enzyme activity, which regulates a higher biohydrogen production. Therefore, when

the bacterial community reaches significant numbers, or namely the stationary phase, biological hydrogen production decreases and become stable, which may be due to the decreasing rate of quorum sensing.

To summarize, biological hydrogen production is significantly affected by the community of inter-bacterial species. After the lag phase, the logarithmic (log) or exponential phase occurs, where bacterial growth or biomass accumulation begins. During the exponential phase, cell doubling mechanism occurs through binary fission. The new count of bacteria that appears each time is proportionate to the current population. Also, this is the stage where the number of bacteria doubles periodically [96]. Nonetheless, during the 1g/L inoculum concentration of *Cereibacter sp.*, only part of the log phase is achieved. This may be due to the low concentration of cells, which resulted a lower cell division rate. Hence, with a 10g/L inoculum of *Cereibacter sp.*, a complete growth curve can be achieved in Figure 4.8. During the steady state, the rate of dividing cells is equal to the rate of dying cells, thus no net increase is observed in the number of viable cells. The entry of bacteria into stationary phase can be caused by various reasons such as limited nutrients available, stress factors such as changes in osmolarity, pH or temperature, and accumulation of toxic metabolites [97], [98].

To carry out preliminary dark and light biodegradation, and co-culture hybrid fermentation, a proper inoculum needs to be prepared for biological hydrogen production. A proper inoculum needs to be at an active growth stage and size, could form by-products from fermentation, and free from contamination. Therefore, the cells available in the log phase are retrieved for hydrogen fermentation [99]. With a 10g/L inoculum growth study, the log phase of *Bacillus sp.* and *Cereibacter sp.* appeared at the 24th hour of fermentation time. As a consequence, both bacteria inoculums are obtained in 24 hours for the following experimental work. Objective 1, encompassing the study of cell morphology, identification of bacterial strains, analysis of growth dynamics, and simultaneous hydrogen production, has been established up to this chapter.

CHAPTER 5: PRELIMINARY STAGE DARK AND PHOTO FERMENTATION

5.1 Overview

Dark fermentation is able to produce biological hydrogen in the absence of light and oxygen. Obligate or facultative anaerobes can be employed to act on the substrate to generate hydrogen through the acidogenic pathway [100]. Moreover, light fermentation employs cells such as PNSB to convert biomass to biological hydrogen in the presence of light. The simple reactor configuration is the advantage for fermentation technology to produce green hydrogen [101].

From the previous experimental work, which included morphology, DNA sequencing, and growth curve studies of dark and light fermentative bacteria, a parametric study on mono-culture fermentation will be performed in this section. The growth curve study from a 10g/L inoculum concentration indicated that dark and photo fermentative bacteria had the highest growth rate at 24 hours of fermentation time. At this stage, cells are the most active in the bioprocess reaction [99]. Thus, dark and light fermentative cells at 24 hours pre-culture will be extracted for this experimental study.

For the preliminary experimental study, the hydrogen production was performed in a 30mL (Figure 5.1) test tube for three days. The fermentation test tubes were flushed with argon gas and closed with stoppers to create anaerobic condition. Liquid samples and biological hydrogen production were collected and analyzed periodically up to 72 hours. In dark and photo fermentation, the parameters studied were various types and concentrations of carbon sources, different types of micronutrients introduced, and the initial inoculum concentration's effect on biological hydrogen production.
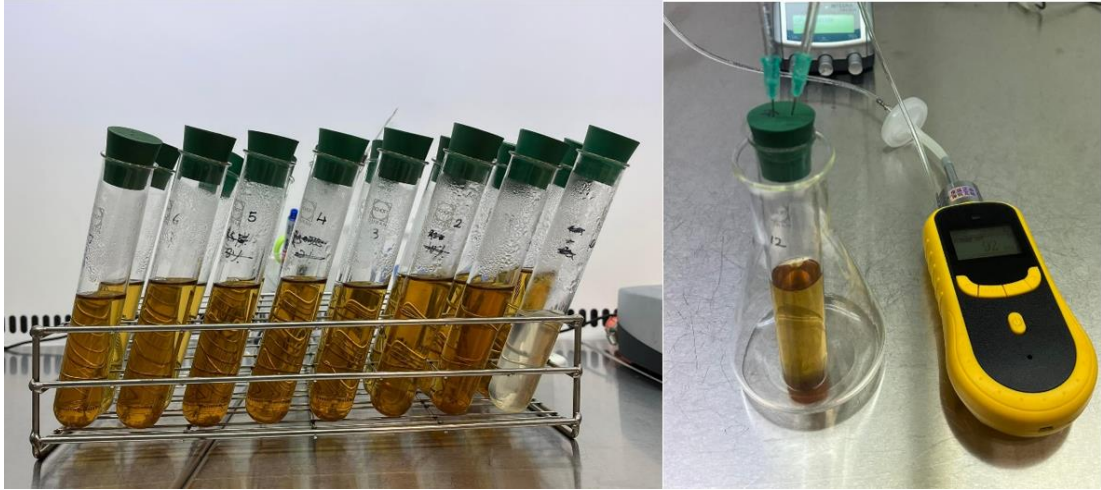
Figure 5.1: Demonstration of dark and light fermentation study in 30mL test tubes.

The following section demonstrates the biological hydrogen production and pH changes throughout the fermentation process based on various parameters.

5.2 Effect of Various Types and Concentrations of Carbon Sources on Dark Fermentation

The biological hydrogen production and pH changes in dark fermentative *Bacillus sp.* were studied based on various types and numbers of monosaccharides used in experiments. The monosaccharides utilized for optimization were xylose and glucose, with sugar levels ranging from 0g/L to 20g/L and increments of 2.5g/L. The main components of plant biomass are cellulose, hemicellulose, and lignin. After pretreatment and saccharification of plant biomass, glucose and xylose are the most abundant monosaccharides in biomass hydrolysates [102], [103]. Thus, glucose and xylose were used in the biological hydrogen fermentation experiments. Figure 5.2 demonstrates the biological hydrogen production by dark fermentative *Bacillus* sp. over 3 days. For xylose, the optimal condition for biological hydrogen production by *Bacillus* sp. was a concentration of 17.5g/L, followed by the second and third optimal conditions of 15g/L and 12.5g/L. The cumulative biological hydrogen production was 415ppm, 355ppm, and 302ppm for 17.5g/L, 15g/L, and 12.5g/L xylose addition, respectively. For glucose, the optimal condition for biological hydrogen production was a concentration of 20g/L, with 385ppm of biological hydrogen accumulated. The

graph shows that the higher the carbon source introduced, the higher the biological hydrogen formation. Detailed results for biological hydrogen production and pH changes are tabulated in Appendix 3, Appendix 4, Appendix 5, Appendix 6, Appendix 7, and Appendix 8.
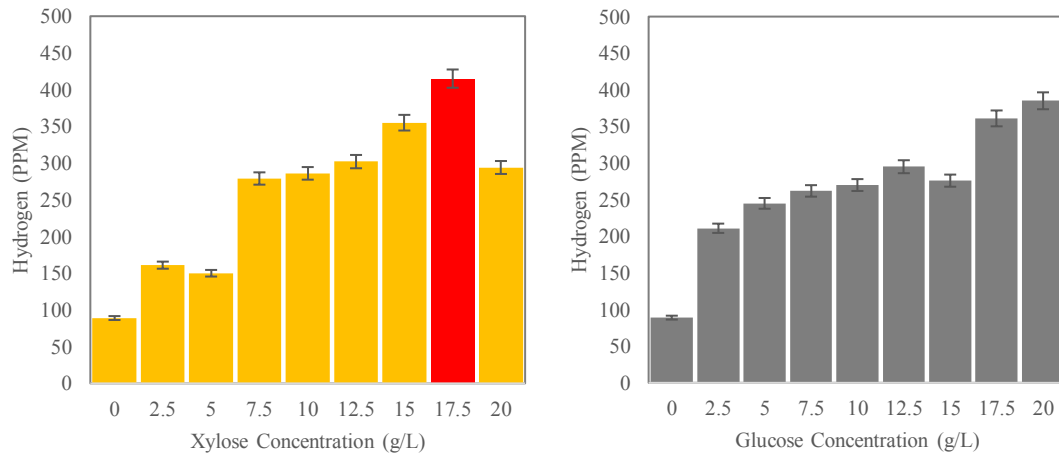
Figure 5.2: Cumulative biological hydrogen production by *Bacillus sp.* based on various types and concentrations carbon source.

A research report has demonstrated that with the proper carbon source addition, the inhibition of metabolites and feedstocks can be alleviated, thus improving bacterial metabolism and increasing by-product productivity, as seen in the case of biological hydrogen production [104]. For xylose addition, the optimal biological hydrogen accumulation was 415ppm, a 366% increase compared to 89ppm in the absence of xylose. Similarly, the addition of 20g/L glucose showed approximately a 432% improvement in biological hydrogen accumulation compared to 0g/L glucose. However, excessive addition of a carbon source may inhibit by-product formation in the fermentation process. In the case of dark fermentation by *Bacillus* sp., a 20g/L xylose concentration resulted in 294ppm of biological hydrogen. Research studies have shown that with a higher feedstock concentration, bacterial metabolism may shift from hydrogen fermentation to acid fermentation, which increases toxicity, causes pH reduction, reduces enzyme activity, and ultimately affects biological hydrogen yield [60], [98]. Furthermore, the addition of xylose shows a higher accumulation of biological hydrogen in dark fermentation, at 415ppm, compared to 385ppm with glucose. The fermentation pH was analyzed and is demonstrated in Figure 5.3, which

illustrates the pH changes of dark fermentation by *Bacillus sp.* when xylose was used as the feedstock. After mixing the culture media formula in deionized water, the nature pH appeared to be 6.68 for dark fermentative broth. Also, from the results, it shows that with a higher xylose addition, a greater pH difference can be observed after the biodegradation. For example, with a 20g/L xylose addition into the fermentation broth, the pH value dropped from 6.68 to 5.81, resulting in a pH drop of 0.87. The least pH changes can be observed when 0g/L xylose concentration was introduced, with a pH difference of only 0.45.
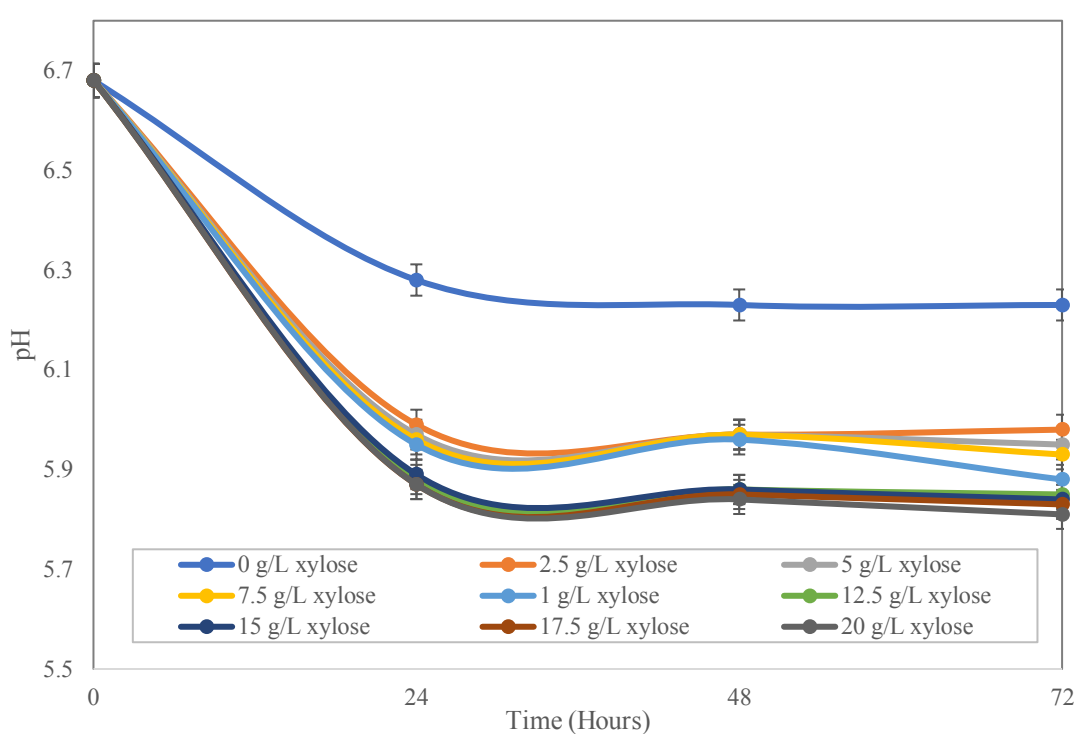
Figure 5.3: pH changes of *Bacillus sp.* based on different xylose concentration.

Thus, it can be concluded that the higher the substrate concentration, the lower the final fermentation pH value. Furthermore, pH changes were analyzed for various glucose concentrations. Figure 5.4 demonstrates the pH changes when glucose was used as the substrate for comparison. From Figure 5.4, it is evident that the pH dropped significantly when glucose concentrations ranging from 2.5g/L to 20g/L were added, whereas no change was observed at 0g/L glucose concentration. The pH difference was the least at 0g/L glucose concentration, with a final pH value of 6.01, resulting in a small pH difference of 0.67. After analyzing the pH, it was found that the higher the

substrate concentration, the lower the final pH value achieved throughout the fermentation period. This indicates that higher concentrations of carbon sources provide more easily biodegradable substrates for organic acid accumulation. However, lower substrate concentrations resulted in limited hydrolysis rates and acidification, resulting in the production of lesser organic acids [60].
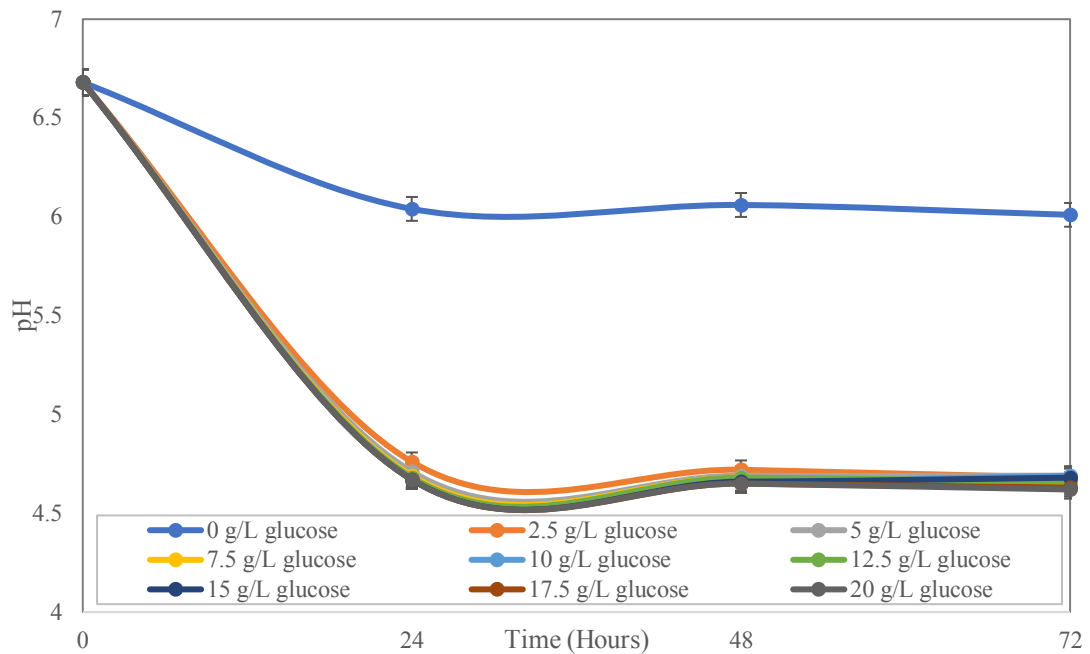
Figure 5.4: pH changes of *Bacillus sp.* based on different glucose percentage.

As compared to xylose fermentation, glucose resulted in a higher pH change during the dark fermentation process. The highest pH change for glucose was 2.06 pH units, while the highest pH drop for xylose addition was 0.87. The utilization of different carbon sources may initiate different metabolic pathways for *Bacillus sp.* during the dark biodegradation. It is known that extra energy is required to transport xylose across the bacterial membrane. The transportation of xylose is energized by a high-energy phosphate compound related to ATP, where 1 mol xylose:1 mol ATP is required for xylose transportation into the cells of *Bacillus sp.*. On the other hand, glucose transportation utilizes phosphoenolpyruvate-dependent phosphotransferase system, and extra energy is not required for [105]. Therefore, acid by-products accumulation is higher when glucose is introduced as the substrate for dark fermentation.

After a parametric study on different xylose and glucose concentrations, it was observed that dark fermentation had a higher biological hydrogen accumulation when xylose was used as the substrate. This may be due to the higher concentration of organic acids formed during glucose fermentation. It was reported that the accumulation of acetate and butyric acids was higher in glucose fermentation compared to xylose fermentation [59]. Furthermore, most studies have shown that the optimum pH for biological hydrogen production from fermentation is between pH 5 to 6. The near-neutral condition facilitates the transportation of nutrients and cells by maintaining the surface charge on the bacteria cell membrane [106]. Acidic fermentation conditions may affect hydrogenase activity and change the bacteria metabolism pathway, thus affecting biological hydrogen production [107], [108]. After comparing Figure 4.11 and Figure 4.12, it was found that the introduction of glucose into the fermentation medium resulted in acidic fermentation conditions, with a final pH of 4.62-4.69. However, for xylose, the final pH of 5.81-5.98 resulted in a more neutral fermentation medium compared to glucose fermentation. To conclude, it can be deduced that the hydrogen-producing enzyme of *Bacillus* sp. may have the highest activity with xylose addition, and the operating pH is optimal for biological hydrogen generation. The following dark fermentation parametric studies based on various metal ions and inoculum concentration are carried out based on 17.5g/L xylose concentration.

5.3 Effect of Various Types and Concentrations of Carbon Sources on Photo Fermentation

PNSB anaerobic fermentation can utilize a wide range of feedstocks to produce hydrogen and carbon dioxide in the presence of light. This makes it an attractive option for complete conversion of VFAs present in dark fermentation effluent streams [99]-[101], as well as industrial and agricultural wastes. In the preliminary stage of photo fermentation by *Cereibacter sp.*, experiments were conducted using simple sugars, such as glucose and xylose. Various concentrations of carbon sources (ranging from 0g/L to 20g/L) were studied to investigate biological hydrogen production and pH changes in photo fermentation [109]–[111].

As shown in Figure 5.5, the optimal biological hydrogen accumulation by *Cereibacter* sp. occurred with 10g/L xylose and 17.5g/L glucose concentrations introduced into the culture medium, resulting in 168 ppm and 141 ppm of biological hydrogen accumulation for xylose and glucose, respectively. Previous studies have reported that providing optimum nutrition can balance microbe interaction with substrates, improve microbial metabolism, and increase biological hydrogen productivity [104]. Figure 5.5 also shows that higher carbon source concentrations result in higher biological hydrogen accumulation after fermentation. However, further increases in carbon source concentration result in decreasing biological hydrogen production. Biological hydrogen production and pH changes for *Cereibacter* sp. based on various carbon sources are tabulated in Appendix 3, Appendix 4, Appendix 5, Appendix 6, Appendix 7, and Appendix 8.
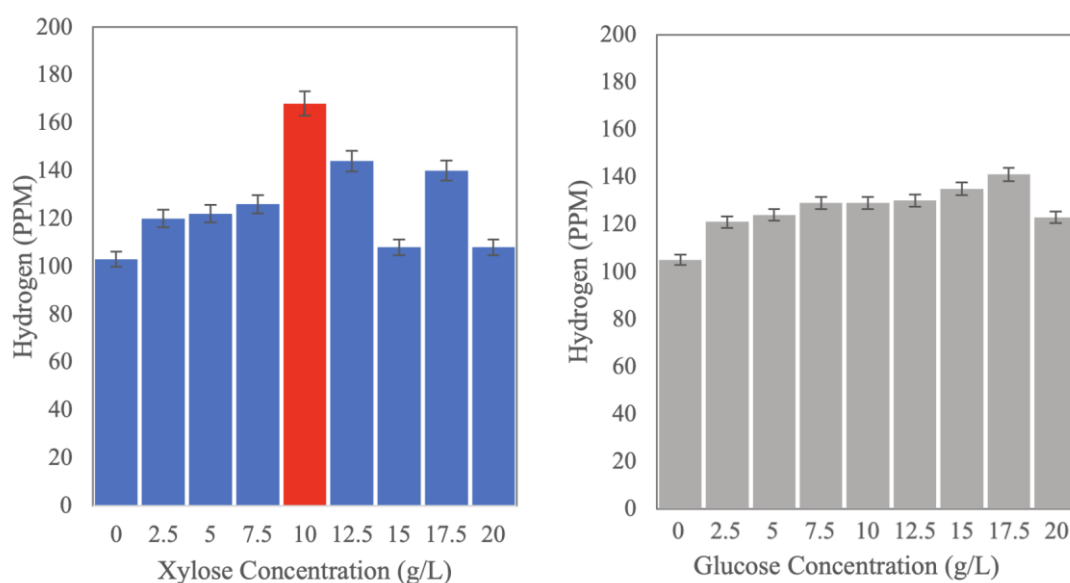
Figure 5.5: Cumulative hydrogen production by *Cereibacter sp.* based on various types and concentrations carbon source.

For xylose concentrations above 10g/L and glucose concentrations above 17.5g/L, biological hydrogen production inhibition can occur, leading to a reduction in hydrogen accumulation. A research study showed that as substrate concentration increases, there is a higher accumulation of VFAs after light fermentation due to variations in the metabolism pathway [112]. As a result, the fermentation medium becomes more acidic with a higher concentration of VFAs, inhibiting nitrogenase

activity required for biological hydrogen formation [107]. In light fermentation by *Cereibacter sp.*, the addition of xylose appears optimal for accumulating higher biological hydrogen, with 19% higher biological hydrogen formation observed with xylose than glucose. A similar study on photo fermentation found that xylose was the optimal carbon source for higher substrate-to-biological hydrogen conversion efficiency. The experimental work reported that 4.73 mol H_2 /mol glucose and 5.24 mol H_2/mol xylose were obtained when glucose and xylose were used as carbon sources in light fermentation by *Rhodobacter sphaeroides*. Xylose was the optimal carbon source in light fermentation for higher substrate to biological hydrogen conversion efficiency [113]. The pH values during photo fermentation were analyzed and are demonstrated in Figure 5.6. The initial nature pH value for *Cereibacter sp.* culturing broth was measured as 6.61 (without adjustment). The pH changes showed similar trends for various xylose concentrations, with curves increasing linearly during the first 48 hours followed by a significant drop in the final 24 hours of photo fermentation. Figure 5.6 also indicates that the higher the xylose concentration, the more acidic the fermentation broth becomes after light fermentation. Therefore, introducing a 20g/L xylose concentration into the *Cereibacter sp.* fermentation medium resulted in the most acidic condition after three days.
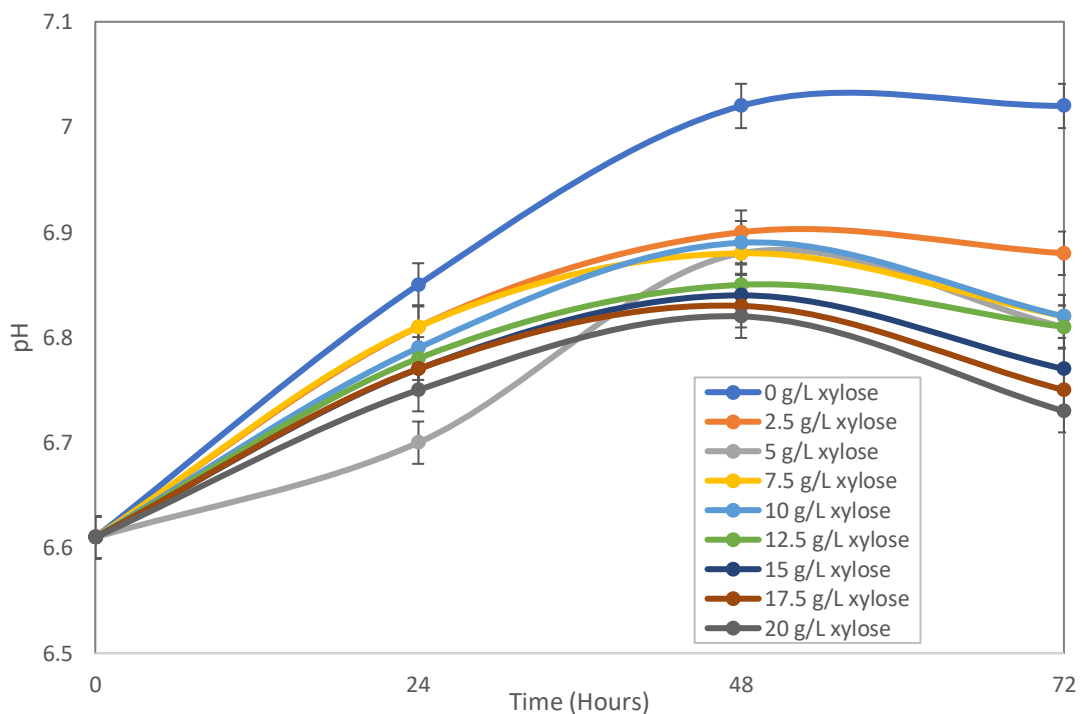
Figure 5.6: pH changes of *Cereibacter sp.* based on various xylose concentration.

The pH changes for glucose and xylose as carbon sources were recorded and compared. Figure 5.7 shows the pH trends for various initial glucose concentrations. The pH changes for glucose show similar trends to xylose pH curves, where the pH value increases linearly for 2 days, followed by a significant drop after 48 hours. For both glucose and xylose, the pH build-up during photo fermentation may be due to the accumulation of polyhydroxybutyrate (PHB), which is formed by *Cereibacter sp.* as one of the by-products [114]. Furthermore, the pH drop after 48 hours can be explained by the accumulation of CO_2 during the light fermentation process. During photo biodegradation, the oxidation of carbon source produces CO_2, which can lower the pH value. Hence, once *Cereibacter sp.* starts to produce biological hydrogen, there is a clear pH drop due to the formation and dissolution of CO_2 [113]. In addition, Figure 5.7 illustrates that the higher the glucose initial concentration, the more acidic the final fermentation media of light fermentative *Cereibacter sp.*, which is similar to xylose as the light fermentative substrate.
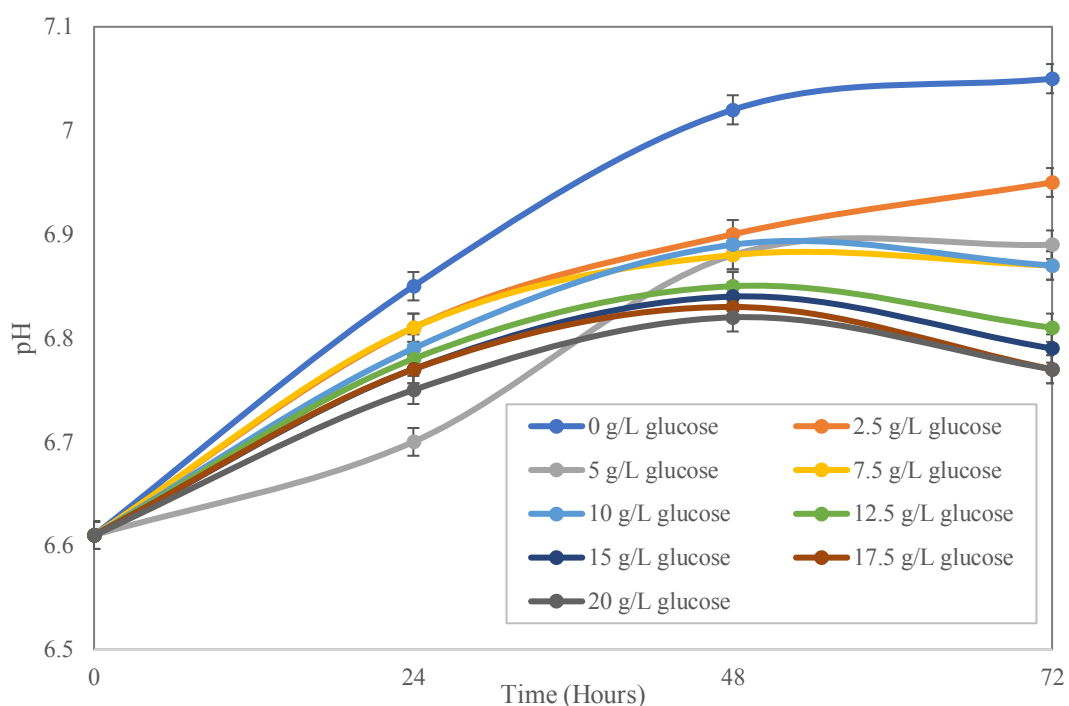
Figure 5.7: pH changes of *Cereibacter sp.* based on various glucose concentration.

Zhang et al. (2020) reported that the higher the substrate concentration, the more VFAs were accumulated after photo fermentation. PNSBs, including *Cereibacter sp.*, can utilize VFAs such as acetic acid, propionic acid, and pentanoic acid for further biological hydrogen evolution. However, butyric acid cannot be used by *Cereibacter sp.* for biological hydrogen production. Therefore, a higher substrate concentration may result in the accumulation of more butyric acid. Excess butyric acid may remain unconsumed for biological hydrogen formation, resulting in a reduction of the fermentation medium's pH [112]. The study showed that the addition of 20g/L glucose to *Cereibacter sp.* fermentation broth resulted in the most acidic pH after 72 hours of photo fermentation. After conducting a parametric study on different xylose and glucose concentrations, it was found that *Cereibacter sp.* produced higher biological hydrogen from xylose. PNSBs may prefer xylose for the optimal biological hydrogen formation pathway [113]. Therefore, the following parametric studies on various micronutrients and inoculum concentrations were carried out based on a 10g/L xylose concentration.

5.4 Effect of Various Micronutrients on Dark Fermentation

The most abundant monosaccharides in plant biomass are glucose and xylose. Based on previous experimental data, an optimum concentration of 17.5g/L xylose was found for the dark fermentative metabolism pathway to produce biological hydrogen. Therefore, dark fermentative *Bacillus* sp. will be experimented with various types of micronutrients based on 17.5g/L xylose concentration. Transition metals have unique inorganic and redox properties that may serve as cofactors for produced enzymes. The unfilled d-orbitals of transition metals make them redox-active and enable metal cofactors to serve as structural and catalytic roles in biological metabolism [115]. Various micronutrients such as iron, copper, nickel, manganese, cobalt, zinc, and calcium were tested, and their effect on biological hydrogen production by dark fermentation was investigated. It was found that metal ions have a significant effect on the microbial activity of fermentative bacteria. These nanomaterials can act as oxygen scavengers during anaerobic fermentation, reducing the oxidation-reduction potential and providing a more suitable anaerobic condition for biological hydrogen evolution [116] In the following section, cumulative biological hydrogen production

and pH changes with various metal ions including manganese, iron, zinc, copper, cobalt, nickel, and calcium are demonstrated.

Figure 5.8 demonstrates the effect of various metal ions on biological hydrogen yield from dark fermentation. The hydrogen production and pH changes were recorded periodically up to three days. The results are tabulated in Appendix 9, Appendix 10, Appendix 11, and Appendix 12. Figure 5.8 shows that the optimal metal ion for biological hydrogen production by *Bacillus* sp. was cobalt (II) chloride hexahydrate, with a total cumulative biological hydrogen production of 200ppm. During dark fermentation, acids produced by the process can corrode cobalt (II) chloride hexahydrate, releasing Co^{2+} into the fermentation environment. These metal ions can be reduced by the organic compound, resulting in a biochemical reaction in terms of electron transfer and enhanced biological hydrogen evolution [117]. Compared to the controlled condition without the introduction of metal ions, the cumulative biological hydrogen was 111ppm. The biological hydrogen was improved by 80%. Moreover, Figure 5.8 shows that all the fermentation media with micronutrients increased the biological hydrogen accumulation compared to the controlled condition. The addition of metal ions significantly improved biological hydrogen yield from the fermentation due to the large specific surface area and quantum size of nanoparticles that facilitate electron transfer between NADPH-ferredoxin oxidoreductase and hydrogenase. The hydrogenase activity can be improved through the redox reaction [65]. In conclusion, Figure 5.8 demonstrates that the addition of metal ions significantly enhances biological hydrogen yield from the fermentation process.
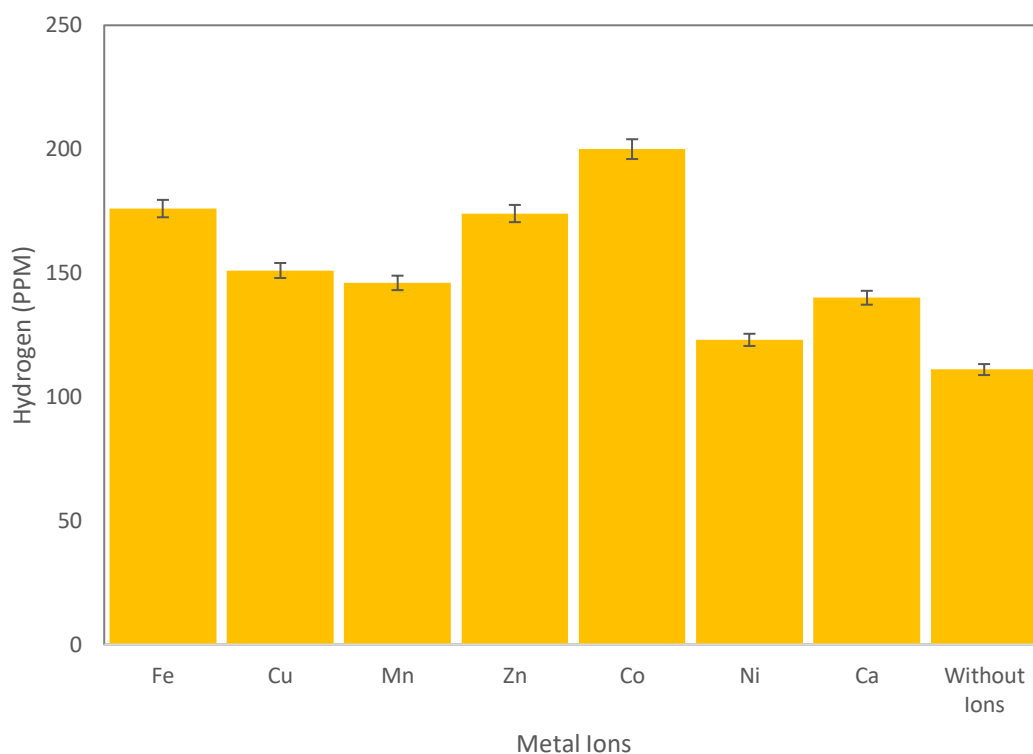
Figure 5.8: Cumulative hydrogen production by *Bacillus sp.* based on various micronutrients.

Additionally, a study revealed that the addition of 0.4g/L micronutrients increased the biological hydrogen yield from the dark fermentation process. However, excessive addition of micronutrients (>0.4g/L) may inhibit enzyme activity and reduce biological hydrogen production due to disruption of the microbial structure caused by excess contact between the nanoparticles and the cells [72]. Therefore, the concentration of cobalt (II) chloride hexahydrate should be investigated in co-culture hybrid fermentation to enhance biological hydrogen yield.

In Figure 5.9, pH trends with various metal ion additions are illustrated. After the introduction of micronutrients into the dark fermentation media, the initial pH of each condition was recorded and ranged from 6.39 to 6.46. The pH was periodically recorded up to 3 days of dark fermentation. A research study reported that metal ions play a significant role in substrate biodegradation, enhancing COD removal and substrate degradation in dark fermentation when introduced into the fermentation media [118]. For instance, Fe metal ions assist in the release of electrons during microbial conversion of sugar to molecular hydrogen, while Mg activates molecules to enter the acidogenic process [119]. The addition of Co, Fe, and Ni bind into the

active site of hydrogenase, promoting electron transfer to hydrogenase and ferredoxin. Ferredoxin acts as an important redox mediator, converting pyruvate into VFAs and CO2 due to its low reduction potential [72], [117], [120]. Thus, when metal ions are included in dark fermentation, a higher production rate of fermentative by-products can be obtained, regardless of biological hydrogen, VFAs, or CO_2. Consequently, a more acidic environment can be observed when metal ions are included in dark fermentation, as shown in Figure 5.9. Fermentation medium with the addition of manganese, iron, zinc, copper, cobalt, and calcium metal ions showed a final pH range of 5.54 to 5.72 acidic conditions. Compared to the fermentation media without metal ions (controlled condition), the final pH achieved was 5.84, the highest among all the pH trends. This condition can be explained by the higher metabolism rate in dark fermentation when micronutrients are introduced. Therefore, the higher the rate of organic bioconversion into VFAs by-products, the lower final pH value, leading to a more acidic fermentation media.
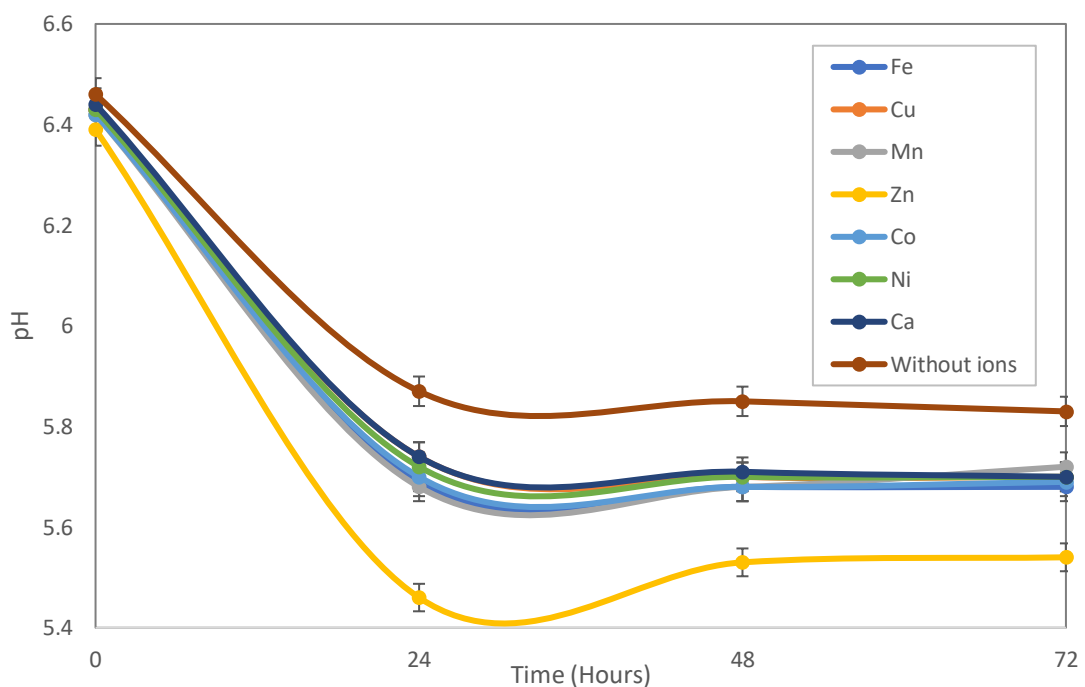
Figure 5.9: pH changes of *Bacillus sp.* based on various micronutrients.

Moreover, the effect of various metal ions on photo fermentation was also studied and the results are illustrated in the following section.

5.5 Effect of Various Micronutrients on Photo Fermentation

From the previous parametric study on types and concentration of feedstocks, photo fermentation showed optimum biological hydrogen production from 10g/L xylose concentration. In this study, photo fermentative *Cereibacter sp.* was experimented with various types of metal ions, 10g/L xylose concentration was added as the carbon source. The metal ions experimented are iron, zinc, copper, manganese, nickel, cobalt, and calcium. These transition metals are redox active, which may serve as a cofactor and provide a catalytic role in biological metabolism. The cumulative hydrogen production and pH changes among several metal ions and controlled condition (without ions) are compared.

Figure 5.10 illustrates the effect of metal ions on cumulative biological hydrogen yield by photo fermentation. The hydrogen production and pH changes were recorded periodically for *Cereibacter* sp. based on various micronutrients. The results are tabulated in Appendix 9, Appendix 10, Appendix 11, and Appendix 12. Figure 5.10 is showing that manganese ion is the optimal micronutrient for biological hydrogen evolution by *Cereibacter sp.*, with 159ppm biological hydrogen accumulated after 3 days of fermentation. Nickel and copper ions were found to be the second and third optimal metal ions for photo fermentative biological hydrogen production, with 149ppm and 144ppm biological hydrogen accumulated.
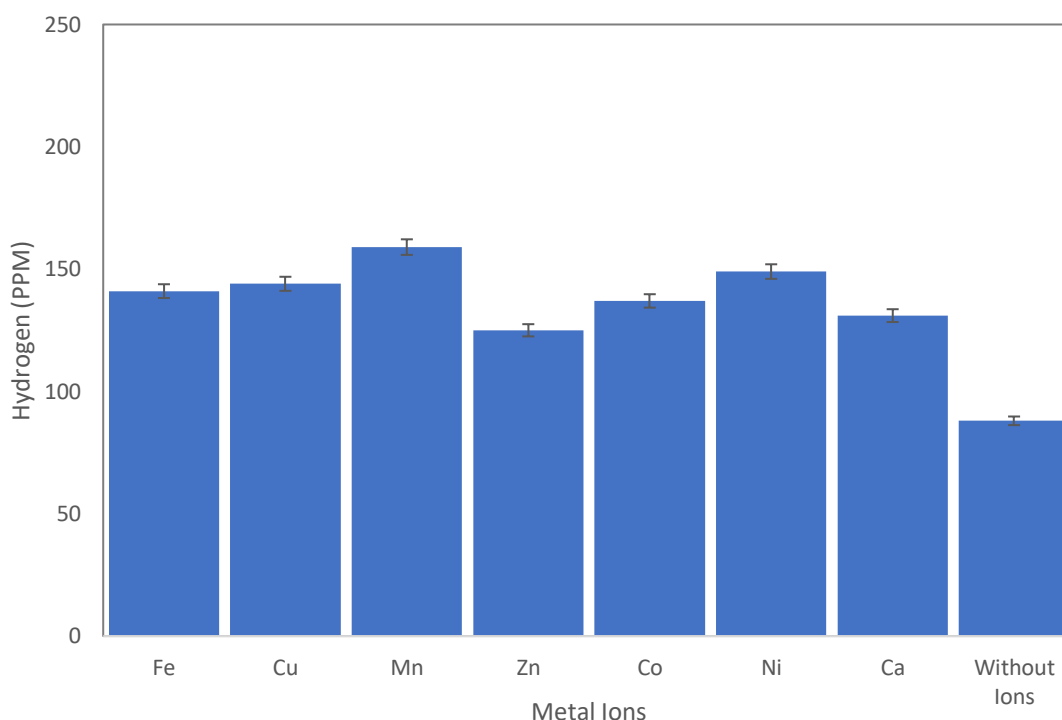
Figure 5.10: Cumulative hydrogen production by *Cereibacter sp.* based on various micronutrients.

During the anaerobic fermentation of bacteria, trace elements are vital for the synthesis of key enzymes and signal transduction. With an optimal concentration of metal ions added, nitrogenase activity can be stimulated, hence increasing hydrogen formation. A similar result was obtained when 50 μM concentration of Mn^{2+} was added. The highest biological hydrogen production by PNSB was observed, compared to other concentrations of Mn^{2+} addition [66]. Furthermore, another study reported that the addition of Zn^{2+} may affect intracellular enzyme synthesis, activity, and stability of mixed PNSB. The results showed that 2mg/L of Zn^{2+} had enhanced the substrate electrons' diversion by 26% towards hydrogen formation. A further increase in Zn^{2+} showed a negative effect on the hydrogen production metabolism of PNSB [121]. Al-Mohammedawi (2020) also revealed that the co-addition of Fe 80μM : Mo 8μM had enhanced biological hydrogen formation by 93% from PNSB. Further increase in micronutrients above the optimum concentration could lead to coagulation, which changes the surface charge distribution of the cells. A negative influence towards biological hydrogen evolution may occur [122].

To summarize, the biological hydrogen formation pathway by PNSB can be significantly affected by the types and concentration of metal ions. For *Cereibacter*

sp., it can be observed that manganese is the optimum for hydrogen formation metabolism. Nonetheless, the concentration of Mn^{2+} addition should be investigated again in hybrid fermentation to ensure the highest microbial activity for biological hydrogen generation. Furthermore, the pH changes were recorded when various micronutrients were experimented with in light fermentation. The initial pH of various photo fermentation mediums was studied and recorded after the addition of various micronutrients. The initial pH of various fermentation broths had a similar pH value, which ranged from 6.71 to 6.81 pH value. The pH was recorded periodically up to 3 days of photo fermentation.
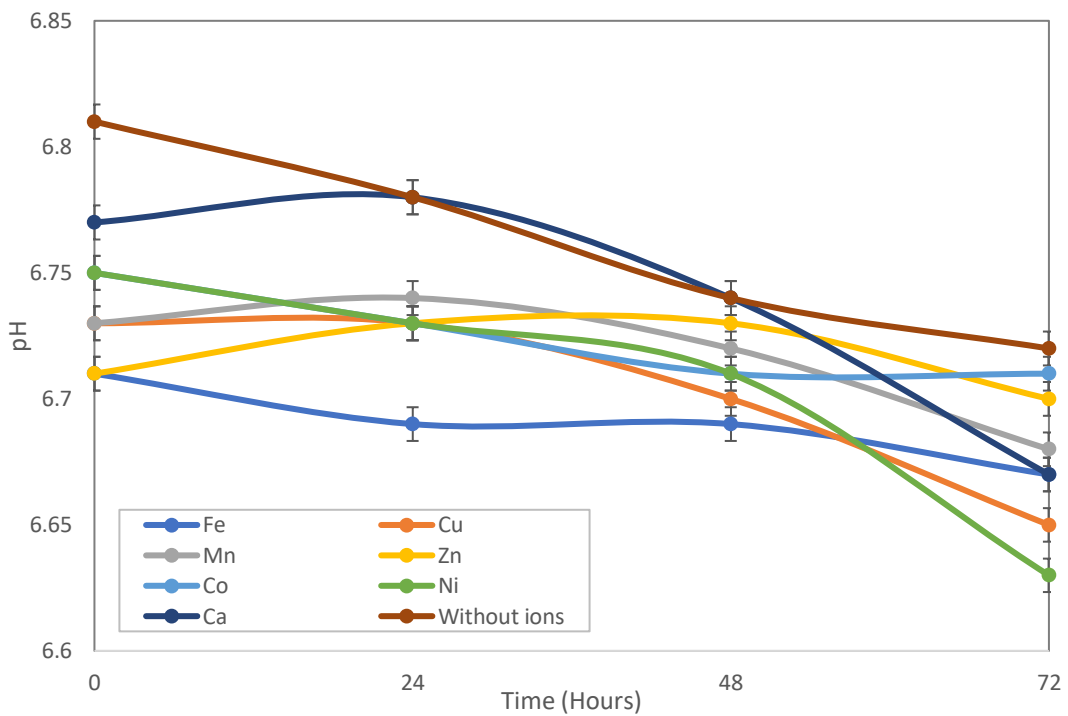
Figure 5.11: pH changes of *Cereibacter sp.* based on various micronutrients.

The addition of metal ions has been proven to activate various enzymes. For instance, a research study revealed that the addition of micronutrients enhanced the activity of PNSB, resulting in the production of higher acid by-products [123]. Thus, high acid formation rate may cause pH to decrease in a higher rate instead of PHB build-up that causes the pH to increase. Another study reported that the addition of activated carbon to PNSB mixture for light fermentation significantly increased the production of VFAs and ethanol by-products. Additionally, the hydrogen metabolism

pathway increased by 33.33% with the addition of micronutrients. This proves that the addition of micronutrients provides many fixed carriers for PNSB and buffers pH changes caused by VFAs accumulation in photo fermentative media [124]. Furthermore, the introduction of metal ions may improve COD removal by enhancing the energy metabolism pathway of PNSB, thus resulting in a higher rate of by-products in the light fermentation process [125]. Therefore, fermentation media with the introduction of metal ions showed a lower pH compared to the controlled condition (without metal ions), which may be due to the higher acid concentration formed and regulated by the micronutrients. After the parametric study on metal ions, the following section demonstrates the effect of inoculum concentration on biological hydrogen evolution by dark and photo fermentation

5.6 Effect of Microbes Concentration on Dark Fermentation

In the previous parametric study on carbon sources, it was found that a concentration of 17.5g/L xylose was optimal for *Bacillus sp.* to generate biological hydrogen through dark fermentation. In this study, the effect of various inoculum percentages on biological hydrogen production by dark fermentative *Bacillus sp.* was investigated, using a 17.5g/L xylose concentration. Inoculum concentration was varied from 2g/L to 10g/L, with intervals of 2g/L. The cumulative hydrogen production and pH changes were studied for a period of three days. The results are tabulated in Appendix 13, Appendix 14, Appendix 15, and Appendix 16.

The size of the bacterial inoculum is a critical parameter in liquid-culture fermentation research, as it can significantly affect culture parameters such as cell growth rate, substrate utilization, and culture morphology [126]. Figure 5.12 illustrates the effect of different inoculum sizes on the cumulative biological hydrogen yield. The results show that 2g/L inoculum size is optimal for biological hydrogen formation, with 158ppm generated. Furthermore, it can be observed from Figure 5.12 that lower inoculum sizes result in higher biological hydrogen production.
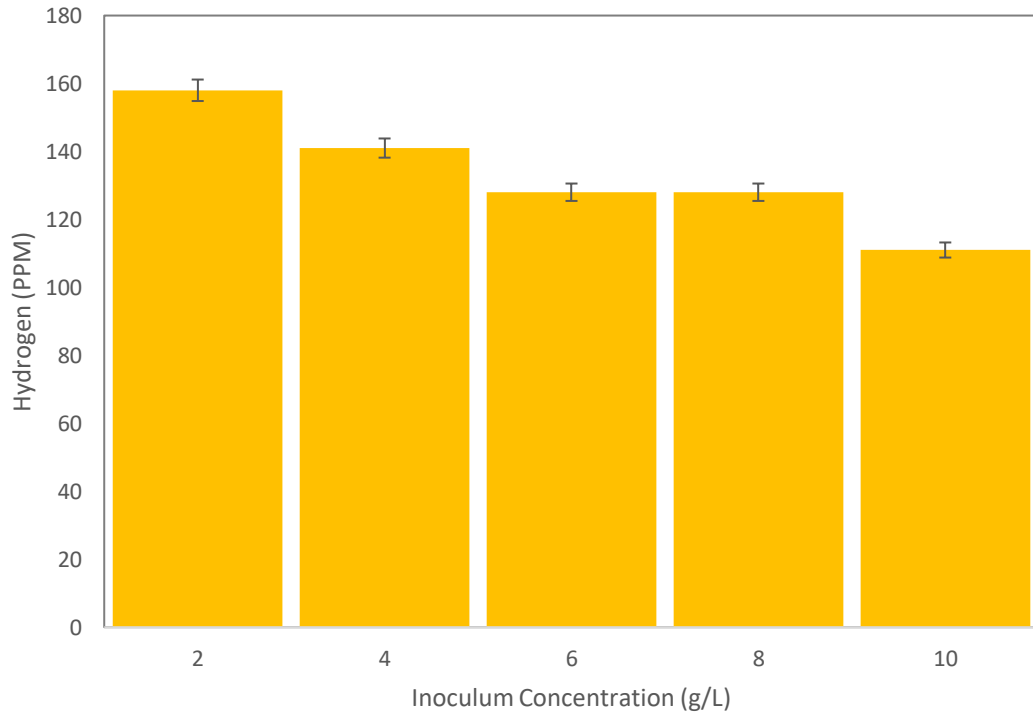
Figure 5.12: Cumulative hydrogen production by *Bacillus sp.* based on various size of inoculum.

A study has reported that optimal inoculum size can maximize biological hydrogen formation in a fermentation process. However, a further increase in initial inoculum concentration may result in low biological hydrogen yield due to the unavailability of insoluble substrates inside bacterial flocs [75]. Moreover, a higher inoculum size may result in a higher VFAs formation rate. The acidic conditions may inhibit the hydrogen-producing enzyme by *Bacillus sp.* and lower the hydrogen generation [60]. Furthermore, a higher biological hydrogen yield occurs when a lower inoculum size is introduced. This may be due to the quorum sensing system, which is related to bacterial community concentration [63]. The inter-species cell may send extracellular signalling molecules called autoinducers to increase their inter-species community size. The quorum sensing mechanism may regulate a higher rate of hydrogenase enzyme production. This may result in higher metabolism by hydrogenase to form biological hydrogen [64]. Hence, the lower the inoculum size, the higher the rate of quorum sensing and enzymes production, finally, the higher the biological hydrogen yield.

Additionally, Ulhiza et al. (2018) experimented with biological hydrogen yield from different yeast concentration, such as 1g/L, 5g/L, and 9g/L inoculum size. The

study revealed that biological hydrogen formation was the maximum when 5g/L inoculum concentration was utilized. The biological hydrogen yields were 38μmol, 52 μmol and 32 μmol for 1g/L, 5g/L, and 9g/L inoculum size, respectively [127]. The study has also reported that different strains may require a different inoculum size for optimal biological hydrogen yield. Hence, the inoculum concentration for *Bacillus* sp. should be investigated once again in hybrid fermentation to optimize biological hydrogen production.

The pH changes for various inoculum size were investigated and illustrated in Figure 5.13. Figure 5.13 shows the pH changes for dark fermentation up three days. Initially, the pH was recorded as 6.57, 6.55, 6.53, 6.51, and 6.46 for 2g/L, 4g/L, 6g/L, 8g/L, and 10g/L inoculum, respectively. The pH changes were recorded periodically up to 72 hours. Figure 5.13 shows that the higher the inoculum size, the more acidic or lower final pH achieved after fermentation.
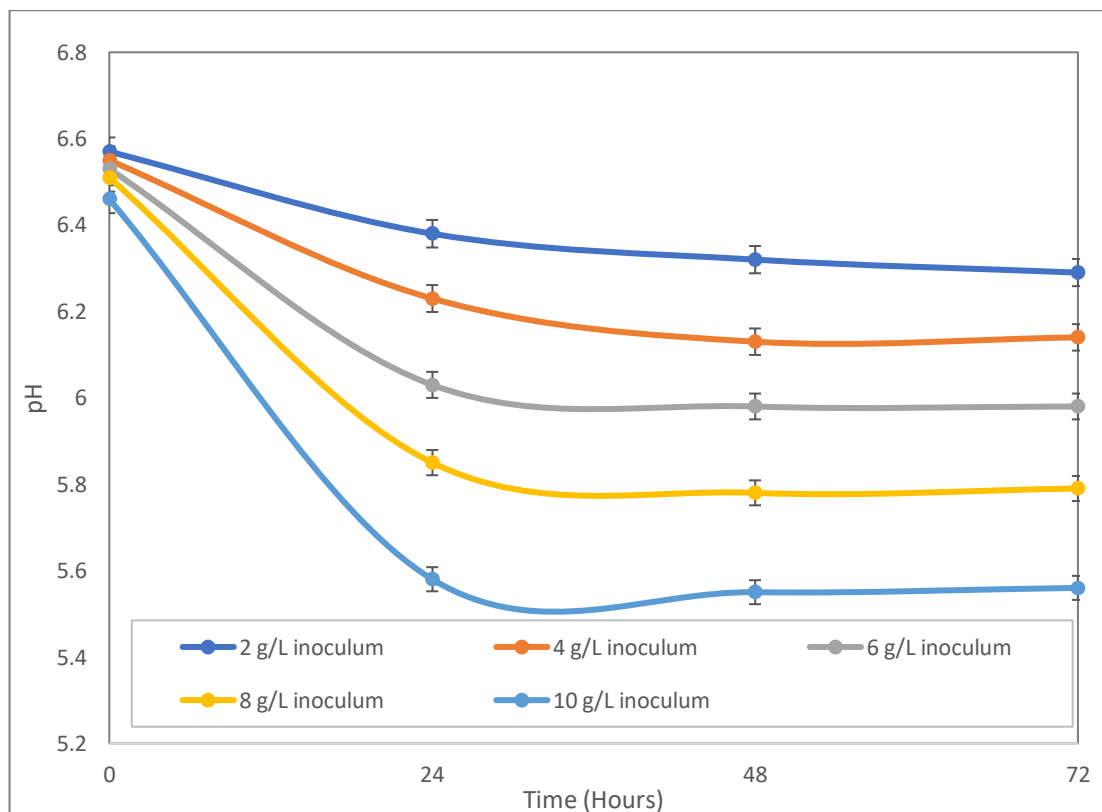
Figure 5.13: pH changes of *Bacillus sp.* based on various size of inoculum.

The inoculum concentration plays an important role in the production of lactic acid through fermentation. A study conducted by Wardani et al. (2017) investigated the effect of different inoculum concentrations on lactic acid fermentation using *L. plantarum* Dad 13. The results showed that the rate of acid production increased with an increase in the size of the inoculum. Low acid production at lower inoculum sizes was attributed to the low density of the starter culture [128]. A similar trend was observed in the case of *Lactobacillus casei,* where the rate of lactose utilization and acid formation increased with the increase in inoculum size up to 2g/L. However, further increases in inoculum concentration did not improve acid production from whey substrate. [129]. The pH of the final product was found to decrease with an increase in inoculum size due to higher acid concentrations, which could potentially affect the biological formation from the fermentation process. Additionally, in dark fermentative *Bacillus sp.*, higher concentrations could result in higher VFA accumulation and lower pH environment, leading to the inhibition of hydrogenase activity and reduced biological hydrogen production [60]. The effect of inoculum concentration on photo fermentation was also studied and will be discussed in the following section.

5.7 Effect of Microbes Concentration on Photo Fermentation

In this study, various types and concentrations of carbon sources were investigated for their effect on light fermentation. The optimal substrate concentration for photo fermentative *Cereibacter sp.* to produce biological hydrogen was found to be 10g/L xylose. Therefore, the study focused on investigating the effect of different inoculum sizes on biological hydrogen production using 10g/L xylose as the substrate. Inoculum sizes ranging from 2g/L to 10g/L concentration were tested, and the resulting trends in biological hydrogen production and pH were analyzed.

Figure 5.14 presents the outcomes of the study, showing the different biological hydrogen production rates obtained with varying inoculum sizes. The detailed results are tabulated in Appendix 13, Appendix 14, Appendix 15, and Appendix 16. The optimal biological hydrogen production rate of 147 ppm was achieved with a 4g/L inoculum size of *Cereibacter sp.* However, as the inoculum size increased above 4g/L, the cumulative hydrogen production rate decreased. Therefore,

the study concluded that a 4g/L inoculum size was optimal for light fermentative biological hydrogen production. Additionally, the figure suggests that a higher inoculum size results in lower biological hydrogen production rates.
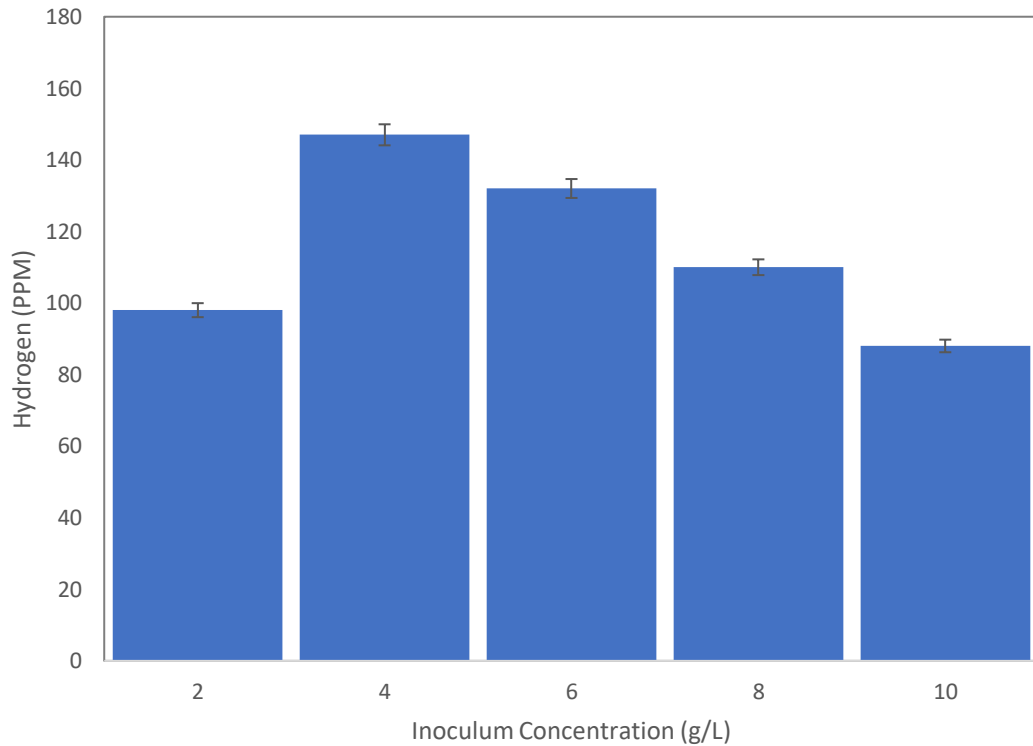
Figure 5.14: Cumulative hydrogen production by *Cereibacter sp.* based on various size of inoculum.

Low initial inoculum size may reduce biological hydrogen formation due to limited bio-catalyst concentration. However, further increase in initial inoculum concentration may result in a lower biological hydrogen yield due to the unavailability of insoluble substrates inside bacterial flocs [75]. Proper substrate and bacteria ratio should be considered to alleviate the inhibition of metabolites and substrates, hence improve microbial metabolism and increase hydrogen productivity [104]. Besides, lower biological hydrogen resulting from a lower inoculum size can be explained by the quorum sensing system related to the bacteria community concentration [63]. The interspecies bacteria may introduce extracellular signalling molecules called autoinducers to increase the interspecies community concentration. Nitrogenase enzyme production may be regulated, and hence higher biological hydrogen evolution [64]. In conclusion, a lower inoculum size resulted in a higher rate of quorum sensing and enzyme production, thereby increasing the rate of biological hydrogen production.

In addition, light can be captured by PNSB to perform complex biochemical reactions. From the reactions, it can synthesize intracellular molecules to sustain cell growth. Similar to biological hydrogen production, PNSB requires light to regulate the hydrogen metabolism pathway [130]. From the experimental study, it can be observed that the higher the inoculum size of PNSB, the more turbid the fermentation broth after 3 days of fermentation. Therefore, the light penetration into the fermentation media may be inhibited due to the high turbidity of higher dry cell weight. This may affect the metabolism of PNSB in biological hydrogen formation. Shui et al. (2022) investigated the effect of light perturbation on biological hydrogen evolution from PNSB. The parameters investigated were 4000 Lux, 5000 Lux, 6000 Lux, and 7000 Lux of light perturbation. The study revealed that the maximum hydrogen yield achieved was 124.3 mL H_2/g TS from 6000 Lux light perturbation, compared to 104 mL H_2/g TS without light perturbation. The biological hydrogen yield enhancement was 20% [131]. This may be due to the light perturbation, which made the light distributed uniformly in the fermentation reactor and increased the area of PNSB to receive light, thereby improving the rate of hydrogen production [132]. Therefore, a higher initial concentration of PNSB resulted in higher turbidity of fermentation broth. In consequence, light penetration into the photo fermentative media can be significantly affected, resulting in a lower biological hydrogen producing rate. The inoculum size of *Cereibacter sp.* in co-culture hybrid fermentation should be investigated to ensure optimal symbiotic effect with dark fermentative *Bacillus sp.* to generate biological hydrogen. The pH trends for photo fermentation based on various initial inoculum sizes were analyzed and illustrated in Figure 5.15.

The pH changes of photo fermentation were recorded periodically up to three days of fermentation. Initially, light fermentation pH was recorded as 6.59, 6.67, 6.71, 6.77, and 6.81 for 2g/L, 4g/L, 6g/L, 8g/L, and 10g/L inoculum sizes. Figure 5.15 illustrates that the higher the initial inoculum size, the greater the pH drop after three days of light fermentation.
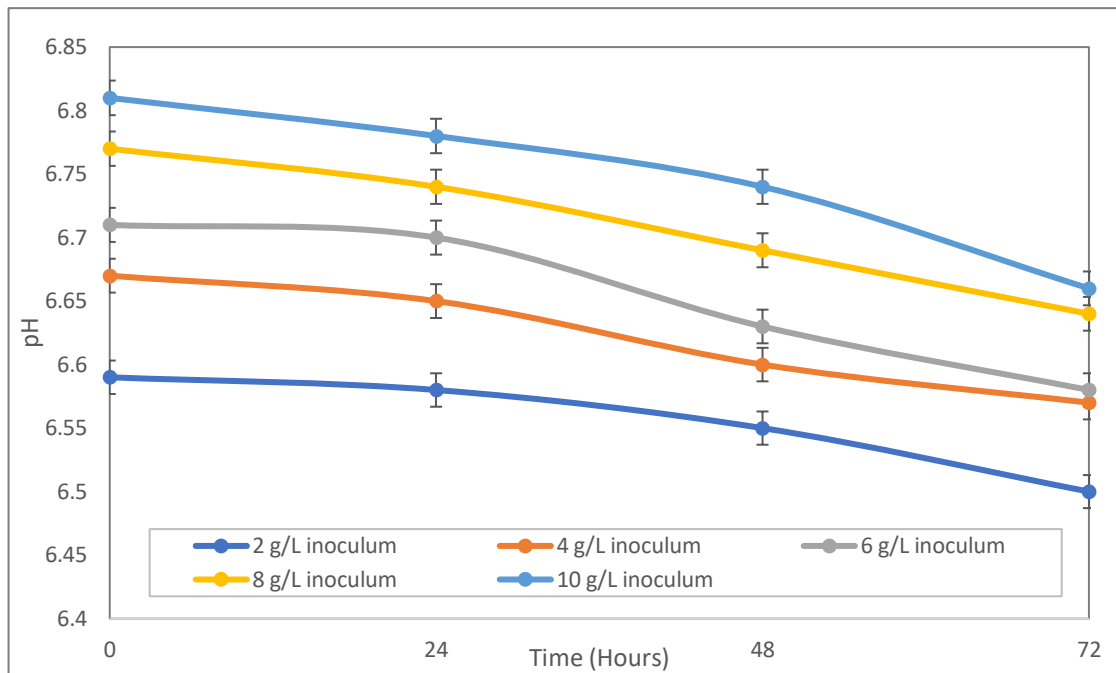
Figure 5.15: pH changes of *Cereibacter sp.* based on various size of inoculum.

The liquid metabolites in photo fermentation primarily consist of VFAs. After enzymatic hydrolysis releases sugar, it is further broken down into VFAs and utilized by PNSB to generate hydrogen molecules through nitrogenase activity and a supplied light source [133]. Compared to the pH trend of *Bacillus* sp., the pH is reducing at a slower rate due to the formation of PHB which will increase the pH [115]. Zhang et al. (2021) conducted an experiment on VFAs production from various inoculation volume ratios. According to the study, the total VFAs accumulation was maximum, around 3900 mg/L, with a high inoculation volume ratio. This can be explained by a high inoculation volume ratio, resulting in a lower consumption rate of VFAs than the PNSB formation rate, hence higher accumulation in VFAs [134]. With a lower initial inoculum size, the PNSB biomass formation rate is lower than the VFAs consumption rate, resulting in a lower concentration of VFAs at the end of fermentation. Therefore, a higher initial inoculum size may lead to a higher pH drop. For example, the pH drop for 10g/L inoculum size was 0.15, while that for a 2g/L inoculum was 0.09. The final pH values recorded were 6.50, 6.57, 6.58, 6.64, and 6.66 for 2g/L, 4g/L, 6g/L, 8g/L, and 10g/L inoculum sizes. Following the preliminary parametric study, the subsequent section showcases the outcomes for co-culture hybrid fermentation. Objective 2, which involves the parametric study of both dark and photo fermentation in mono-cultures, has been established up to this chapter.

CHAPTER 6: CO-CULTURE HYBRID FERMENTATION

6.1 Overview

In dark fermentation, organic substrates are decomposed to generate hydrogen, carbon dioxide, and VFAs. However, the organic feedstock is not fully utilized, and only a portion of the substrate is converted into biological hydrogen. As a consequence, the biological hydrogen yield from the dark fermentation process is relatively low [135], [136]. Previous studies have shown that the accumulation of VFAs could cause enzyme inhibition, leading to decreased hydrogen formation. Additionally, since the fermentation effluent contains a high concentration of VFAs, it must be treated before being released into the environment, as VFAs have negative impacts on our surroundings [137], [138]. To fully utilize the VFAs from the dark fermentation effluent, PNSB can be used for further hydrogen production through the light fermentation process. The VFAs produced from dark fermentation can be transformed into more hydrogen and increase the overall hydrogen yield, while simultaneously alleviating inhibition in both fermentation processes [139]–[141]. In our study, a single-stage co-culture hybrid fermentation (Figure 6.1(B)) was performed due to its less laborious and costly features [142]. The dark fermentation broth by *Bacillus sp.* was observed to be white (Figure 6.1(C)), while the photo fermentation by *Cereibacter sp.* shows red-coloured fermentation broth (Figure 6.1(A)). In the single-stage co-culture hybrid fermentation, the fermentation broth was observed to be yellowish/orange due to the growth and mixture of both microbes.

Figure 6.1: Comparison of light (A) and dark (C) fermentation with single stage hybrid fermentation (B).

The biological hydrogen yield from single stage co-culture hybrid fermentation was investigated. The ratio of dark and photo fermentative microbes, substrate concentration, types and amount of metal ions, pH, and temperature are chosen as the affecting variables towards hydrogen production from hybrid fermentation. Obtained results for hybrid fermentation will be demonstrated in the following section.

6.2 Optimization and Model Validation (Inoculum Ratio and Xylose Concentration)

It has been demonstrated that RSM (Respond Surface Methodology) under Design-Expert software (StatEase, Inc., USA) has optimized various fermentation processes. Several research studies have utilized RSM to optimize various bioprocesses to improve the production of targeted useful by-products, such as bioethanol, xylitol, pyruvic acid, and biological hydrogen production [143]–[145]. For the co-culture hybrid fermentation study, CCD (Central Composite Design) under RSM was used to optimize hydrogen production. From the preliminary stage of dark fermentation, the optimal conditions for biological hydrogen production were 17.5g/L xylose concentration and 2g/L inoculum size. For photo fermentation, the optimal conditions for biological hydrogen generation were 10g/L xylose concentration and 4g/L inoculum size. Therefore, for the hybrid fermentation study, parameters ranging from

0g/L to 17.5g/L xylose concentration, 0.1g/L to 2g/L *Bacillus* sp. inoculum size, and 0.1g/L to 4g/L *Cereibacter* sp. inoculum size were investigated. Twenty sets of experimental runs using RSM were performed to understand the effect of dark/light fermentative bacteria ratio and substrate concentration on biological hydrogen evolution from hybrid fermentation. The hydrogen production was recorded periodically and tabulated in Appendix 17. The independent variables are tabulated in Table 6.1:

Table 6.1: The Independent and Response Variables in Central Composite Design

Experiment Run	Substrate Concentration		*Cereibacter sp.* Inoculum		*Bacillus sp.* Inoculum	
	C	Code	B	Code	A	Code
1	0	-1	0.1	-1	0.1	-1
2	17.5	1	0.1	-1	0.1	-1
3	0	-1	4	1	0.1	-1
4	17.5	1	4	1	0.1	-1
5	0	-1	0.1	-1	2	1
6	17.5	1	0.1	-1	2	1
7	0	-1	4	1	2	1
8	17.5	1	4	1	2	1
9	0	-1	2.05	0	1.05	0
10	17.5	1	2.05	0	1.05	0
11	8.75	0	0.1	-1	1.05	0
12	8.75	0	4	1	1.05	0
13	8.75	0	2.05	0	0.1	-1
14	8.75	0	2.05	0	2	1
15	8.75	0	2.05	0	1.05	0
16	8.75	0	2.05	0	1.05	0
17	8.75	0	2.05	0	1.05	0
18	8.75	0	2.05	0	1.05	0
19	8.75	0	2.05	0	1.05	0
20	8.75	0	2.05	0	1.05	0

After obtaining the results for each experimental run, 3D contour plots were generated and illustrated in Figure 6.2. When examining the effect of biological

hydrogen yield versus various *Bacillus* sp. and *Cereibacter* sp. inoculum sizes, it was found that xylose concentration had a significant effect on hydrogen production from hybrid fermentation. Biological hydrogen formation was optimized when the initial xylose concentration was 17.5g/L. Some experimental runs without the addition of xylose resulted in unsatisfactory biological hydrogen yield. In microbial metabolic reactions, carbon sources are vital for cells to serve as substrates in metabolic networks. The supplied substrates may be decomposed to supply a pool of amino acids and other molecules to make up a cell, leading to a higher rate of by-product formation [146]. Therefore, the presence of xylose carbon source enhanced biological hydrogen production. The 3D contour plots indicate that the higher the xylose concentration, the higher the biological hydrogen yield. According to Figure 6.2, the optimal condition for co-culture hybrid fermentation hydrogen production is 17.5g/L xylose. Furthermore, the influence of dark and photo fermentative bacteria inoculum sizes on biological hydrogen yield was analyzed by RSM. The 3D contour plot in Figure 6.2(B) shows that the optimal inoculum concentrations for *Bacillus* sp. and *Cereibacter* sp. are 1g/L and 2g/L, respectively. The contour plot shifted upwards, which signifies the optimization of biological hydrogen generation when the A-axis (*Bacillus* sp.) and B-axis (*Cereibacter* sp.) are at 1 and 2, respectively, creating a dark-photo fermentative bacteria ratio of 1:2. Therefore, proper dark and photo fermentative bacteria inoculum can have a strong effect on biological hydrogen production in co-culture hybrid fermentation.
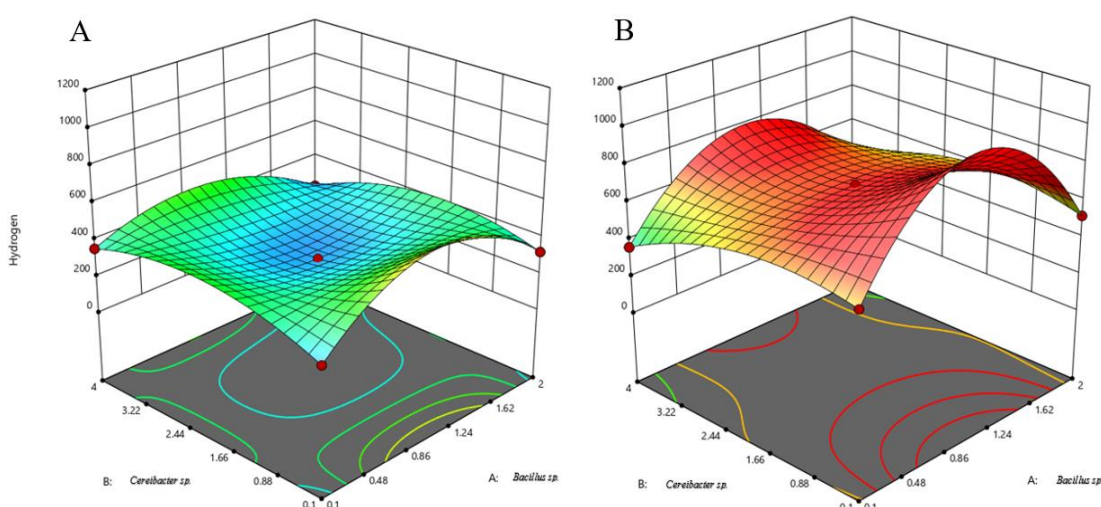
Figure 6.2: Three-dimensional contour plots for biological hydrogen yield (A) without xylose and (B) 17.5g/L xylose addition.

Several critical experimental runs were performed to determine the biological hydrogen yield, and the results were plotted in Figure 6.3 for comparison. Sets 8 and 10 utilized 17.5g/L xylose concentration for hybrid fermentation, while sets 11, 12, 14, and 15 used 8.75g/L xylose for hydrogen production. The main parameter that varied between these experimental runs was the inoculum ratio of *Bacillus* sp. and *Cereibacter* sp. From the comparisons between sets 11, 12, 14, and 15, it was found that a higher concentration of light fermentative bacteria led to a higher biological hydrogen yield. For instance, set 11 with a D/L ratio of 10/1 yielded an unsatisfactory cumulative hydrogen of 293 ppm, whereas set 12 with a D/L ratio of 1/4 yielded a hydrogen production of 434 ppm due to the high concentration of light fermentative bacteria. This may be due to the fact that the VFAs formed by *Bacillus* sp. were decomposed by the high concentration of *Cereibacter* sp. for further biological hydrogen evolution.
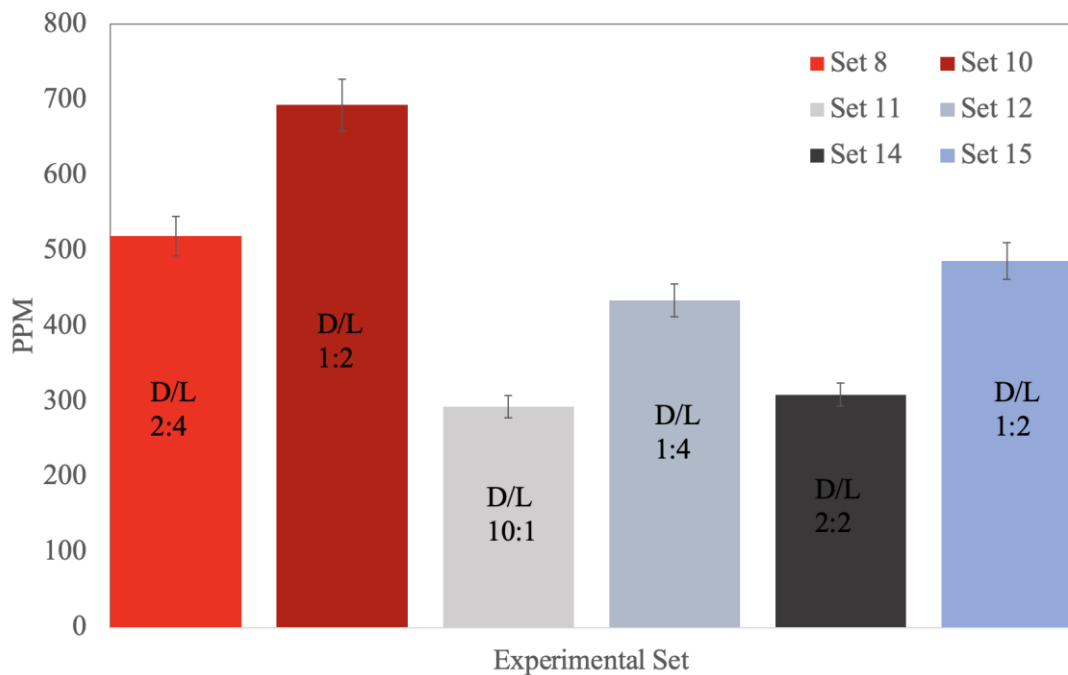
Figure 6.3: Comparison of biological hydrogen yield from several experimental runs (effect of D/L ratio and xylose concentration).

A pH study for each experimental set is presented in Figure 6.4. The pH changes for the 20 sets of experiment are tabulated in Appendix 17. Figure 6.4 shows that in set 11, the pH decreases linearly due to the accumulation of VFAs. However, an insufficient amount of light fermentative bacteria could not transform the VFAs

formed for hydrogen metabolism. In contrast, set 12 showed a sharp increase in pH after 48 hours of fermentation. This can be explained by the fact that there is sufficient inoculum of *Cereibacter* sp. that utilized VFAs from dark fermentation to form biological hydrogen. The metabolism may increase PHB formation which causes the pH to increase [115]. Furthermore, set 14 with an inoculum ratio of 1:1 between 2g/L *Cereibacter* sp. and 2g/L *Bacillus* sp. resulted in the accumulation of 309ppm of biological hydrogen. The biological hydrogen yield from an inoculum ratio of D/L=1/1 was relatively low, possibly due to the accumulation of VFAs in the medium, which inhibited hydrogen-producing enzyme activity [147]. As shown in Figure 6.4, the pH dropped significantly during the fermentation process. Several research studies have shown that the optimum dark/light bacteria ratio for enhanced biological hydrogen accumulation and hydrogen production rate is 1:2. This ratio balances the VFAs production rate from dark fermentation and VFAs consumption rate from photo fermentation. The presence of sufficient light fermentative bacteria, *Cereibacter* sp., can ferment VFAs metabolites produced from dark fermentation. Hence, VFAs accumulation can be avoided, and inhibition of hydrogenase and nitrogenase enzyme activity can also be alleviated [54], [147]. It can be observed that the pH changes for set 8, 10, and 15 fluctuate throughout the fermentation process. This indicates that there is some interaction between dark and photo fermentative bacteria [148]. The VFAs forming and consumption rate is balanced with a D/L ratio of 1:2. Thus, in this experimental work, it was observed that an inoculum ratio of D/L=1/2 was optimal in co-culture dark/light fermentation. Experimental sets 8, 10, and 15 showed high-yield biological hydrogen production with accumulated yields of 519ppm, 693ppm, and 486ppm, respectively. For set 10 and 15, xylose concentration had a significant effect on hydrogen formation, where set 10 (17.5g/L xylose) resulted in higher hydrogen accumulation than set 15 (8.75g/L xylose). The pH changes for set 10 in Figure 6.4 showed a deeper curve compared to set 15, which signifies that xylose concentration has a significant effect on the symbiotic relationship between *Bacillus* and *Cereibacter* species. However, for experimental sets 8 and 10, both with 17.5g/L xylose concentration, the biological hydrogen accumulation varied even with a D/L ratio of 1:2. The inoculum size may have a significant effect on biological hydrogen formation from co-culture hybrid fermentation. The inoculum size for set 8 was D/L of 4g/L:2g/L, where set 10 was D/L of 2g/L:1g/L. The lower inoculum size resulted in a higher accumulation of biological hydrogen. This situation can be explained by the quorum

sensing feature, where a higher rate of quorum sensing resulted in higher enzyme production during the bacteria's doubling mechanism. Thus, a higher rate of biological hydrogen production was achieved due to maximal enzyme activity [95]. Besides, the unusual trend of pH for set 8, 10, and 15 indicate the interaction of *Bacillus* and *Cereibacter* sp., where *Bacillus* sp. produce VFAs during the metabolism, followed by adaption of *Cereibacter* with the acidic environment, hence start using VFAs as the substrate in the metabolism.
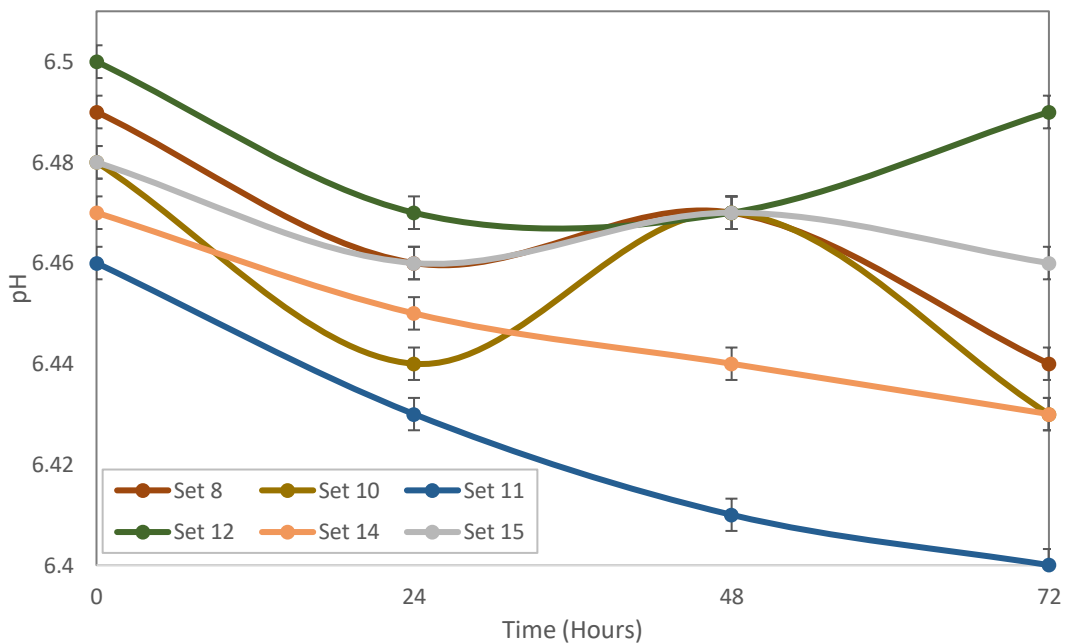
Figure 6.4: pH changes for various experimental set.

In the following section, the effect of initial pH was investigated for hybrid hydrogen fermentation.

6.3 Effect of Initial pH on Biological Hydrogen Production by Hybrid Fermentation

Based on previous findings, the optimum inoculum size for *Bacillus* sp. and *Cereibacter* sp. for hybrid fermentation is 1g/L and 2g/L, respectively. Therefore, a ratio of 1:2 dark/light fermentative bacteria is utilized for the initial pH parametric study. pH is one of the most important factors that manipulate anaerobic fermentation for biological hydrogen formation. Microorganisms can be categorized as acidophiles,

which have the best growth rate at pH < 5, neutrophiles that grow optimally at pH 5 to 9, and alkaliphiles that have optimal growth at pH > 9 [63]. This part of the experimental work aims to investigate the effect of the initial pH on co-culture biological hydrogen formation. The results are tabulated in Appendix 18 and presented in Figure 6.5. Moreover, xylose concentrations of 15g/L, 17.5g/L, and 20g/L were experimented with once again to ensure the optimal substrate concentration for co-culture hydrogen fermentation.

From Figure 6.5, it is shown that the optimal xylose concentration for biological hydrogen production from hybrid fermentation is 17.5g/L. As compared among 15g/L, 17.5g/L, and 20g/L xylose concentration, hydrogen production with 17.5g/L substrate concentration outperformed other conditions, regardless of any initial pH condition. This signifies that RSM contour plots from the previous study are reliable. Additionally, the most suitable initial pH for biological hydrogen accumulation was pH 8 for all concentrations of xylose.
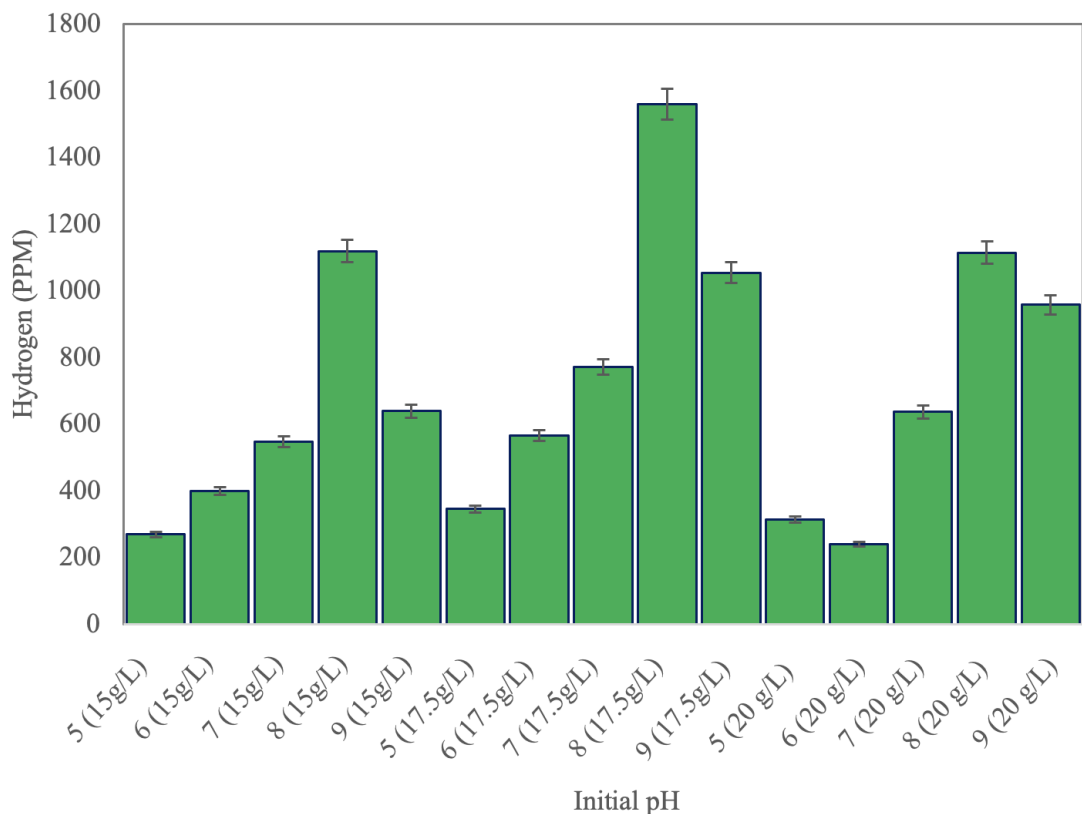
Figure 6.5: Cumulative biological hydrogen based on various initial pH.

Figure 6.6 illustrates the pH profile with the optimal substrate concentration (17.5g/L xylose concentration). Previous studies have shown that the optimal growth

condition for *Bacillus* sp. is a neutral pH of 7, while for PNSB *Cereibacter* sp., it is between 6.5 to 7.5 [149], [150]. With an initial pH of 8, the operating pH dropped to 7.23, which is close to neutral pH. This may be the reason why an initial pH of 8 is the most suitable for co-culture hybrid fermentation. The small pH changes during hybrid fermentation is due to the interaction of *Bacillus* and *Cereibacter* sp. in VFAs and PHB formation during their co-culture symbiotic effect. In an experimental research study, Zagrodnik (2015) investigated the effect of pH on co-culture hybrid fermentation for biological hydrogen production and found that the optimum biological hydrogen formation was obtained when the fermentation broth was controlled at a neutral pH (pH 7) [53]. Therefore, in the present hybrid fermentation, an initial pH of 8 is optimal for maximum hydrogenase and nitrogenase activity to produce biological hydrogen. Moreover, changes in pH in the fermentation environment could alter the shape of the enzyme's active site and affect the folding of the enzyme molecule. This situation could decrease the enzyme's ability to bind with the substrate and even inhibit its function as an enzyme [151]. Hence, an optimum pH is essential for the enzyme to reach its maximum activity.
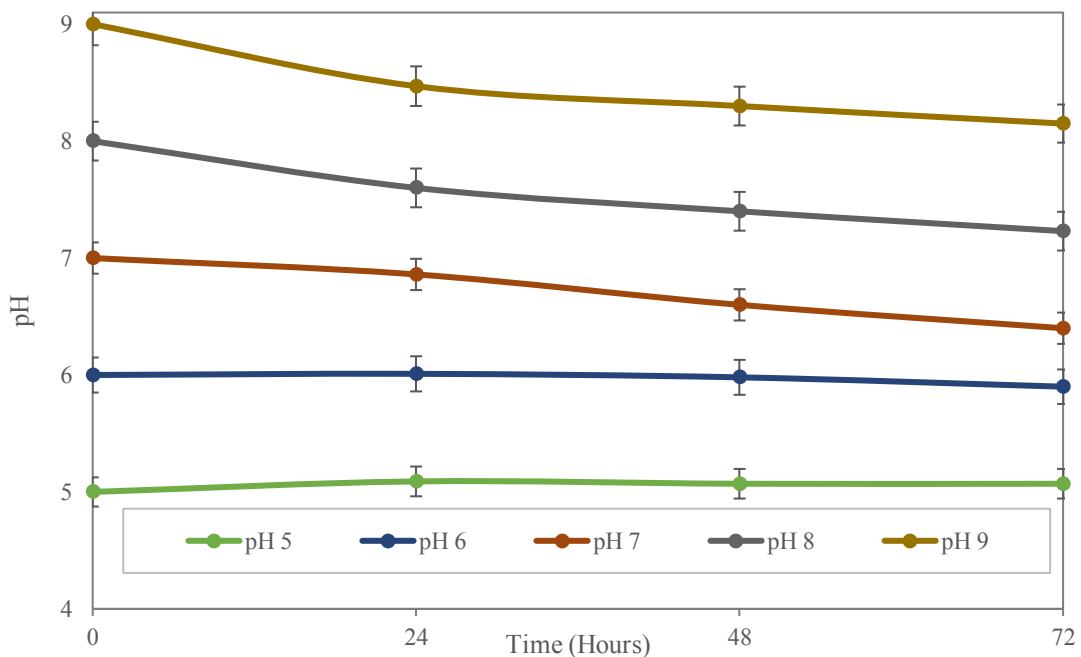
Figure 6.6: pH profile with various initial pH.

After investigating the effect of pH on hybrid fermentation, the following section demonstrates the effect of temperature on biological hydrogen production from hybrid fermentation.

6.4 Effect of Temperature on Biological Hydrogen Production by Hybrid Fermentation

Temperature is another important operating parameter that affects microbial activity and xylose hydrolysis. Microorganisms' adaptation to temperature can be differentiated into mesophilic (20-40°C), thermophilic (40-65°C), and extreme thermophilic (65-80°C) conditions [78]. It has been demonstrated a higher temperature could increase bacteria's ability to produce more hydrogen molecule from fermentation, provided with an appropriate range. However, studies have also found that at an extremely high temperature, bacteria's ability to produce biological hydrogen would decrease [152]–[154]. Consequently, the optimum temperature for co-culture hybrid fermentation to produce biological hydrogen needs to be investigated as there are two types of microbes in their symbiotic effect. Different microbes may prefer a different operating temperature for by-products formation from biodegradation.

Bacillus sp. and Cereibacter sp. are both mesophilic bacteria. Nevertheless, an investigation was carried out to study the growth of Bacillus sp. at various temperature. The study found that the critical temperature for Bacillus sp. is 53°C. Further increase in temperature may inhibit their culturability, hence cease the growth of Bacillus sp. [155]. For Cereibacter sp., biodegradation ability appears up to high temperatures of 50°C [156]. Thus, an elevation in temperature did not stop both bacteria in their hydrogen-forming metabolisms but increased their rate of reaction. The hydrogen production based on various temperature were recorded periodically, and the results are tabulated in Appendix 19 and presented in Figure 6.7. According to Figure 6.7, the optimum temperature for biological hydrogen production by both bacteria was 50°C, with biological hydrogen of 1330ppm accumulated. This may possibly be due to the rapid hydrogenase and nitrogenase activity to generate biological hydrogen at optimum temperature, which was 50°C. However, a high fermentation temperature may inhibit the microbial activity to produce biological hydrogen, as illustrated in Figure 6.7.
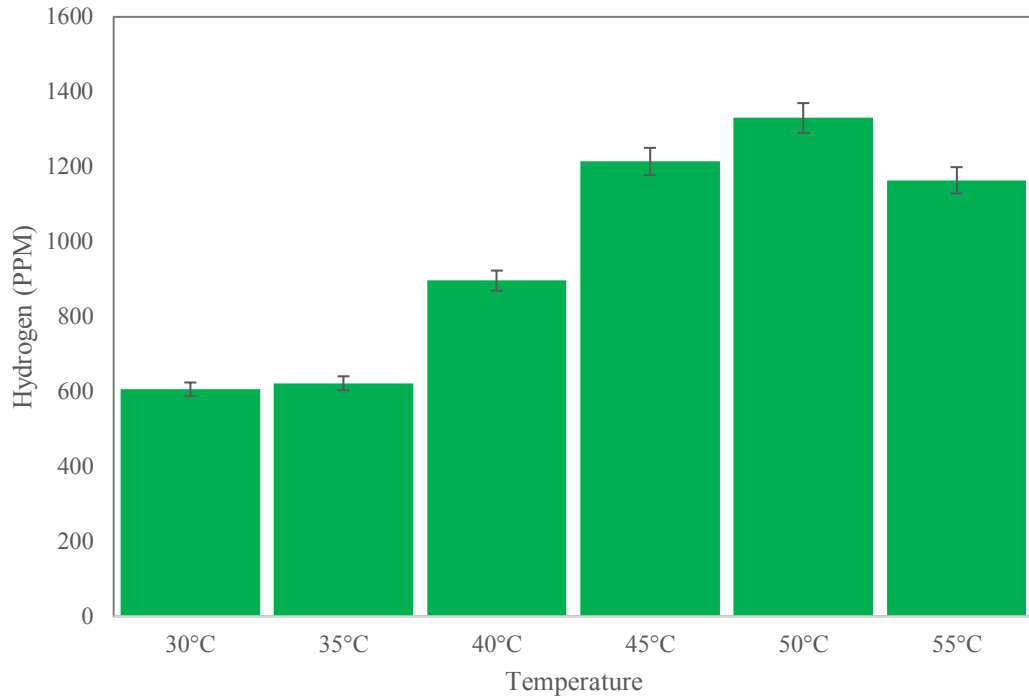
Figure 6.7: Cumulative biological hydrogen based on various operating temperature.

Jiang and Zhu (2021) reviewed the effect of mesophilic and thermophilic conditions on the fermentation of wheat starch for biological hydrogen production. They found that the maximum biological hydrogen production was achieved under thermophilic conditions, compared to mesophilic conditions, when anaerobic sludge was used as the inoculum. In addition, thermophilic conditions were also preferred for fermenting a cheese whey powder solution during dark fermentation, with a maximum hydrogen yield of 111 mL hydrogen/g total sugar achieved [78]. This is because the active microbial activity, along with rapid decomposition of organic matter, during thermophilic conditions is ideal for biological hydrogen fermentation. Furthermore, thermophilic conditions result in a higher gas production rate and shorter retention time during fermentation, which is suitable for biogas generation [157]. Figure 6.8 shows the biological hydrogen profile for each operating temperature.

Xiao et al. (2013) conducted experiments to study the effect of temperature on hydrogen-producing enzymes. The authors found that with increasing temperature, the activity of the hydrogen-generating enzyme increased rapidly and then decreased over time. The higher the temperature, the faster the rate at which the highest hydrogen level was reached. However, they also reported that when the operating temperature

was controlled at 37°C, the cumulative biological hydrogen yield was at its maximum at the end of fermentation [158]. In our experimental study, the optimal cumulative hydrogen yield from hybrid fermentation was achieved at 50°C after 72 hours. However, in Figure 6.8, the slope (m) for 50°C is 1/2, indicating that hydrogen production is reaching the stationary phase. On the other hand, for the operating temperature of 35°C, the slope (m) is 1, which shows that rapid hydrogen formation from hybrid fermentation is still ongoing. Overall, the optimal hydrogen production from 35°C might be achieved after a longer period of co-culture biodegradation. Nonetheless, thermophilic conditions are still preferred if the fermentation period is limited, as they result in higher yields of biogas production in a shorter retention time [157].
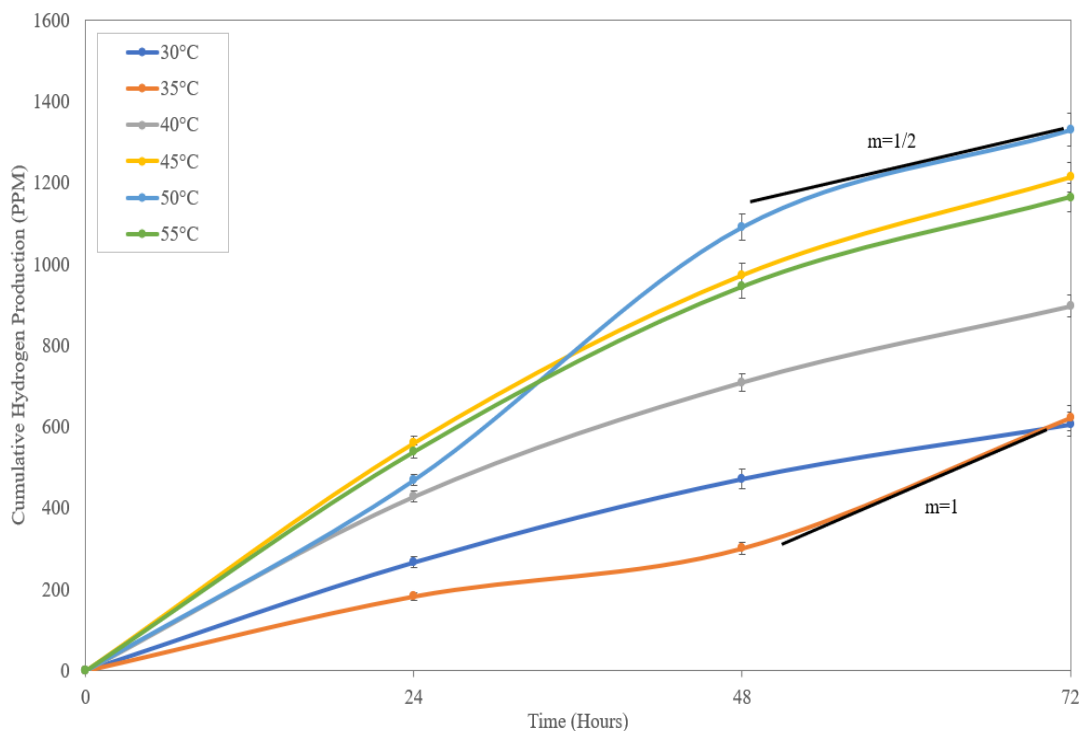
Figure 6.8: Biological hydrogen profile from various operating temperature.

Therefore, the optimum temperature for the hybrid fermentation by *Bacillus sp.* and *Cereibacter sp.* to produce biological hydrogen with a shorter retention time is 50°C. Further investigation into the effect of micronutrients, including Co^{2+} and Mn^{2+}, on hydrogen fermentation was conducted and the results will be demonstrated in the next section.

6.5 Effect of Metal Ion Concentration on Biological Hydrogen Production by Hybrid Fermentation

The aforementioned parametric study on various micronutrients found that 50μM of Co^{2+} and Mn^{2+} were optimal for dark and light fermentations, respectively. However, the concentration of each metal ion should be investigated again for hybrid fermentation, as variations in concentration could significantly affect co-culture hybrid fermentation. Thus, the concentration of Co^{2+} and Mn^{2+} was investigated to optimize biological hydrogen production by hybrid fermentation. The results are tabulated in Appendix 20.

As shown in Figure 6.9, the addition of metal ions significantly improved biological hydrogen production from co-culture fermentation. The optimal concentrations for hybrid fermentative hydrogen formation were 20μM of both Co^{2+} and Mn^{2+} ions. The addition of metal ions may be reduced by the organic compound, thereby creating electron transfer that leads to biological hydrogen formation [117]. Moreover, the facilitated electron transfer may improve the synthesis of hydrogenase and nitrogenase enzymes, as well as signal transduction, leading to improved biological hydrogen production from hybrid fermentation [65], [66]. However, increasing the concentration of metal ions further may inhibit microbial activity, leading to a decrease in biological hydrogen production. For instance, 100μM of Mn^{2+} resulted in an unsatisfactory biological hydrogen yield of 324ppm, which is lower than that of the fermentation broth without the addition of Mn^{2+}, which generated 439ppm. This occurred because excess metal ions may create a toxic environment, inducing efflux and storage [159].
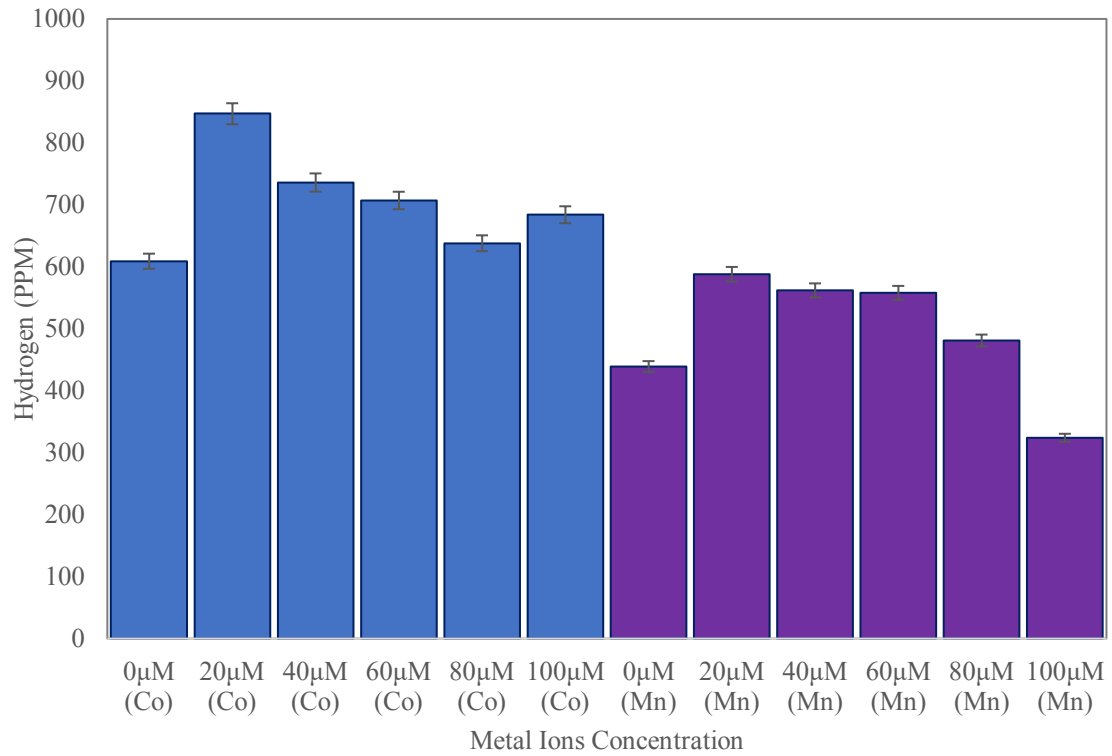
Figure 6.9: Cumulative biological hydrogen based on various Co^{2+} and Mn^{2+} concentration.

Furthermore, the ratio of Co^{2+} and Mn^{2+} ions should also be investigated if both ions are required in hybrid fermentation. To do that, RSM software will be utilized in the following optimization process to investigate the optimum ratio and concentration of Co^{2+} and Mn^{2+} in co-culture hybrid fermentation. Besides, parameters such as initial pH and temperature will be included in RSM parameters to investigate the biological hydrogen yield.

6.6 Optimization and Model Validation (Initial pH, Temperature, and Metal Ions Concentration)

Microbial consortia offer significant advantages over pure cultures in terms of producing hydrogen by-products. This is because microbial consortia have a wider variety of genes and a more diverse metabolism, which allows them to utilize less substrate during their metabolic pathways. Additionally, the diverse array of cells in microbial consortia can coordinate their specific tasks by exchanging signals or trading metabolites [160], [161]. Therefore, co-culture hybrid fermentation using *Bacillus* sp. and *Cereibacter* sp. is preferred for biological hydrogen production.

In a previous co-culture fermentation study, the optimal bacteria ratio and concentration of xylose were investigated as D/L=1:2 and 17.5g/L, respectively, using RSM analysis. A further parametric study found that the optimal initial pH ranged between 7 and 9, and the optimal operating temperature ranged between 45°C and 50°C. Furthermore, the best performing metal ions for hybrid fermentation were found to be Co^{2+} and Mn^{2+}, with concentrations ranging from 0μM to 20μM. In this part of the study, RSM will be used again to find the optimum conditions for co-culture biological hydrogen fermentation. Therefore, the independent variables that will be investigated are pH between 7 and 9, temperature between 45°C and 50°C, and 0μM to 20μM of Co^{2+} and Mn^{2+} concentration. Table 6.2 shows the operating parameters from each experimental run:

Table 6.2: The Independent Variables and Responding Variable for Hybrid Fermentation

Experiment Run	Co^{2+} Concentration (μM)		Mn^{2+} Concentration (μM)		Temperature (°C)		pH	
	A	Code	B	Code	C	Code	D	Code
1	0	-1	0	-1	45	-1	7	-1
2	20	1	0	-1	45	-1	7	-1
3	0	-1	20	1	45	-1	7	-1
4	20	1	20	1	45	-1	7	-1
5	0	-1	0	-1	50	1	7	-1
6	20	1	0	-1	50	1	7	-1
7	0	-1	20	1	50	1	7	-1
8	20	1	20	1	50	1	7	-1
9	0	-1	0	-1	45	-1	9	1
10	20	1	0	-1	45	-1	9	1
11	0	-1	20	1	45	-1	9	1
12	20	1	20	1	45	-1	9	1
13	0	-1	0	-1	50	1	9	1
14	20	1	0	-1	50	1	9	1
15	0	-1	20	1	50	1	9	1
16	20	1	20	1	50	1	9	1
17	0	-1	10	0	47.5	0	8	0

18	20	1	10	0	47.5	0	8	0
19	10	0	0	-1	47.5	0	8	0
20	10	0	20	1	47.5	0	8	0
21	10	0	10	0	45	0	8	0
22	10	0	10	0	50	0	8	0
23	10	0	10	0	47.5	0	7	-1
24	10	0	10	0	47.5	0	9	1
25	10	0	10	0	47.5	0	8	0
26	10	0	10	0	47.5	0	8	0
27	10	0	10	0	47.5	0	8	0
28	10	0	10	0	47.5	0	8	0
29	10	0	10	0	47.5	0	8	0
30	10	0	10	0	47.5	0	8	0

30 sets of experimental runs were generated using Design-Expert software. After obtaining the results for each experiment, 3D contour plots were generated and are illustrated in Figure 6.10. The results are tabulated in Appendix 21. The plots form Figure 6.10 depict the effect of temperature, initial pH, and metal ion concentration on biological hydrogen production. After RSM analysis, the optimal temperature for hybrid fermentation to produce biological hydrogen was found to be 50°C, and the optimal initial pH was 9. In addition, the optimal concentration of Co^{2+} metal ions was found to be 20μM, while the optimal concentration of Mn^{2+} metal ions was found to be 0μM.
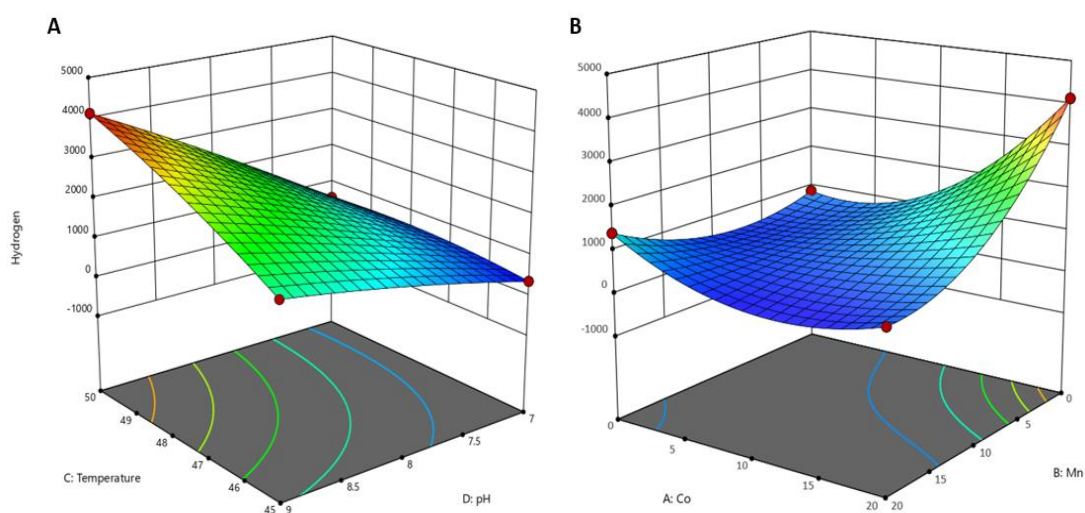
Figure 6.10: Three-dimensional contour plots for biological hydrogen yield (A) Temperature and Initial pH and (B) Co^{2+} and Mn^{2+} concentration.

A few critical experimental sets were selected for comparison, and the cumulative biological hydrogen yield for each set is illustrated in Figure 6.11. For experimental sets 2 and 6, the operating parameters were similar, except for the operating temperature. Both sets utilized an initial pH of 7 and 20μM of Co^{2+} metal ions. However, the biological hydrogen yield for set 6 was higher compared to set 2, with hydrogen accumulation of 574ppm compared to 228ppm. The situation can be explained by the different operating temperatures utilized for each experimental set. The elevated temperature seems to have triggered enzymatic activity, resulting in a higher volume of biological hydrogen production [162].

In addition, for experimental sets 13, 14, and 15, operating parameters such as a temperature of 50°C and an initial pH of 9 were utilized. The only difference for these sets was the different ratio of metal ions was investigated. For instance, experimental set 13 fermented xylose without the addition of any metal ions, while set 14 and set 15 utilized 20μM of Co^{2+} and Mn^{2+}, respectively. The biological hydrogen accumulations from sets 13, 14, and 15 were 961ppm, 4127ppm, and 1271ppm, respectively. After the comparison of sets 13, 14, and 15, it was found that the introduction of Co^{2+} to hybrid fermentation had enhanced biological hydrogen production. Inclusion of Mn^{2+} metal ions appeared to inhibit hydrogen production, resulting in a lower hydrogen yield compared to the fermentation broth with Co^{2+}.

Thus, the RSM analysis revealed that Co^{2+} and Mn^{2+} could not coexist simultaneously in hybrid fermentation. 20µM of Co^{2+} was found to be the optimum concentration for *Bacillus sp.* and *Cereibacter sp.* co-culture hybrid fermentation.
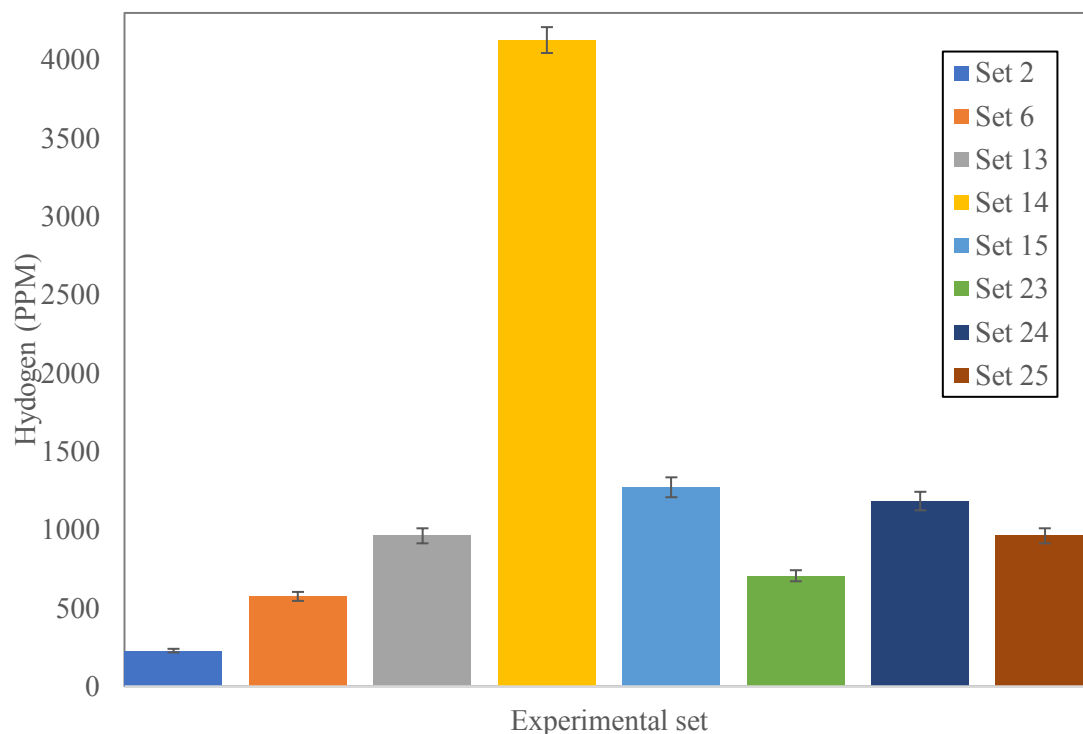
Figure 6.11: Comparison of biological hydrogen yield from several experimental runs (effect of pH, temperature, and metal ions).

Another comparison was made between experimental sets 23, 24 and 25. The operating temperature (45°C) and ratio of metal ions were similar for all three experimental sets. However, the initial pH was 7, 8, and 9 for experimental sets 23, 25, and 24, respectively. Figure 6.12 shows the pH profile for each experimental set. Research has reported that with higher temperature introduced to the fermentation process, the rate of by-products formation is higher. For instance, the formation rate of volatile fatty acids and ethanol will be enhanced [163]. Thus, when compared to the previous pH study, with elevated temperature for hybrid fermentation, the pH dropped significantly faster. Figure 6.12 shows that with an initial pH of 9 (set 24), the final pH dropped to 7.27, which is close to neutral. For sets 23 and 25, the final pH dropped to 6.3 and 6.62, respectively, which is slightly acidic compared to experimental set 24. The neutral pH may be optimum for biological hydrogen evolution from hybrid fermentation as proven in the previous study. Moreover, high temperature may trigger

a higher rate of bacterial metabolism. As a consequence, initial pH 9 was found to be the optimum when paired with high temperature fermentation.
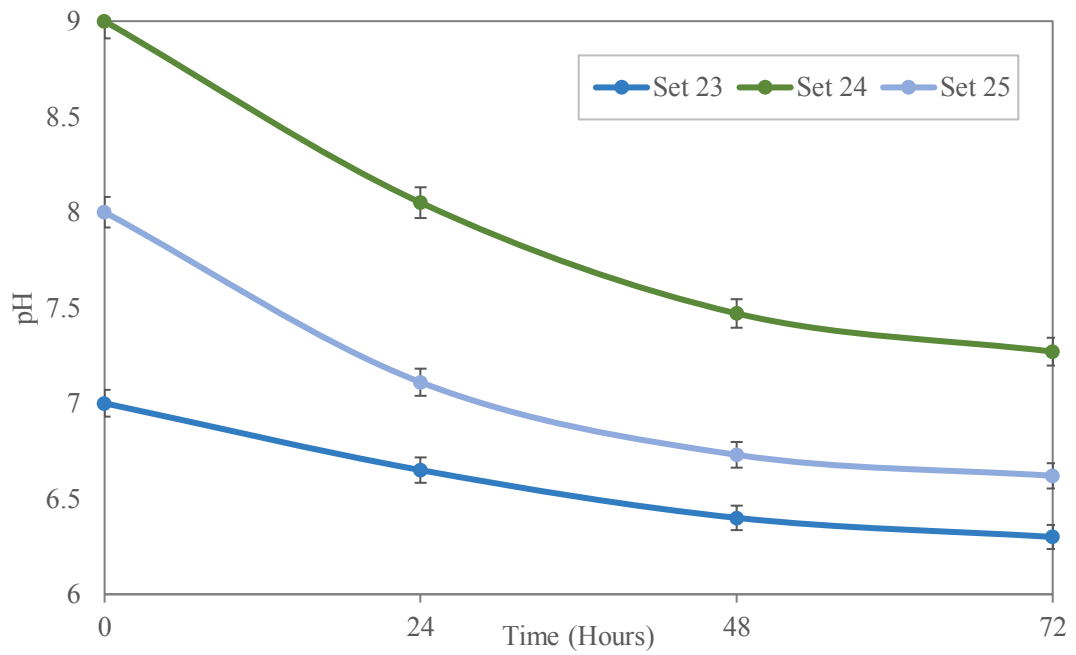
Figure 6.12: pH profile for various experimental set.

Finally, after obtaining the optimal conditions for co-culture hydrogen fermentation, the biological hydrogen production was up scaled to a 200mL conical flask and 2L bioreactor. Biological hydrogen yield was investigated for 96 hours and compared with dark or light fermentation individually.

CHAPTER 7: CO-CULTURE HYBRID FERMENTATION WITH OPTIMIZED OPERATING CONDITIONS

7.1 Overview

This chapter focuses on augmenting biological hydrogen production through dark-light hybrid fermentation. Previous research has shown that hybrid biodegradation can enhance biological hydrogen yield and substrate conversion efficiencies. Furthermore, single stage integration has been found to be more cost-effective than multi-stage hybrid fermentation [164]. Therefore, this study will upscale the single-stage hybrid fermentation process to a 200mL conical flask and 2L bioreactor for hydrogen evolution.

7.2 200mL Hybrid Fermentation in Optimized Conditions

The parametric study and RSM analysis have reported that the optimum conditions for hybrid fermentation to generate biological hydrogen are a 17.5g/L xylose concentration, 1g/L and 2g/L dark and light fermentative inoculum respectively, an initial pH of 9, an operating temperature of 50°C, and the addition of 20μM of Co^{2+}. After determining these optimal conditions, the experiment was upscaled to a 200mL conical flask to produce biological hydrogen. Liquid samples were collected and analyzed periodically every four hours for four days. Detailed results are tabulated in Appendix 22. Figure 7.1 illustrates that rapid biological hydrogen production occurs throughout the fermentation process.
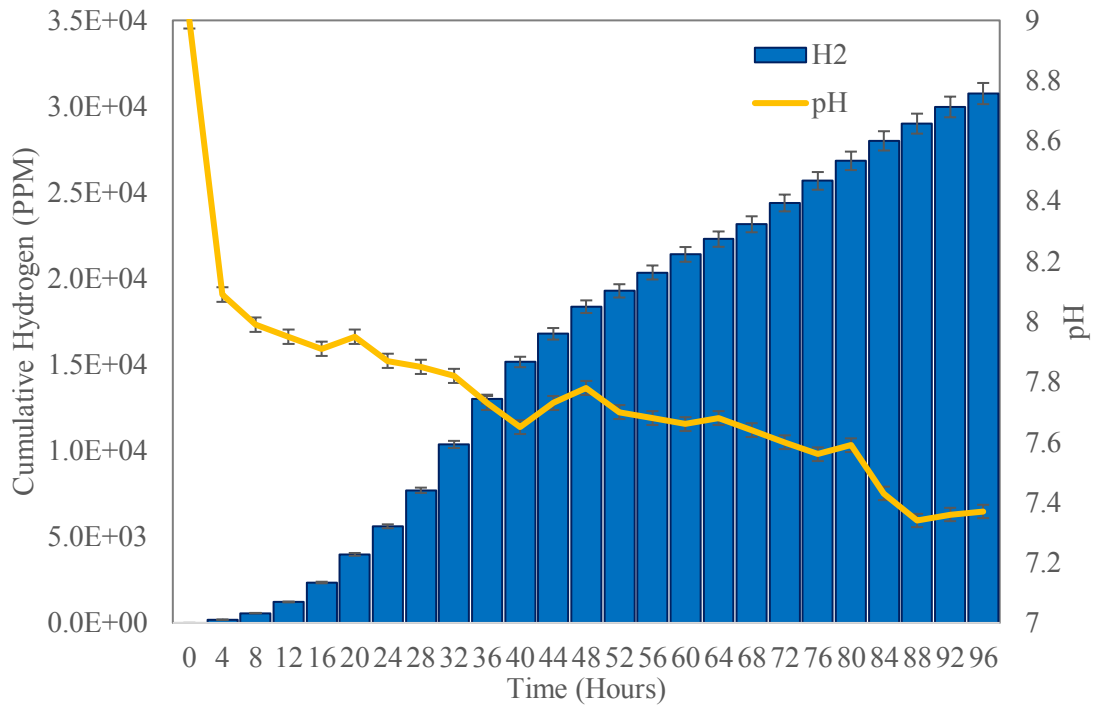
Figure 7.1: Optimized hybrid fermentation for biological hydrogen production in a 200mL conical flask.

Rapid biological hydrogen production occurred during the first 24 hours of single strain dark and light fermentation, followed by a decline, resulting in unsatisfactory biological hydrogen accumulation. However, after 96 hours of co-culture hybrid fermentation, the accumulated biological hydrogen yield was 30749 ppm, which was significantly higher than the yield of 4668 ppm and 2564 ppm obtained from single strain dark and light fermentation with 10g/L inoculum concentration, respectively. The biological hydrogen yield was enhanced by 658% and 1199%, respectively, compared to co-culture fermentation. Under more optimum conditions for single strain dark and light fermentation, inoculating *Bacillus* sp. and *Cereibacter* sp. with 1g/L inoculum concentration resulted in yields of 5739 ppm and 3654 ppm, respectively. This represents an enhancement of 535% and 842% compared to dark and light fermentation, respectively. In conclusion, the co-culture symbiotic effect and the optimum conditions experimented with have significantly enhanced biological hydrogen production, outperforming single strain dark and light fermentation. Furthermore, the final pH was recorded as 7.37, which is neutral and suitable for *Bacillus* sp. and *Cereibacter* sp. in hydrogen generating metabolism. The initial pH of 9 dropped to neutral when VFAs produced were accumulated in the fermentation broth. Coupling of dark and light fermentation could improve biological

100

hydrogen production yield while simultaneously increasing organic COD removal. Theoretically, it is possible to recover a higher volume of hydrogen atoms from xylose as gas through hybrid fermentation [165]. Dissolved hydrogen and oxidation reduction potential (ORP) were analyzed throughout the hybrid fermentation process.

ORP, also known as redox potential, is a dynamic process parameter that tracks microorganism metabolism in fermentation. It measures a substance's ability to oxidize or reduce other substances. ORP indicates the anaerobic degree of the fermentation broth. Bioprocess metabolism strongly depends on the oxidation or reduction state in fermentation media. High ORP or positive ORP values are preferred by aerobic microorganisms, while strict anaerobes prefer low negative ORP values in their metabolic pathways [166]. *Bacillus* sp. and *Cereibacter* sp. are both facultative anaerobic bacterium [167], [168]. These bacteria can adjust their metabolism according to the ORP state. Hydrogen production from organic biodegradation occurs under anaerobic conditions, with negative ORP values. Thus, regardless of single strain or co-culture hydrogen fermentation, an ORP value below 0 is preferred. As shown in Figure 7.2, the initial ORP value was recorded as 0 mV during the initial state of fermentation, then sharply decreased to -61 mV. After 12 hours of fermentation, the ORP values fluctuated between -20 mV and -52 mV. An experimental work was carried out to study the ORP and hydrogen production rate in fed-batch light fermentation. The authors revealed that after 72 hours of light fermentation, fresh acid medium was fed into the fermentation broth, resulting in an ORP value drop and promoting hydrogen production rate [166]. The fluctuating ORP value can be explained by the interaction of dark and light fermentative bacteria in co-culture biodegradation. The sharp decrease in ORP value indicates that *Bacillus* sp. may produce VFAs and accumulate them in the fermentation broth. The explanation can also be proven by the decreasing pH in Figure 7.1. After the rapid VFAs production by *Bacillus* sp., *Cereibacter* sp. may adapt to the acidic environment and start utilizing VFAs as the substrate for hydrogen conversion. The VFAs consumption by light fermentation may result in lower VFAs accumulation and higher hydrogen accumulation, thus increasing the ORP value. Besides, after the sharp decrease in pH from 0 to 4th hours of fermentation, the pH value dropped linearly after that. *Cereibacter* sp. had effectively consumed the VFAs, thus maintaining the pH profile at a linear rate. As a consequence, the ORP values fluctuated between -20 mV and -52

mV, indicating the VFAs production and consumption between dark and light fermentative metabolism. Furthermore, dissolved hydrogen was analyzed together with ORP value. Figure 7.2 shows that ORP value reflected dissolved hydrogen (ppb) in hybrid fermentation broth. It can be observed that the lower the ORP value, the higher the dissolved hydrogen in fermentation media.
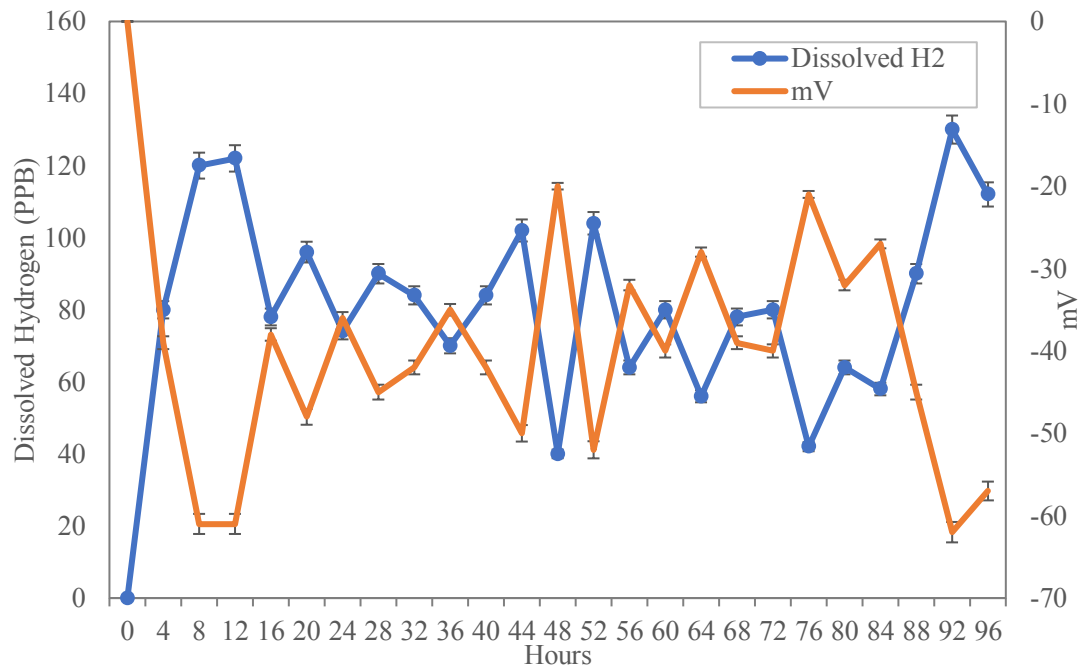
Figure 7.2: ORP and dissolved oxygen in 200mL hybrid fermentation.

A study was conducted to investigate hydrogen fermentation under various intracellular redox states using different carbon sources. The research reported that different carbon sources have different redox potentials depending on the chemical molecules. Substrates with low redox potential significantly enhance the NADPH-dependent hydrogenase activity in the cells, thus promoting higher hydrogen evolution [169]. This may be the reason why lower ORP values resulted in a higher concentration of dissolved hydrogen in the fermentation media. After the successful 200mL fermentation, the biological hydrogen generation process was upscaled to a 2-liter bioreactor.

7.3 2L Bioreactor for Hybrid Fermentation in Optimized Conditions

The advantage of using a bioreactor is that it is a closed system that employs multiple sensors, motor-driven impellers for agitation, instruments for temperature control, and gassing equipment to create an anaerobic condition. Moreover, for scientists who need to improve productivity and save time in the bioprocess reaction, a bioreactor can be employed to produce a high quantity of cells, improve cell growth reproducibility, and increase cultivation efficiency. The wide range of bioreactor applications includes basic research and development, biopharmaceutical manufacturing, food, and chemical production [170]. A continuous fermentation can also be developed through a bioreactor to increase the yield of by-products from biodegradation [171]. In this experimental study, a 2L continuous stirred tank bioreactor (CSTR: Eppendorf Bioflo 320) is utilized for upscaled fermentation, with a working volume of 1.75L. The experimental setup is illustrated in Figure 7.3:
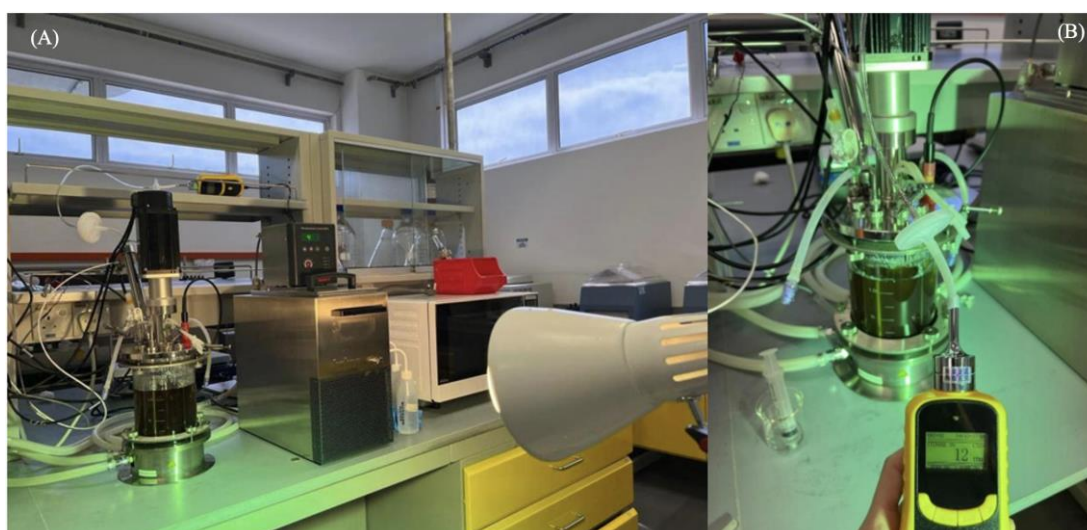
Figure 7.3: (A) Co-culture fermentation with illumination provided and (B) real time hydrogen detected from a 2L fermenter.

In the upscaled experiment, hydrogen production was performed in a batch fermentation. Firstly, the fermentation media was prepared, with the initial pH adjusted to 9 and metal ions introduced. The media was then poured into the bioreactor and autoclaved at 121°C. A separate bottle containing the carbon source was autoclaved at 110°C. *Bacillus* sp. and *Cereibacter* sp. were pre-cultured for 24 hours before the batch fermentation. To inoculate microorganisms and carbon source into the CSTR, the system integrated pump was utilized to feed the carbon source and

cultures into the bioreactor. Moreover, the fermentation media was continuously measured by a pH sensor throughout the fermentation process, allowing for real-time pH observation and data logging through the control software. To regulate the fermentation temperature, the bioreactor was placed in a thermowell, with a water jacket helping to maintain the temperature at 50°C. Furthermore, the temperature sensor equipped with the bioreactor was used to monitor the temperature of the culture medium, allowing for fermentation at a desired temperature. To analyze the hydrogen formation, a hydrogen detector was connected to one of the outlets from the CSTR. The data logging feature helped to record the real-time hydrogen production from hybrid fermentation. A research study revealed that the hydrogen production rate from fermentation significantly increased with agitation [172]. Throughout the hybrid fermentation process, the agitation speed was 10rpm for 22 hours, followed by 100rpm until the 96th hour of fermentation [173]. The biological hydrogen production and pH profile of co-culture fermentation are tabulated in Appendix 23 and illustrated in Figure 7.4. From Figure 7.4, a sharp decrease in pH can be observed from 0 to the 16th hour of hybrid fermentation, while biological hydrogen production increased rapidly during this period.
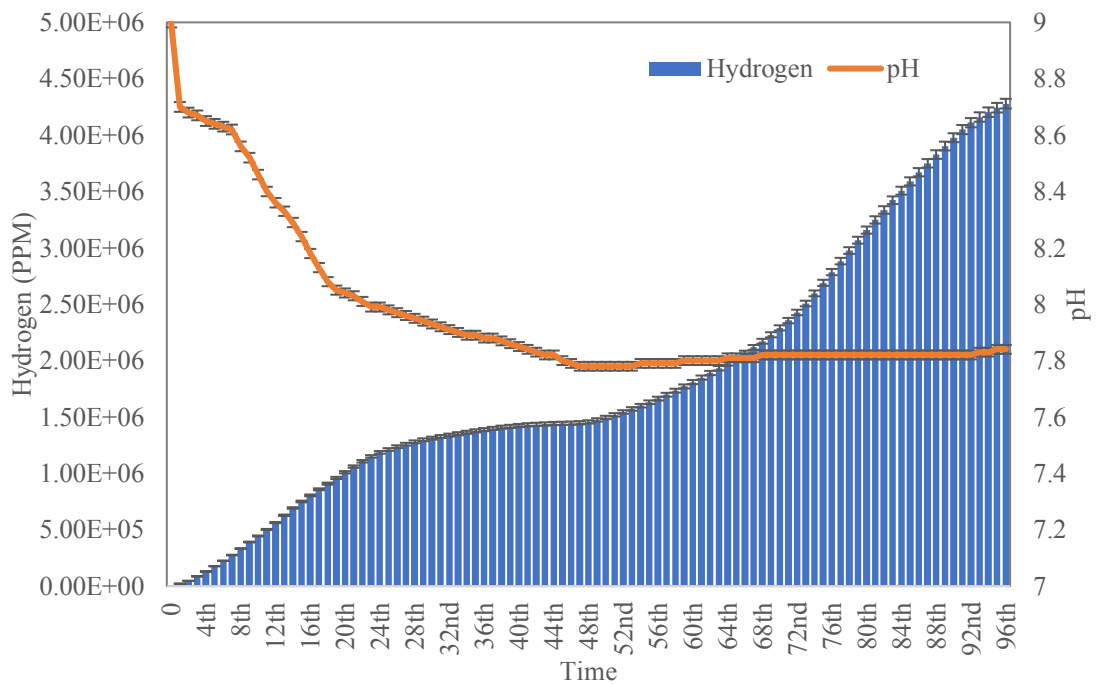
Figure 7.4: Biological hydrogen and pH profile of co-culture fermentation in CSTR.

The optimum operating conditions trigger high-rate acidogenic metabolism by *Bacillus sp.*, resulting in the accumulation of VFAs and biological hydrogen as the by-products [100]. Furthermore, a linear decrease in pH can be observed from the 16th to the 46th hour of fermentation, accompanied by a decrease in biological hydrogen production rate during this period of biodegradation. One possible explanation for this situation is that *Cereibacter* sp. may begin to utilize the VFAs by-products generated from dark fermentation, thus slowing down the rate of pH decrease. The accumulated VFAs may start to inhibit the hydrogenase activity from *Bacillus* sp., thus reducing the biological hydrogen production rate [108]. At the same time, *Cereibacter sp.* is adapting into the new acidic environment for its metabolism. Starting from the 46th hours onwards, the pH profile fluctuated between 7.78 and 7.84, while the biological hydrogen producing rate increased rapidly. At this stage of fermentation, rapid nitrogenase activity from *Cereibacter sp.* utilized VFAs as a substrate to produce biological hydrogen, thus alleviate the inhibition of hydrogenase from *Bacillus sp.*. Therefore, rapid hydrogen production rate appeared once again after two days of fermentation. The simultaneous biochemical reaction resulted in a rapid hydrogen production rate and a balanced VFAs production and consumption rate between *Bacillus* sp. and *Cereibacter* sp., resulting in fluctuating pH at the end of fermentation. Compared to the hybrid fermentation in a 200mL conical flask, the pH profile in the CSTR was maintained in the range of 7.78 and 7.84, while the pH profile in the 200mL conical flask kept decreasing, resulting in a final pH of 7.37 after four days of fermentation. This could be due to the effect of agitation on hybrid fermentation. The stirring mechanism may increase the metabolism of photo fermentative bacteria by decreasing the light shading effect and increasing the light saturation effect. As a result, the *Cereibacter* cells can absorb light energy more easily and shorten the residence time, thus promoting their metabolism [174], [175]. Thus, with a higher rate of metabolism, VFAs consumption rate and hydrogen production rate increased, and therefore the pH profile was maintained at a constant rate. An experimental study also showed that the stirring condition had a positive influence on mixed photoheterotrophic culture, resulting in a higher hydrogen production rate [172]. After combining the findings from preliminary mono-culture fermentation and the parametric study of hybrid fermentation, along with the aid of RSM software, the optimal operating conditions for co-culture fermentation involving *Bacillus* and *Cereibacter* have been determined. Chapter 6 and Chapter 7 establish Objective 3,

which focuses on the optimization of co-culture hybrid fermentation by *Bacillus paramycoides* and *Cereibacter azotoformans* using Response Surface Methodology. After obtaining enhanced biological hydrogen production from hybrid fermentation in a proper bioreactor, a simulation study for data validation and proposed metabolic pathway will be demonstrated in the following section.

CHAPTER 8: PROPOSED MECHANISTIC PATHWAY AND KINETIC MODELLINNG

8.1 Overview

A metabolic pathway is defined as a set of connected reactions or biochemical interactions that feed into one another. The metabolism of cells can utilize multiple starting substrates and convert them into products through a series of intermediates [176]. Constructing metabolic networks of pathways is an essential step in understanding the mechanisms of pathway engineering, medical diagnostics, and drug determination [177]–[179]. The most common pathways are anabolic and catabolic pathways. For instance, plants generate sugar from different raw materials through anabolic reaction, while animals digest food and break down food molecules to generate energy through catabolic pathway. Enzymes play a vital role in catalyzing chemical reactions in metabolic pathways. Figure 8.1 provides a simple demonstration of how enzymes work to generate products from substrates.
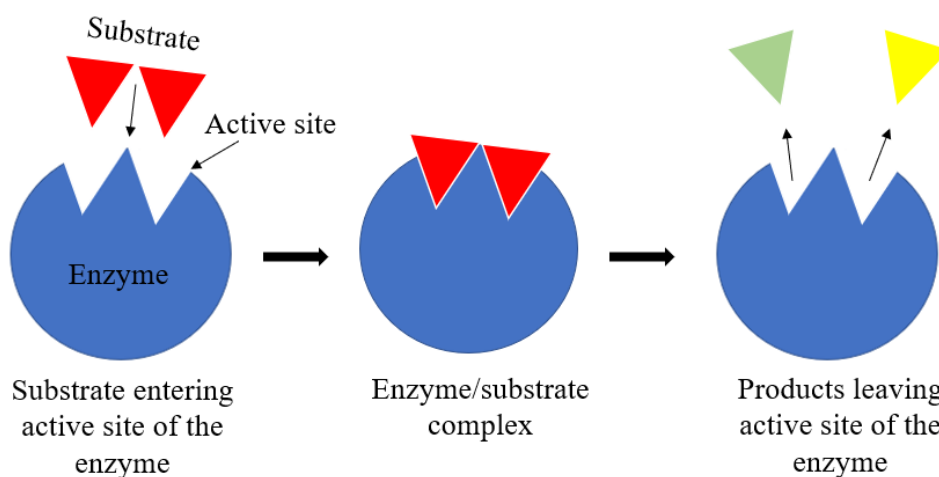
Figure 8.1: Lock-and-key model of substrate-enzyme interaction.

An enzyme's active site is a location within the enzyme where a substrate binds, and the reaction takes place. Enzymes are proteins with a unique mixture of amino acid side chains located at the active site. The side chains of the enzyme are characterized by various properties, including size, acidity or basicity, charge, and hydrophilicity or hydrophobicity. This special combination of side chains creates a specific chemical environment at the enzyme's active site, allowing only a specific chemical substrate to bind to the enzyme's active site at one time. In bioprocess

engineering, it is essential to understand the pathway from substrate to by-products in a specific metabolism. Once the main metabolic regulation can be fully understood, a specific pathway mutation for metabolic engineering can be created to generate the desired amount of useful by-products [180].

8.2 Proposed Metabolism in Co-culture Hybrid Fermentation

Bacillus sp. are acidogenic bacteria that decompose carbon sources, such as biomass wastes, into volatile fatty acids [181]. During anaerobic acidification, by-products such as hydrogen, carbon dioxide, and ethanol are formed along the metabolic pathway [182]. Without sunlight, dark fermentation is a promising approach for treating large amounts of organic wastes. Additionally, dark fermentation effluent can be further decomposed to produce polyhydroxyalkanoate (PHA), methane, or extra hydrogen by-products [183]–[185]. In our project, PNSB utilize the dark fermentation effluent to produce additional biological hydrogen. During light fermentation, PNSB produce hydrogen via catalytic reactions, specifically the tricarboxylic acid cycle (TCA) [48]. Based on the results observed from co-culture hybrid fermentation, a hypothetical metabolic pathway is proposed and illustrated in Figure 8.2:
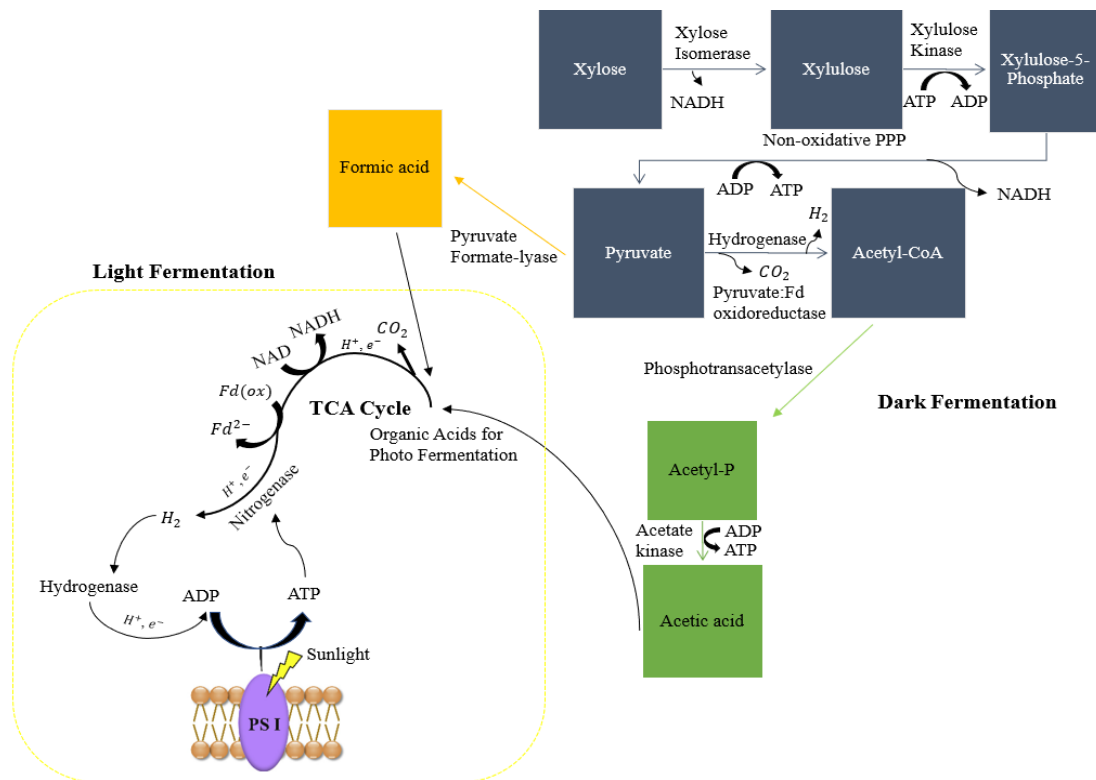
Figure 8.2: Proposed metabolic pathway for co-culture hybrid fermentation [186]–[188].

108

During the dark fermentation process by *Bacillus sp.*, numerous enzymes are secreted as part of their metabolism [189]. One of the pathways used by *Bacillus sp.* to consume xylose is the isomerase pathway, which converts xylose to xylulose using xylose isomerase and then phosphorylates it to xylulose-5-phosphate using xylulose kinase. This is a typical pathway used by prokaryotes, such as *Bacillus* strain bacteria [186]. When xylose is broken down by *Bacillus* sp. to produce energy, molecules such as pyruvate, nicotinamide adenine dinucleotide (NADH), and adenosine triphosphate (ATP) are formed. During this process, NAD^+ is reduced to form NADH and H^+ ions. Furthermore, pyruvate is further converted to acetylcoenzyme A (acetyl-CoA), and molecules such as CO_2 and hydrogen are formed by pyruvate-ferrodoxin oxidoreductase and hydrogenase enzymes. Additionally, pyruvate may be transformed into formate by pyruvate formate-lyase enzyme, and the formate formed can be readily converted into CO_2 and hydrogen by *Bacillus sp.*. Finally, acetate kinase enzyme converts acetyl-CoA to acetate, with ATP generated along the pathway [187]. The short-chain organic acids generated from dark fermentation can be further metabolized by PNSB to produce higher amounts of biological hydrogen [89].

During the light fermentation process, organic VFAs are consumed as the electron donor to produce biological hydrogen under anaerobic, nitrogen-limited, and light-supplied conditions [190]. VFAs are fed into the TCA cycle for oxidation reactions to produce electrons and CO_2. The electrons produced are transported from the TCA to nitrogenase through successive reduction and oxidation of electron carriers, such as $(Fd)_{red}/(Fd)_{ox}$ and $NAD^+/$ NADH, responsible for the oxidation and reduction processes. Additionally, protons resulting from the carbon source consumption and central metabolism are transported to the nitrogenase, which reduces them to produce biological hydrogen [188]. However, in the light fermentation process, uptake hydrogenase may utilize hydrogen as the electron donor and catalyze its splitting into electron and proton [48]. Moreover, with a light source provided, the photosystem (PS) unit is stimulated to transport protons for ATP production. The ATP produced can be utilized by nitrogenase enzyme for hydrogen-producing metabolism. To understand the mechanisms of dark and photo fermentative reactions, kinetic modelling is vital for quantitatively understanding and predicting their metabolic behaviour in biodegradation processes. To do so, a sequential hybrid fermentation was performed for the kinetic modelling, as illustrated in Figure 8.3:
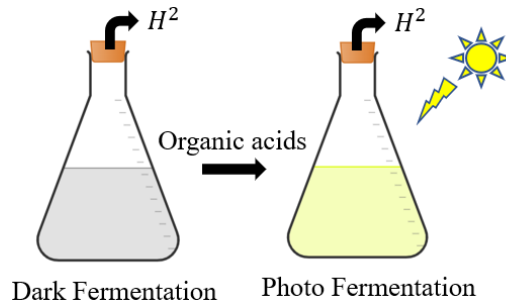
Figure 8.3: Illustration of sequential dark/light fermentation.

Initially, with the optimized conditions experimented, dark fermentation was performed for 2 days for biological hydrogen production. Moreover, the fermentation media was sterilized under UV ray prior to photo fermentation, followed by inoculation for light fermentation process for 2 days. The biological hydrogen production, xylose consumption, and acids production and consumption was quantified throughout the sequential dark/light fermentation.

8.3 Reaction Mechanism and Kinetic Modelling for Sequential Hybrid Fermentation

The proposed metabolic pathway indicates that dark fermentation produces biological hydrogen, acetic acid, and formic acid as by-products. Stoichiometrically, one mole of xylose requires five moles of water to produce one mole of formic acid, nine moles of molecular hydrogen, and four moles of carbon dioxide. Similarly, during the acetate pathway, one mole of xylose requires three moles of water to form one mole of acetic acid, six moles of hydrogen, and three moles of carbon dioxide. The dark fermentation reaction can be described using Equations 8.1 - 8.2 [53].

$$C_5H_{10}O_5 + 5\,H_2O \rightarrow HCOOH + 9\,H_2 + 4\,CO_2 \qquad (8.1)$$

$$C_5H_{10}O_5 + 3\,H_2O \rightarrow CH_3COOH + 6\,H_2 + 3\,CO_2 \qquad (8.2)$$
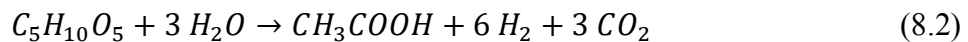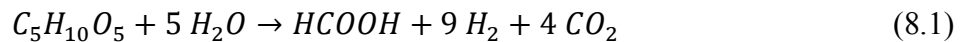
During light fermentation, VFAs produced from dark fermentation can be utilized as the carbon source to produce extra biological hydrogen. Theoretically, with light source provided, one mol of formate can produce one mol of hydrogen and carbon dioxide. Besides, four moles of hydrogen and two moles of carbon dioxide

can be produced when one mol of acetate react with two moles of water. The stoichiometry of photo fermentation can be described in Equations 8.3 - 8.4 [53].

$$HCOOH + Sunlight \rightarrow H_2 + CO_2 \qquad\qquad (8.3)$$

$$CH_3COOH + 2\,H_2O\ + Sunlight \rightarrow 4H_2 + 2CO_2 \qquad\qquad (8.4)$$
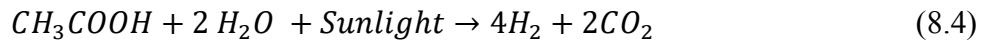
Computer simulation plays a vital role in defining the mechanisms and modelling the dynamic changes of metabolic rates in bioprocess reactions [191]. It is a helpful for optimizing the cost of final products, regardless of the number of tries. Although simulation models cannot fully represent lab or pilot-scale experiments, they are still a powerful tool for selecting further research directions. For example, the Ordinary Differential Equation (ODE) can be used to simulate various bioprocesses. One of the most precise algorithms for solving numerical ODEs is the Runge-Kutta family, which leads to better fitting estimates of functions to real curves, thereby significantly reducing errors [192]. A simulation study reported that Fagbemi et al. (2019) successfully predicted biogas production from anaerobic degradation by utilizing the 4th order Runge-Kutta method. Additionally, the results of their proposed model matched well with those of two other numerical models [193]. Furthermore, Liu and colleagues successfully simulated ethanol production from rice wine fermentation using the 4th order Runge-Kutta method. They investigated the ethanol production rate at various temperatures and achieved a highly accurate kinetic model ranging from 95% to 99% [194]. Therefore, this study used the Runge-Kutta method in our kinetic modelling study of hydrogen fermentation. By considering the ODE in the simplest form of dy/dx=f(x,y), with an initial situation of $y(x_0) = y_0$, the first-order Runge-Kutta method can be defined as:

$$y_1 = y_0 + hf(x_0, y_0) \qquad\qquad (8.5)$$

The first-order Runge-Kutta method is similar to the Euler's method, where h represents the step size for numerical simulation [192]. Theoretically, the value of y can be calculated at any point during a given duration. However, using a single and constant step method may not accurately simulate various complex cases. Therefore,

the second-order Runge-Kutta method is proposed. The second-order Runge-Kutta method can be described as:

$$y_1 = y_0 + \frac{1}{2}(k_1 + k_2) \tag{8.6}$$

Where $k_1 = hf(x_0, y_0)$ and $k_2 = hf(x_0 + h, y_0 + k_1)$. To further increase the accuracy in numerical modelling, the 3rd order Runge-Kutta equation is proposed and can be described as:

$$y_1 = y_0 + \frac{1}{6}(k_1 + 4k_2 + k_3) \tag{8.7}$$

Where $k_1 = hf(x_0, y_0)$, $k_2 = hf[x_0 + (\frac{1}{2})h, y_0 + (\frac{1}{2})k_1]$, and $k_3 = hf(x_0 + h, y_0 + k_1)$. The 4th order Runge-Kutta method adapts a weighted average slope at various number of points [195]. Hence, it offers higher accuracy than the lower order ones. The equation of 4th order Runge Kutta method can be described as:

$$y_1 = y_0 + \frac{1}{6}(k_1 + 2k_2 + 2k_3 + k_4) \tag{8.8}$$

Where $k_1 = hf(x_0, y_0)$, $k_2 = hf[x_0 + (\frac{1}{2})h, y_0 + (\frac{1}{2})k_1]$, $k_3 = hf[x_0 + (\frac{1}{2})h, y_0 + (\frac{1}{2})k_2]$, and $k_4 = hf(x_0 + h, y_0 + k_3)$. Since the 4th order Runge-Kutta method offers higher accuracy, the following mathematical model for sequential hybrid fermentation utilized the 4th order Runge-Kutta formula. Equations 8.9 – 8.12 shows the stoichiometry of dark (Equations 8.9 – 8.10) and light (Equations 8.11 – 8.12) fermentation with forward reaction rate constants included, such as k_1, k_2, k_3, and k_4 for respective equations.

$$C_5H_{10}O_5 + 5\ H_2O \xrightarrow{k_1} HCOOH + 9\ H_2 + 4\ CO_2 \tag{8.9}$$

$$C_5H_{10}O_5 + 3\ H_2O \xrightarrow{k_2} CH_3COOH + 6\ H_2 + 3\ CO_2 \tag{8.10}$$

$$HCOOH + Sunlight \xrightarrow{k_3} H_2 + CO_2 \tag{8.11}$$

$$k_4$$

$$CH_3COOH + 2\,H_2O\ + Sunlight \rightarrow 4H_2 + 2CO_2 \qquad (8.12)$$
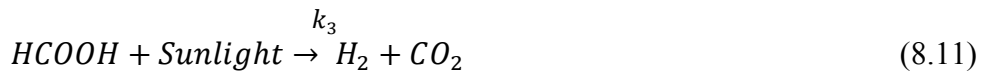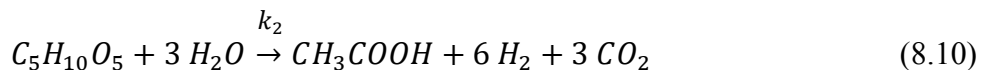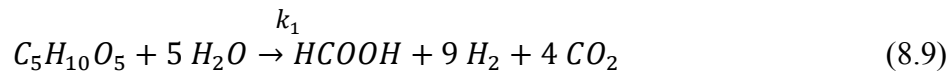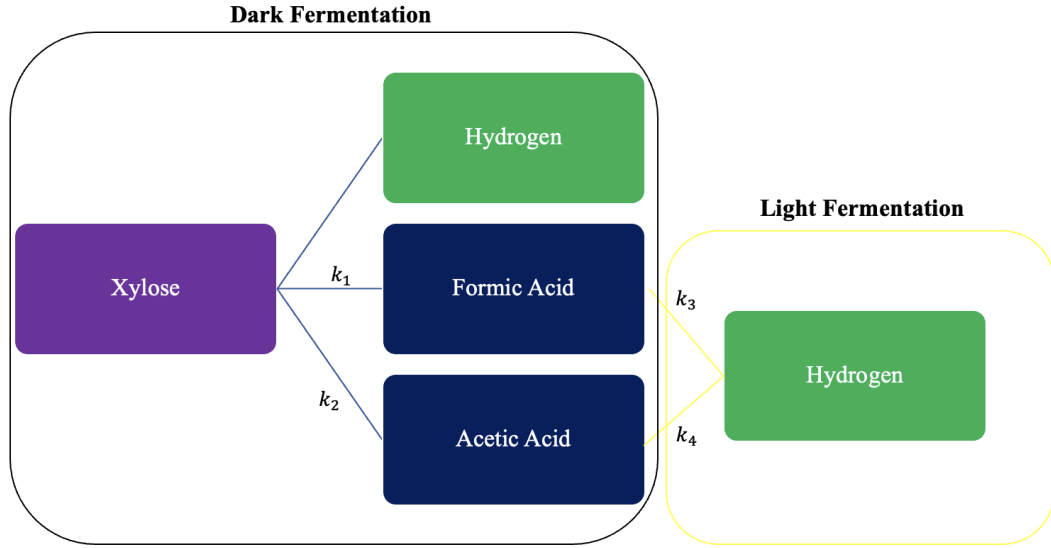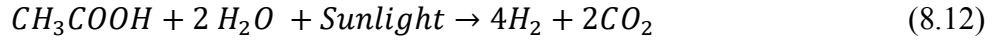
Figure 8. 4: Reaction kinetic based on stoichiometry equations.

From the stoichiometric relations shown in Equations 8.9 – 8.12, differential rate of reaction for each molecule, $C_5H_{10}O_5$, H_2O, $HCOOH$, CH_3COOH, H_2, and CO_2 can be defined in Equations 8.13 – 8.23.

Dark Fermentation

$$\frac{d[C_5H_{10}O_5]}{dt} = -k_1[C_5H_{10}O_5][H_2O]^5 - k_2[C_5H_{10}O_5][H_2O]^3 \qquad (8.13)$$

$$\frac{d[HCOOH]}{dt} = k_1[C_5H_{10}O_5][H_2O]^5 \qquad (8.14)$$

$$\frac{d[CH_3COOH]}{dt} = k_2[C_5H_{10}O_5][H_2O]^3 \qquad (8.15)$$

$$\frac{d[CO_2]}{dt} = 4k_1[C_5H_{10}O_5][H_2O]^5 + 3k_2[C_5H_{10}O_5][H_2O]^3 \qquad (8.16)$$

$$\frac{d[H_2]}{dt} = 9k_1[C_5H_{10}O_5][H_2O]^5 + 6k_2[C_5H_{10}O_5][H_2O]^3 \qquad (8.17)$$

$$\frac{d[H_2O]}{dt} = -5k_1[C_5H_{10}O_5][H_2O]^5 - 3k_2[C_5H_{10}O_5][H_2O]^3 \qquad (8.18)$$

Photo Fermentation

$$\frac{d[HCOOH]}{dt} = -k_1[HCOOH] \tag{8.19}$$

$$\frac{d[CH_3COOH]}{dt} = -k_2[CH_3COOH][H_2O]^2 \tag{8.20}$$

$$\frac{d[CO_2]}{dt} = k_1[HCOOH] + 2k_2[CH_3COOH][H_2O]^2 \tag{8.21}$$

$$\frac{d[H_2]}{dt} = k_1[HCOOH] + 4k_2[CH_3COOH][H_2O]^2 \tag{8.22}$$

$$\frac{d[H_2O]}{dt} = -2k_2[CH_3COOH][H_2O]^2 \tag{8.23}$$

Before performing the kinetic modelling using Runge-Kutta method, concentration data for each molecule were collected for dark and photo fermentation separately. Water is available in excess, thus its concentration during the fermentation process is considered essentially constant and therefore it is ignored in kinetic modelling. Furthermore, hydrogen detector can only detect hydrogen gas in biogas production from fermentation process. In a consequence, only hydrogen is considered in our kinetic modelling. The concentrations for each molecule are demonstrated in Table 8.1:

Table 8.1: Experimental data of (a) xylose consumption and by-products formation in dark fermentation and (b) VFAs consumption and hydrogen formation in photo fermentation.

(a) Dark Fermentation			
Fermentation Time (hours)	Number of Mol		
	$C_5H_{10}O_5$	$HCOOH$	CH_3COOH	H_2
0	0.1167	0.0001	0.0001	0
4	0.1165	0.00015	0.00015	0.001492
8	0.1163	0.00025	0.00025	0.003045
12	0.1161	0.0004	0.0004	0.004723
16	0.1159	0.0005	0.0005	0.006359
20	0.1157	0.00065	0.00065	0.007575
24	0.1156	0.0008	0.0008	0.009017
28	0.1154	0.00095	0.00095	0.010417
32	0.1152	0.00115	0.00115	0.012049
36	0.115	0.0013	0.0013	0.014148
40	0.1148	0.00145	0.00145	0.014963
44	0.1146	0.0016	0.0016	0.017365
48	0.1144	0.00175	0.00175	0.01802

(b) Photo Fermentation			
	$C_5H_{10}O_5$	$HCOOH$	CH_3COOH	H_2
0	0.1144	0.00175	0.00175	0
4	0.1144	0.001675	0.001675	0.000292
8	0.1144	0.0016	0.0016	0.000576
12	0.1144	0.0015	0.0015	0.000868
16	0.1144	0.0014	0.0014	0.001122
20	0.1144	0.0013	0.0013	0.001333
24	0.1144	0.0012	0.0012	0.001451
28	0.1144	0.0011	0.0011	0.001677
32	0.1144	0.001	0.001	0.001904
36	0.1144	0.0009	0.0009	0.002002
40	0.1144	0.00085	0.00085	0.002209
44	0.1144	0.0008	0.0008	0.002377
48	0.1144	0.00075	0.00075	0.002459

The forward reaction constants k were calculated using the built-in solver function in Excel (Microsoft 365). The calculated reaction constants were optimized to find the best values of k that represent the experimental data, with the condition of $k > 0$. Additionally, the R^2 value was utilized to evaluate the model fitting. The closer the R^2 to 1, the higher the model fitting accuracy. Table 8.2 shows the optimized values for kinetic parameters, k, and R-squared value for the kinetic analysis.

Table 8.2: Kinetic parameters and R-squared value for the kinetic modelling.

(a) Dark Fermentation			
Reaction Rate Constant (mol/h)		R^2	Error %
k_1	0.0000000000059921	-	-
k_2	0.0000000018454	-	-
Model Fitting with Experimental Data			
Actual xylose VS Simulated xylose		0.998	0.2
Actual hydrogen VS Simulated hydrogen		0.997	0.3
Actual formic acid VS Simulated formic acid		0.992	0.8
Actual acetic acid VS Simulated acetic acid		0.992	0.8
(b) Photo Fermentation			
k_3	0.0176519	-	-
k_4	0.000005737	-	-
Model Fitting with Experimental Data			
Actual hydrogen VS Simulated hydrogen		0.998	0.2
Actual formic acid VS Simulated formic acid		0.991	0.9
Actual acetic acid VS Simulated acetic acid		0.991	0.9

After obtaining the kinetic parameters, the experimental data versus simulated concentration of each molecule in dark and photo fermentation are shown in Figure 8.4 and Figure 8.5.
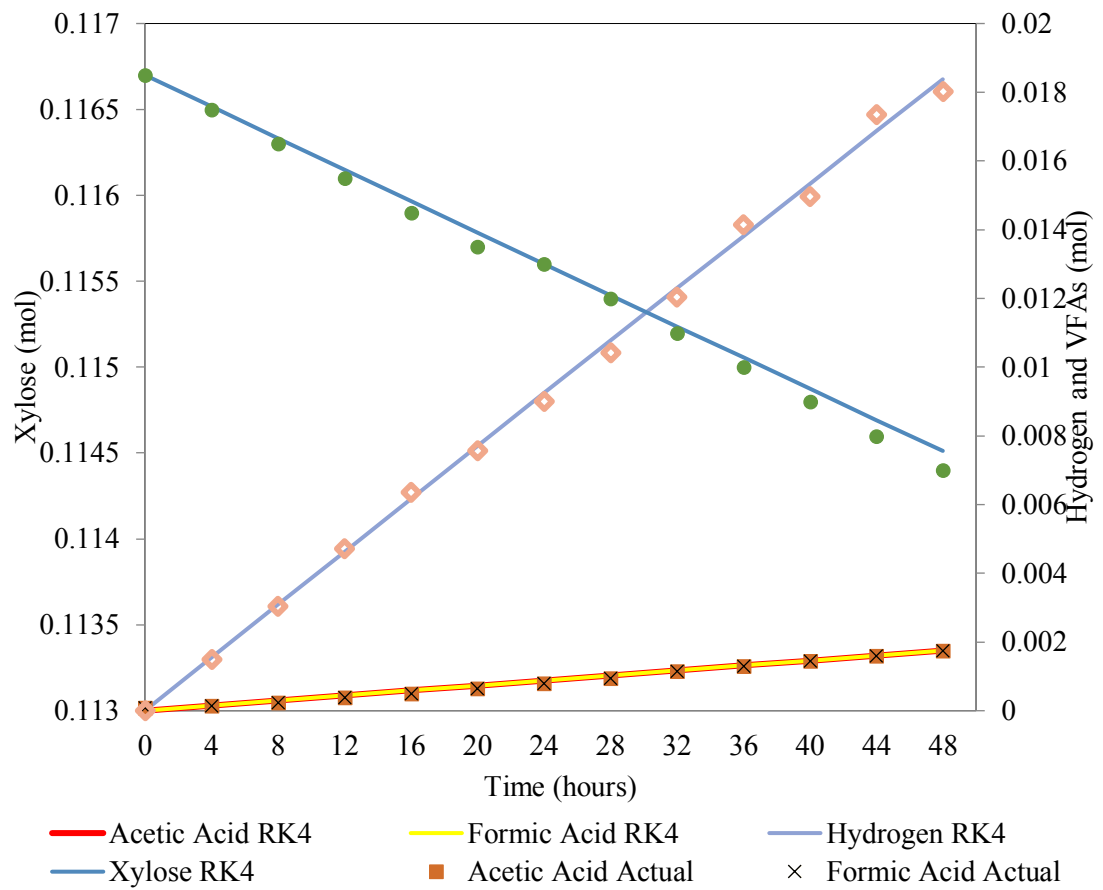
Figure 8.5: Experimental data versus simulated concentrations of $C_5H_{10}O_5$, $HCOOH$, CH_3COOH, and H_2 in dark fermentation.
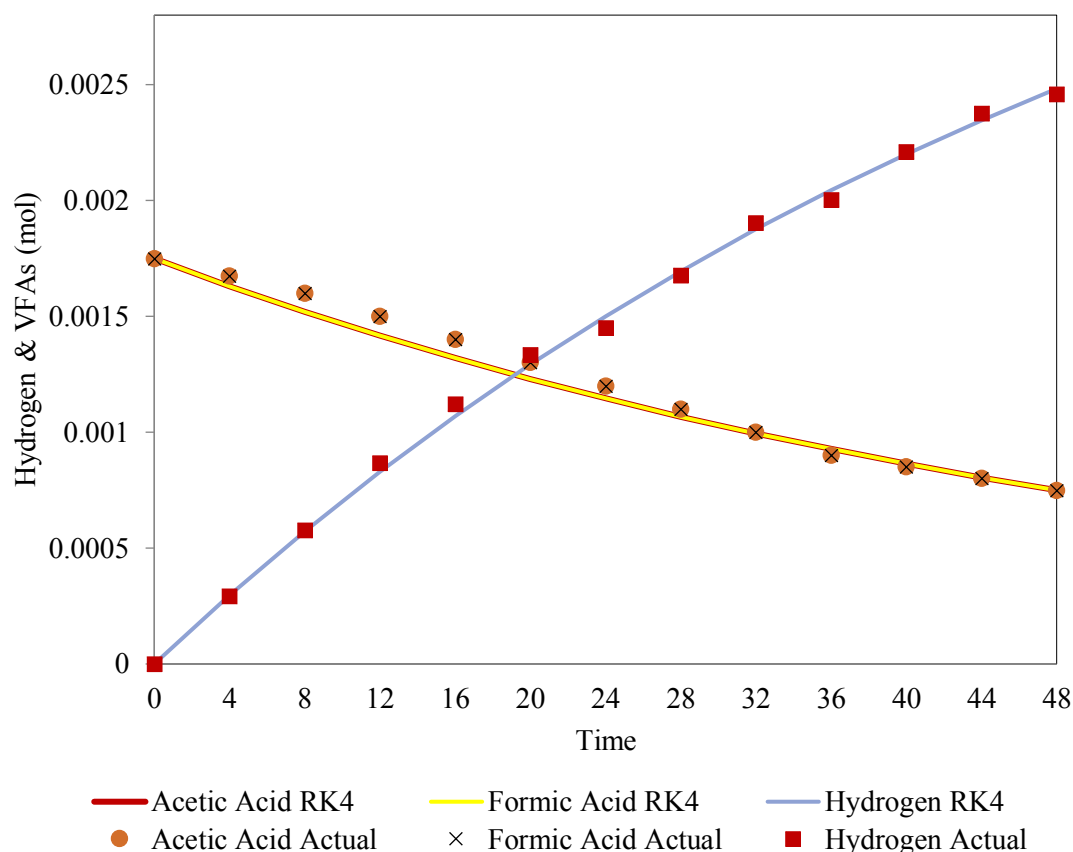
Figure 8.6: Experimental data versus simulated concentrations of $HCOOH$, CH_3COOH, and H_2 in photo fermentation.

Based on the illustrations in Figure 8.4 and 8.5, the kinetic modelling by 4th order Runge-Kutta method fits very well with the profile of actual data. The R-squared values ranged between 0.991 and 0.998 which signifies that the model is useful to describe the sequential dark and light fermentation in optimized conditions. Therefore, our proposed model is suitable to estimate the biological hydrogen production from sequential hybrid fermentation. Nevertheless, to achieve lab scale transition into industrial application for biological hydrogen generation, the proposed numerical modelling could play a critical role to understand the kinetic mechanisms in enhancing useful by-products formation. Objective 4, which aims to propose co-culture fermentation metabolic pathway for xylose conversion and perform 4th order Runge Kutta method for data validation, has been established in this chapter. Finally, Table 8.3 demonstrated the benchmarking of the experimental results with other literature studies to compare the biological hydrogen yield.

Table 8. 3: Comparison on biological hydrogen production with various study.

Types of substrates	Organism	Hydrogen yield	References
Xylose	*Bacillus paramycoides* and *Cereibacter azotoformans*	3.92 L H_2/ L medium	This study
Glucose from rice straw hydrolysate	*Bacillus cereus* and *Rhodopseudomonas rutila*	1.82 mol H_2/mol glucose	[19]
Glucose	*Clostridium acetobutylicum* and *Rhodobacter sphaeroides*	2.533 L H_2/ L medium	[53]
Fruit and vegetable waste (FVW) and cheese whey powder (CWP)	DF + PF mixed culture	0.7937 L H_2 /g COD when FVW:CWP ratio was 1:1	[61]
Milk whey permeate	*Enterobacter cloacae* and *Rhodobacter capsulatus / Rhodopseudomonas palustris*	319.35 mmol H_2/ L day	[148]
Glucose (13.7 g/L)	Mixed culture	1.2 mol/mol glucose	[196]
Sucrose (20 g COD/L)	Mixed culture	1.5 mol/mol sucrose	[197]
Cheese whey wastewater	Mixed cultures (anaerobic bacteria from UASB reactor)	3.1 mol H_2 / mol lactose	[198]
Wheat straw	*Thermoanaerobacterium thermosaccharolyticum* M18	3.53 mmol/g substrate	[199]
Corn leaves	*Caldicellulosiruptor saccharolyticus*	1.80 mol H_2/mol glucose	[200]
Starch	*Clostridium acetobutylicum* and *Rhodobacter sphaeroides*	3.23 L H_2 / L medium	[201]

CHAPTER 9: CONCLUSION AND RECOMMENDATIONS

9.1 Conclusions

In this chapter, a conclusion will be presented to summarize the key findings of the research project. Initially, morphology, gram staining, and DNA sequencing were performed to identify the bacterial strains. Based on the generated phylogenetic tree and DNA sequencing results, the strains were identified as *Bacillus paramycoides* and *Cereibacter azotoformans*. The growth behaviour study and simultaneous biological hydrogen production of photo fermentative *Cereibacter azotoformans* and dark fermentative *Bacillus paramycoides* were investigated. The results indicated that a 1g/L inoculum produced higher biological hydrogen compared to a 10g/L inoculum, attributed to the quorum sensing mechanism. Furthermore, a complete lag, log, and stationary phase were observed with a 10g/L inoculum of bacteria. During the log phase at 24 hours, the most active phase of the inoculum was retrieved for subsequent experimental studies. Objective 1, which involved strain identification and determination of the appropriate inoculum phase for the parametric study, has been achieved.

Moreover, mono-culture fermentation was conducted in 30mL test tubes, varying carbon sources, substrate concentrations, types of metal ions, and inoculum concentrations. For dark fermentation, it was observed that *Bacillus* sp. produced significantly higher biological hydrogen from xylose compared to glucose. The inhibition of hydrogenase enzymes for hydrogen production was attributed to the acidic environment when glucose was utilized as the substrate. Additionally, the optimal addition of Co^{2+} ions enhanced biological hydrogen production in *Bacillus* sp. due to the large specific surface area and quantum size of nanoparticles, facilitating electron transfer between NADPH-ferredoxin oxidoreductase and hydrogenase, thus improving hydrogenase activity through the redox reaction. Furthermore, it was found that lower inoculum sizes resulted in higher biological hydrogen generation, attributed to the quorum sensing mechanism and near neutral pH, enhancing biological hydrogen yield from low *Bacillus* sp. inoculum sizes. Regarding photo fermentation, it was also observed that *Cereibacter* sp. produced significantly higher biological hydrogen from xylose compared to glucose. PNSB preferred xylose in their metabolic pathway for hydrogen formation, whereas higher PHB build-up when glucose was used as the

substrate. The optimal addition of Mn^{2+} ions facilitated the redox reaction in *Cereibacter* sp. metabolism, leading to much higher biological hydrogen production compared to other metal ions. Additionally, it was found that lower inoculum sizes of *Cereibacter* sp. resulted in higher biological hydrogen generation. The high turbidity caused by high inoculum sizes inhibited sunlight penetration into the fermentation broth, thereby hindering the metabolism of *Cereibacter* sp. for hydrogen generation. Objective 2, involving the parametric study of dark and photo fermentation, has been achieved. The optimal parameters established in this preliminary stage have enhanced biological hydrogen production from the novel strains *Bacillus paramycoides* and *Cereibacter azotoformans*.

The optimal ranges for xylose concentration, inoculum size, and types of metal ions were determined through the preliminary stage of dark and photo fermentation. Response Surface Methodology (RSM) software was utilized to analyze the basic data obtained from this stage and identify the optimum conditions. Initially, an optimized inoculum ratio of D/L=1:2 and a xylose concentration of 17.5g/L were obtained from 20 sets of experimental runs using RSM software. The 17.5g/L substrate concentration in hybrid fermentation was found to be suitable for preventing metabolite and feedstock inhibition, improving bacterial metabolism, and increasing by-product productivity. Additionally, with an inoculum ratio of D/L=1:2, the production and consumption rates of VFAs were balanced, and sufficient light fermentative bacteria were present to ferment VFAs metabolites produced from dark fermentation. This approach helps prevent acid accumulation and increases the activity of hydrogenase and nitrogenase enzymes. After obtaining the optimal inoculum ratio and substrate concentration, the effects of initial pH, temperature, and metal ion concentrations on hybrid fermentation were investigated. The optimal initial pH for biological hydrogen evolution through co-culture hybrid fermentation was found to be pH 8, as this close to neutral pH is suitable for hydrogenase and nitrogenase enzymes to produce hydrogen efficiently. Furthermore, the optimal operating temperature for hybrid fermentation was determined to be 50°C, as it promotes rapid hydrogenase and nitrogenase activity, resulting in shorter retention time for biological hydrogen generation. The results also indicated that the optimal concentrations for both Co^{2+} and Mn^{2+} ions were 20μM. The introduction of these metal ions facilitated electron transfer, improving the synthesis of hydrogenase and nitrogenase enzymes as well as signal transduction. Utilizing RSM software once again, the optimal conditions for co-

culture biodegradation were determined to be a fermentation temperature of 50°C, an initial pH of 9, and a 20μM concentration of Co^{2+} ions. The biological hydrogen yield and production rate from the 2L CSTR were measured to be 3920.52 mL H_2/L and 40.84 mL H_2/L h, respectively. The step-by-step optimization process significantly enhanced the biological hydrogen yield from hybrid fermentation compared to mono-culture dark and light fermentation. Finally, a hypothetical metabolic pathway was proposed for hybrid fermentation to generate useful by-products. The 4th order Runge-Kutta method was employed to solve the Ordinary Differential Equations (ODEs) in sequential dark/light fermentation. The kinetic metabolism of sequential hybrid fermentation was simulated to estimate the production and consumption of VFAs and the generation of biological hydrogen. The R-squared values were calculated, ranging from 0.991 to 0.998, indicating high fitting accuracy to the experimental data. Objective 3 and 4 were successfully addressed through the optimization of co-culture fermentation, proposed mechanisms, and kinetic validation using experimental data.

9.2 Recommendations

In this research project, biological hydrogen was successfully obtained through single strain dark and light fermentation, as well as co-culture hybrid fermentation. Based on the experimental work, a few recommendations can be made for further research:

1. Operating pH plays a critical role in bacteria metabolism. In this experimental work, only the initial pH was investigated for hydrogen fermentation. To further enhance the biological hydrogen yield from the fermentation process, an experimental design to maintain the pH can be performed to investigate the effect of controlled pH on *Bacillus paramycoides* and *Cereibacter azotoformans*.

2. The key enzymes to produce biological hydrogen by *Bacillus paramycoides* and *Cereibacter azotoformans* are hydrogenase and nitrogenase enzymes. Due to the limited project timeline, enzymes activity has not yet been investigated. For further hydrogen fermentation projects, experimental work on enzymatic assay should be performed to track enzyme activity to produce hydrogen. In addition, metabolic engineering by designing and applying genetic

modifications can be employed to improve bacteria cell properties for high-quality and quantity by-products formation.

3. The low production rate is the key obstacle for biodegradation processes to produce hydrogen. Various useful by-products from the fermentation process should be explored to increase the value of biodegradation processes. For instance, excess VFAs produced from dark fermentation processes can be used as a preservative in food manufacturing. Also, the simultaneous ethanol and methane production during hydrogen fermentation can be extracted to make alternate biofuels. In photo fermentation, polyhydroxybutyrate (PHB) formation can be utilized to make bioplastic products. Meanwhile, coenzyme Q10 production from PNSB can be extracted to make nutrient supplements for humans. Additionally, *Cereibacter* sp. could produce ammonia as fertilizer in the agriculture sector. To conclude, the biodegradation process to produce biological hydrogen could produce other useful metabolites simultaneously. The valuable products could help in food, fuel, pharmaceutical, and agricultural industries. The fermentation process still offers commercial value if all the useful by-products can be discovered and extracted for commercialization.

4. Various biomass wastes should be experimented with for hybrid fermentation to produce useful bio-products. The current experiment utilized only xylose and glucose as substrates. The exact cost and energy cannot be identified if biomass waste is not utilized for the bio-treatment process. Proper biomass pre-treatment methods should also be identified to ensure compatibility with hybrid fermentation. By doing this, a full feasibility study can be carried out to identify the exact energy and cost required to convert waste into useful bio-products. A proper cost and energy analysis can be calculated from the co-culture biodegradation process.

5. To achieve a higher biological hydrogen production rate from biodegradation process, it is recommended to extend the current research by conducting scaling-up studies to explore the practical application of the hybrid fermentation process for biological hydrogen production. The successful transition from small-scale experiments in 30mL test tubes to larger volumes, such as 200mL conical flasks and 2L bioreactors, highlights the potential

feasibility of the biodegradation process. To gain a comprehensive understanding of its practicality, further investigations at pilot or industrial scale are essential. These scaled-up studies will provide valuable insights into scalability, process stability, and economic viability, ultimately bridging the gap between laboratory research and real-world applications for more sustainable and efficient bioenergy solutions.

9.3 Commercialization of Biological Hydrogen Production

The commercialization of biological hydrogen production via the biodegradation pathway offers significant value in addressing global energy challenges. With the increasing demand for clean energy, this approach presents a unique opportunity to capitalize on the growing market. Based on a compilation of different projections, it is evident that the global annual revenue in the hydrogen production market has the potential to increase from $150 billion in 2021 to surpass $200 billion by 2025 [202]. Within this market, the demand for sustainable hydrogen sources is rising rapidly. Furthermore, fermentative hydrogen production utilizes a variety of feedstocks, such as organic waste and agricultural residues, providing a reliable and diverse resource base. This feedstock flexibility ensures a consistent supply and reduces dependence on specific sources, enhancing the commercial viability of the process. However, the practical application of biological hydrogen production is still on the distant horizon. The future of this field relies not only on research breakthroughs but also on economic considerations, energy policies, environmental factors, and societal influences [203]. While the exploration of alternative fuels is crucial, extensive research is currently being conducted in the field of biological hydrogen production. That is why co-culture hybrid fermentation plays a crucial role, as it involves cultivating two or more microorganisms together, establishing a symbiotic relationship where the metabolic by-products of one organism serve as nutrients for the other. Co-culture fermentation offers significant advantages in terms of enhanced efficiency and stability compared to traditional single-strain fermentation processes. By harnessing the synergistic capabilities of multiple microorganisms, co-culture systems can achieve higher hydrogen yields, faster fermentation rates, and improved substrate utilization efficiency. Moreover, it can be seamlessly integrated into existing industrial processes, such as wastewater treatment

plants or bioethanol production facilities, to maximize resource utilization and generate added value. This integration eliminates the need for standalone infrastructure, making it economically feasible. However, several technical hurdles must be addressed before these technologies can be widely implemented on a practical, large-scale basis. For example, increasing the biofuel production rate and conversion efficiency from fermentation process, implementing a continuous process to treat the biomass wastes from industry, and decreasing the cost of bioprocess plant set-up. Nonetheless, the commercialization value of fermentative hydrogen production lies in its ability to provide a renewable, environmentally friendly, and economically viable energy solution. By leveraging its advantages, capitalizing on market opportunities, and addressing the remaining challenges, fermentative hydrogen production can play a crucial role in the transition towards a sustainable energy future.

REFERENCES

[1]   A. K. Karmaker, M. M. Rahman, M. A. Hossain, and M. R. Ahmed, "Exploration and corrective measures of greenhouse gas emission from fossil fuel power stations for Bangladesh," *J Clean Prod*, vol. 244, p. 118645, Jan. 2020, doi: 10.1016/j.jclepro.2019.118645.

[2]   W. K. Wang, Y. H. Hu, G. Z. Liao, W. L. Zeng, and S. Y. Wu, "Hydrogen fermentation by photosynthetic bacteria mixed culture with silicone immobilization and metagenomic analysis," *Int J Hydrogen Energy*, Dec. 2021, doi: 10.1016/J.IJHYDENE.2021.12.004.

[3]   D. H. Lee, "Biohydrogen yield efficiency and the benefits of dark, photo and dark-photo fermentative production technology in circular Asian economies," *Int J Hydrogen Energy*, vol. 46, no. 27, pp. 13908–13922, Apr. 2021, doi: 10.1016/J.IJHYDENE.2020.08.275.

[4]   X. Li *et al.*, "Revealing the mechanisms of rhamnolipid enhanced hydrogen production from dark fermentation of waste activated sludge," *Science of The Total Environment*, vol. 806, p. 150347, Feb. 2022, doi: 10.1016/J.SCITOTENV.2021.150347.

[5]   A. Velazquez Abad and P. E. Dodds, "Production of Hydrogen," in *Encyclopedia of Sustainable Technologies*, Elsevier, 2017, pp. 293–304. doi: 10.1016/B978-0-12-409548-9.10117-4.

[6]   M. Hermesmann and T. E. Müller, "Green, Turquoise, Blue, or Grey? Environmentally friendly Hydrogen Production in Transforming Energy Systems," *Prog Energy Combust Sci*, vol. 90, p. 100996, May 2022, doi: 10.1016/J.PECS.2022.100996.

[7]   N. Srivastava *et al.*, "Nanoengineered cellulosic biohydrogen production via dark fermentation: A novel approach," *Biotechnology Advances*, vol. 37, no. 6. Elsevier Inc., Nov. 01, 2019. doi: 10.1016/j.biotechadv.2019.04.006.

[8]   L. Vernès, Y. Li, F. Chemat, and M. Abert-Vian, "Biorefinery Concept as a Key for Sustainable Future to Green Chemistry—The Case of Microalgae," pp. 15–50, 2019, doi: 10.1007/978-981-13-3810-6_2.

[9]   E. Borgardt *et al.*, "Impact of clamping pressure and stress relaxation on the performance of different polymer electrolyte membrane water electrolysis cell designs," *Int J Hydrogen Energy*, vol. 44, no. 42, pp. 23556–23567, Sep. 2019, doi: 10.1016/j.ijhydene.2019.07.075.

[10]   A. Anniwaer *et al.*, "Hydrogen-rich gas production from steam co-gasification of banana peel with agricultural residues and woody biomass," *Waste Management*, vol. 125, pp. 204–214, Apr. 2021, doi: 10.1016/j.wasman.2021.02.042.

[11]   H. C. Wu, Z. Rui, and J. Y. S. Lin, "Hydrogen production with carbon dioxide capture by dual-phase ceramic-carbonate membrane reactor via steam reforming of methane," *J Memb Sci*, vol. 598, p. 117780, Mar. 2020, doi: 10.1016/j.memsci.2019.117780.

[12]   I. Moussallem, J. Jörissen, U. Kunz, S. Pinnow, and T. Turek, "Chlor-alkali electrolysis with oxygen depolarized cathodes: History, present status and future prospects," *J Appl Electrochem*, vol. 38, no. 9, pp. 1177–1194, Sep. 2008, doi: 10.1007/s10800-008-9556-9.

[13]   C. Barca, D. Ranava, M. Bauzan, J. H. Ferrasse, M. T. Giudici-Orticoni, and A. Soric, "Fermentative hydrogen production in an up-flow anaerobic biofilm reactor inoculated with a co-culture of Clostridium acetobutylicum and

Desulfovibrio vulgaris," *Bioresour Technol*, vol. 221, pp. 526–533, Dec. 2016, doi: 10.1016/J.BIORTECH.2016.09.072.

[14] V. Kumar, R. Kothari, and S. Singh, "Dark Fermentation: a green way to produce hydrogen and methane," *International Journal of Science, Technology & Society*, vol. 1, no. 1, Jan. 2015, doi: 10.18091/IJSTS.V1I1.12.

[15] C. Mejía-Saucedo, G. Buitrón, M. F. León-Galván, and J. Carrillo-Reyes, "Biomass purge strategies to control the bacterial community and reactor stability for biohydrogen production from winery wastewater," *Int J Hydrogen Energy*, vol. 47, no. 9, pp. 5891–5900, Jan. 2022, doi: 10.1016/J.IJHYDENE.2021.12.007.

[16] L. Zhang, Y. Z. Wang, T. Zhao, and T. Xu, "Hydrogen production from simultaneous saccharification and fermentation of lignocellulosic materials in a dual-chamber microbial electrolysis cell," *Int J Hydrogen Energy*, vol. 44, no. 57, pp. 30024–30030, Nov. 2019, doi: 10.1016/J.IJHYDENE.2019.09.191.

[17] D. C. S. Rorke, P. Lekha, G. E. B. Kana, and B. B. Sithole, "Effect of pharmaceutical wastewater as nitrogen source on the optimization of simultaneous saccharification and fermentation hydrogen production from paper mill sludge," *Sustain Chem Pharm*, vol. 25, p. 100619, Apr. 2022, doi: 10.1016/J.SCP.2022.100619.

[18] T. Tang, Y. Chen, M. Liu, Y. Du, and Y. Tan, "Effect of pH on the performance of hydrogen production by dark fermentation coupled denitrification," *Environ Res*, vol. 208, p. 112663, May 2022, doi: 10.1016/J.ENVRES.2021.112663.

[19] G. H. Dinesh *et al.*, "Simultaneous biohydrogen (H2) and bioplastic (poly-β-hydroxybutyrate-PHB) productions under dark, photo, and subsequent dark and photo fermentation utilizing various wastes," *Int J Hydrogen Energy*, vol. 45, no. 10, pp. 5840–5853, Feb. 2020, doi: 10.1016/j.ijhydene.2019.09.036.

[20] B. F. Liu *et al.*, "Bio-hydrogen production by mixed culture of photo- and dark-fermentation bacteria," *Int J Hydrogen Energy*, vol. 35, no. 7, pp. 2858–2862, Apr. 2010, doi: 10.1016/J.IJHYDENE.2009.05.005.

[21] K.-Y. Show, Y. Yan, and D.-J. Lee, "Bioreactor and Bioprocess Design for Biohydrogen Production," *Biohydrogen*, pp. 391–411, Jan. 2019, doi: 10.1016/B978-0-444-64203-5.00016-2.

[22] S. V. Mohan and A. Pandey, "Biohydrogen Production: An Introduction," in *Biohydrogen*, Elsevier B.V., 2013, pp. 1–24. doi: 10.1016/B978-0-444-59555-3.00001-5.

[23] F. Martins, C. Felgueiras, M. Smitkova, and N. Caetano, "Analysis of fossil fuel energy consumption and environmental impacts in european countries," *Energies (Basel)*, vol. 12, no. 6, p. 964, Mar. 2019, doi: 10.3390/en12060964.

[24] S. Braungardt, J. van den Bergh, and T. Dunlop, "Fossil fuel divestment and climate change: Reviewing contested arguments," *Energy Research and Social Science*, vol. 50. Elsevier Ltd, pp. 191–200, Apr. 01, 2019. doi: 10.1016/j.erss.2018.12.004.

[25] Z. Duan, M. Pi, D. Zhang, P. Zhang, J. Deng, and S. Chen, "High hydrogen evolution performance of Al doped CoP 3 nanowires arrays with high stability in acid solution superior to Pt/C," *Int J Hydrogen Energy*, vol. 44, no. 16, pp. 8062–8069, Mar. 2019, doi: 10.1016/j.ijhydene.2019.02.095.

[26] M. M. Habashy, E. S. Ong, O. M. Abdeldayem, E. G. Al-Sakkari, and E. R. Rene, "Food Waste: A Promising Source of Sustainable Biohydrogen Fuel," *Trends in Biotechnology*. Elsevier Ltd, May 12, 2021. doi: 10.1016/j.tibtech.2021.04.001.

[27] S. Rittmann and C. Herwig, "A comprehensive and quantitative review of dark fermentative biohydrogen production.," *Microbial cell factories*, vol. 11. 2012. doi: 10.1186/1475-2859-11-115.

[28] R. S. Poudyal *et al.*, "Hydrogen production using photobiological methods," in *Compendium of Hydrogen Energy*, Elsevier, 2015, pp. 289–317. doi: 10.1016/b978-1-78242-361-4.00010-8.

[29] S. Shiva Kumar and V. Himabindu, "Hydrogen production by PEM water electrolysis – A review," *Mater Sci Energy Technol*, vol. 2, no. 3, pp. 442–454, Dec. 2019, doi: 10.1016/j.mset.2019.03.002.

[30] A. Basile, S. Liguori, and A. Iulianelli, "Membrane reactors for methane steam reforming (MSR)," in *Membrane Reactors for Energy Applications and Basic Chemical Production*, Elsevier Inc., 2015, pp. 31–59. doi: 10.1016/B978-1-78242-223-5.00002-9.

[31] A. Bakhtyari, M. A. Makarem, and M. R. Rahimpour, "Hydrogen Production Through Pyrolysis," in *Encyclopedia of Sustainability Science and Technology*, Springer New York, 2018, pp. 1–28. doi: 10.1007/978-1-4939-2493-6_956-1.

[32] J. S. Martín del Campo *et al.*, "High-Yield Production of Dihydrogen from Xylose by Using a Synthetic Enzyme Cascade in a Cell-Free System," *Angewandte Chemie International Edition*, vol. 52, no. 17, pp. 4587–4590, Apr. 2013, doi: 10.1002/ANIE.201300766.

[33] M. Tena *et al.*, "Techno-economic evaluation of bioenergy production from anaerobic digestion of by-products from ethanol flex plants," *Fuel*, vol. 309, p. 122171, Feb. 2022, doi: 10.1016/J.FUEL.2021.122171.

[34] Q. Zhang *et al.*, "Sequential dark and photo fermentation hydrogen production from hydrolyzed corn stover: A pilot test using 11 m3 reactor," *Bioresour Technol*, vol. 253, pp. 382–386, Apr. 2018, doi: 10.1016/j.biortech.2018.01.017.

[35] T. M. Vatsala, S. M. Raj, and A. Manimaran, "A pilot-scale study of biohydrogen production from distillery effluent using defined bacterial co-culture," *Int J Hydrogen Energy*, vol. 33, no. 20, pp. 5404–5415, Oct. 2008, doi: 10.1016/J.IJHYDENE.2008.07.015.

[36] N. Akhlaghi and G. Najafpour-Darzi, "A comprehensive review on biological hydrogen production," *International Journal of Hydrogen Energy*, vol. 45, no. 43. Elsevier Ltd, pp. 22492–22512, Sep. 03, 2020. doi: 10.1016/j.ijhydene.2020.06.182.

[37] H. Argun and F. Kargi, "Bio-hydrogen production by different operational modes of dark and photo-fermentation: An overview," *International Journal of Hydrogen Energy*, vol. 36, no. 13. Pergamon, pp. 7443–7459, Jul. 01, 2011. doi: 10.1016/j.ijhydene.2011.03.116.

[38] Y. Zhao and Y. Chen, "Nano-TiO 2 enhanced photofermentative hydrogen produced from the dark fermentation liquid of waste activated sludge," *Environ Sci Technol*, vol. 45, no. 19, pp. 8589–8595, Oct. 2011, doi: 10.1021/es2016186.

[39] D. H. Kim and M. S. Kim, "Hydrogenases for biological hydrogen production," *Bioresour Technol*, vol. 102, no. 18, pp. 8423–8431, Sep. 2011, doi: 10.1016/j.biortech.2011.02.113.

[40] M. Bao, H. Su, and T. Tan, "Biohydrogen production by dark fermentation of starch using mixed bacterial cultures of Bacillus sp and Brevumdimonas sp.," *Energy and Fuels*, vol. 26, no. 9, pp. 5872–5878, Sep. 2012, doi: 10.1021/ef300666m.

[41] N. Akhlaghi and G. Najafpour-Darzi, "A comprehensive review on biological hydrogen production," *International Journal of Hydrogen Energy*, vol. 45, no.

43. Elsevier Ltd, pp. 22492–22512, Sep. 03, 2020. doi: 10.1016/j.ijhydene.2020.06.182.

[42]   H. Argun, F. Kargi, and I. K. Kapdan, "Light fermentation of dark fermentation effluent for bio-hydrogen production by different Rhodobacter species at different initial volatile fatty acid (VFA) concentrations," *Int J Hydrogen Energy*, vol. 33, no. 24, pp. 7405–7412, Dec. 2008, doi: 10.1016/j.ijhydene.2008.09.059.

[43]   X. Li *et al.*, "Effect of salinity and pH on dark fermentation with thermophilic bacteria pretreated swine wastewater," *J Environ Manage*, vol. 271, p. 111023, Oct. 2020, doi: 10.1016/j.jenvman.2020.111023.

[44]   E. Sağır and P. C. Hallenbeck, "Photofermentative Hydrogen Production," in *Biohydrogen*, Elsevier, 2019, pp. 141–157. doi: 10.1016/b978-0-444-64203-5.00006-x.

[45]   H. Sakurai, H. Masukawa, M. Kitashima, and K. Inoue, "Photobiological hydrogen production: Bioenergetics and challenges for its practical application," *Journal of Photochemistry and Photobiology C: Photochemistry Reviews*, vol. 17. Elsevier, pp. 1–25, Dec. 01, 2013. doi: 10.1016/j.jphotochemrev.2013.05.001.

[46]   T. Y. Wu, J. X. W. Hay, L. B. Kong, J. C. Juan, and J. M. Jahim, "Recent advances in reuse of waste material as substrate to produce biohydrogen by purple non-sulfur (PNS) bacteria," *Renewable and Sustainable Energy Reviews*, vol. 16, no. 5. pp. 3117–3122, Jun. 2012. doi: 10.1016/j.rser.2012.02.002.

[47]   J. Y. Park, B. N. Kim, Y. H. Kim, and J. Min, "Whole-genome sequence of purple non-sulfur bacteria, Rhodobacter sphaeroides strain MBTLJ-8 with improved CO2 reduction capacity," *J Biotechnol*, vol. 288, pp. 9–14, Dec. 2018, doi: 10.1016/j.jbiotec.2018.10.007.

[48]   S. Ghosh, U. K. Dairkee, R. Chowdhury, and P. Bhattacharya, "Hydrogen from food processing wastes via photofermentation using Purple Non-sulfur Bacteria (PNSB) – A review," *Energy Conversion and Management*, vol. 141. Elsevier Ltd, pp. 299–314, Jun. 01, 2017. doi: 10.1016/j.enconman.2016.09.001.

[49]   Y. Li *et al.*, "Enhancement of bio-hydrogen yield and pH stability in photo fermentation process using dark fermentation effluent as succedaneum," *Bioresour Technol*, vol. 297, Feb. 2020, doi: 10.1016/j.biortech.2019.122504.

[50]   D. Jiang *et al.*, "Insights into correlation between hydrogen yield improvement and glycerol addition in photo-fermentation of Arundo donax L.," *Bioresour Technol*, vol. 321, p. 124467, Feb. 2021, doi: 10.1016/j.biortech.2020.124467.

[51]   T. Yue *et al.*, "Recycling of shrub landscaping waste: Exploration of bio-hydrogen production potential and optimization of photo-fermentation bio-hydrogen production process," *Bioresour Technol*, vol. 331, p. 125048, Jul. 2021, doi: 10.1016/j.biortech.2021.125048.

[52]   J. Cai *et al.*, "Photosynthetic bacteria improved hydrogen yield of combined dark- and photo-fermentation," *J Biotechnol*, vol. 302, pp. 18–25, Aug. 2019, doi: 10.1016/j.jbiotec.2019.06.298.

[53]   R. Zagrodnik and M. Laniecki, "The role of pH control on biohydrogen production by single stage hybrid dark- and photo-fermentation," *Bioresour Technol*, vol. 194, pp. 187–195, Oct. 2015, doi: 10.1016/j.biortech.2015.07.028.

[54]   S. Ozmihci and F. Kargi, "Effects of starch loading rate on performance of combined fed-batch fermentation of ground wheat for bio-hydrogen production," *Int J Hydrogen Energy*, vol. 35, no. 3, pp. 1106–1111, Feb. 2010, doi: 10.1016/j.ijhydene.2009.11.048.

[55] E. Sağır and P. C. Hallenbeck, "Photofermentative Hydrogen Production," *Biohydrogen*, pp. 141–157, Jan. 2019, doi: 10.1016/B978-0-444-64203-5.00006-X.

[56] R. Zagrodnik and M. Laniecki, "The role of pH control on biohydrogen production by single stage hybrid dark- and photo-fermentation," *Bioresour Technol*, vol. 194, pp. 187–195, Oct. 2015, doi: 10.1016/j.biortech.2015.07.028.

[57] R. K. Srivastava, N. P. Shetti, K. R. Reddy, E. E. Kwon, M. N. Nadagouda, and T. M. Aminabhavi, "Biomass utilization and production of biofuels from carbon neutral materials," *Environmental Pollution*, vol. 276, p. 116731, May 2021, doi: 10.1016/J.ENVPOL.2021.116731.

[58] A. Webster, S. Scherer, K. Fabri, H. Doudican, and M. Felder, "Saccharomyces cerevisiae ferments monosaccharides faster than disaccharides," *Journal of Undergraduate Biology Laboratory Investigations*, vol. 2, no. 1, p. 1, Apr. 2019.

[59] N. Ren, G. Cao, A. Wang, D. J. Lee, W. Guo, and Y. Zhu, "Dark fermentation of xylose and glucose mix using isolated Thermoanaerobacterium thermosaccharolyticum W16," *Int J Hydrogen Energy*, vol. 33, no. 21, pp. 6124–6132, Nov. 2008, doi: 10.1016/J.IJHYDENE.2008.07.107.

[60] Y. Pu *et al.*, "Hydrogen production from acidogenic food waste fermentation using untreated inoculum: Effect of substrate concentrations," *Int J Hydrogen Energy*, vol. 44, no. 50, pp. 27272–27284, Oct. 2019, doi: 10.1016/J.IJHYDENE.2019.08.230.

[61] C. Niño-Navarro, I. Chairez, P. Christen, M. Canul-Chan, and E. I. García-Peña, "Enhanced hydrogen production by a sequential dark and photo fermentation process: Effects of initial feedstock composition, dilution and microbial population," *Renew Energy*, vol. 147, pp. 924–936, Mar. 2020, doi: 10.1016/J.RENENE.2019.09.024.

[62] R. Zagrodnik, "Continuous H2 production during fermentation of the carbon components of lignocellulose hydrolysates: Insight into the influence of pH conditions on the conversion efficiency of individual sugars," *Int J Hydrogen Energy*, vol. 47, no. 84, pp. 35635–35640, Oct. 2022, doi: 10.1016/J.IJHYDENE.2022.08.165.

[63] A. F. Plante, J. M. Dick, R. M. Jones, J. P. Beam, Q. Jin, and M. F. Kirk, "pH as a Primary Control in Environmental Microbiology: 1. Thermodynamic Perspective," *Primary Control in Environmental Microbiology: 1. Thermodynamic Perspective. Front. Environ. Sci*, vol. 6, p. 21, 2018, doi: 10.3389/fenvs.2018.00021.

[64] S. Guo *et al.*, "Enhancement of pH values stability and photo-fermentation biohydrogen production by phosphate buffer," 2020, doi: 10.1080/21655979.2020.1736239.

[65] A. Gadhe, S. S. Sonawane, and M. N. Varma, "Enhancement effect of hematite and nickel nanoparticles on biohydrogen production from dairy wastewater," *Int J Hydrogen Energy*, vol. 40, no. 13, pp. 4502–4511, Apr. 2015, doi: 10.1016/J.IJHYDENE.2015.02.046.

[66] L. Hakobyan, L. Gabrielyan, and A. Trchounian, "Bio-hydrogen production and the F0F1-ATPase activity of Rhodobacter sphaeroides: Effects of various heavy metal ions," *Int J Hydrogen Energy*, vol. 37, no. 23, pp. 17794–17800, Dec. 2012, doi: 10.1016/J.IJHYDENE.2012.09.091.

[67] T. M. Vatsala, S. M. Raj, and A. Manimaran, "A pilot-scale study of biohydrogen production from distillery effluent using defined bacterial co-

culture," *Int J Hydrogen Energy*, vol. 33, no. 20, pp. 5404–5415, Oct. 2008, doi: 10.1016/J.IJHYDENE.2008.07.015.

[68] Y. Asada *et al.*, "Hydrogen production by co-cultures of Lactobacillus and a photosynthetic bacterium, Rhodobacter sphaeroides RV," *Int J Hydrogen Energy*, vol. 31, no. 11, pp. 1509–1513, Sep. 2006, doi: 10.1016/J.IJHYDENE.2006.06.017.

[69] N. Basak, A. K. Jana, D. Das, and D. Saikia, "Photofermentative molecular biohydrogen production by purple-non-sulfur (PNS) bacteria in various modes: The present progress and future perspective," *Int J Hydrogen Energy*, vol. 39, no. 13, pp. 6853–6871, Apr. 2014, doi: 10.1016/J.IJHYDENE.2014.02.093.

[70] E. Özgür and B. Peksel, "Biohydrogen production from barley straw hydrolysate through sequential dark and photofermentation," *J Clean Prod*, vol. 52, pp. 14–20, Aug. 2013, doi: 10.1016/J.JCLEPRO.2013.02.035.

[71] K. Trchounian, A. Poladyan, and A. Trchounian, "Optimizing strategy for Escherichia coli growth and hydrogen production during glycerol fermentation in batch culture: Effects of some heavy metal ions and their mixtures," *Appl Energy*, vol. 177, pp. 335–340, Sep. 2016, doi: 10.1016/J.APENERGY.2016.05.129.

[72] J. Zhang *et al.*, "Cobalt ferrate nanoparticles improved dark fermentation for hydrogen evolution," *J Clean Prod*, vol. 316, p. 128275, Sep. 2021, doi: 10.1016/J.JCLEPRO.2021.128275.

[73] H. Sun *et al.*, "Manganese ferrite nanoparticles enhanced biohydrogen production from mesophilic and thermophilic dark fermentation," *Energy Reports*, vol. 7, pp. 6234–6245, Nov. 2021, doi: 10.1016/J.EGYR.2021.09.070.

[74] A. Matsushika and S. Sawayama, "Effect of initial cell concentration on ethanol production by flocculent Saccharomyces cerevisiae with xylose-fermenting ability," *Appl Biochem Biotechnol*, vol. 162, no. 7, pp. 1952–1960, Nov. 2010, doi: 10.1007/S12010-010-8972-6.

[75] H. Argun, F. Kargi, and I. K. Kapdan, "Effects of the substrate and cell concentration on bio-hydrogen production from ground wheat by combined dark and photo-fermentation," *Int J Hydrogen Energy*, vol. 34, no. 15, pp. 6181–6188, Aug. 2009, doi: 10.1016/J.IJHYDENE.2009.05.130.

[76] S. Eker and M. Sarp, "Hydrogen gas production from waste paper by dark fermentation: Effects of initial substrate and biomass concentrations," *Int J Hydrogen Energy*, vol. 42, no. 4, pp. 2562–2568, Jan. 2017, doi: 10.1016/J.IJHYDENE.2016.04.020.

[77] T. T. Giang, S. Lunprom, Q. Liao, A. Reungsang, and A. Salakkam, "Enhancing hydrogen production from Chlorella sp. Biomass by pre-hydrolysis with simultaneous saccharification and fermentation (PSSF)," *Energies (Basel)*, vol. 12, no. 5, Mar. 2019, doi: 10.3390/EN12050908.

[78] D. Jiang and S. Zhu, "Advances in dark fermentation hydrogen production technologies," *Waste to Renewable Biohydrogen: Volume 1: Advances in Theory and Experiments*, pp. 123–137, Jan. 2021, doi: 10.1016/B978-0-12-821659-0.00007-1.

[79] D. Infantes, A. González Del Campo, J. Villaseñor, and F. J. Fernández, "Influence of pH, temperature and volatile fatty acids on hydrogen production by acidogenic fermentation," *Int J Hydrogen Energy*, vol. 36, no. 24, pp. 15595–15601, Dec. 2011, doi: 10.1016/J.IJHYDENE.2011.09.061.

[80] R. M. M. Ziara, D. N. Miller, J. Subbiah, and B. I. Dvorak, "Lactate wastewater dark fermentation: The effect of temperature and initial pH on biohydrogen

production and microbial community," *Int J Hydrogen Energy*, vol. 44, no. 2, pp. 661–673, Jan. 2019, doi: 10.1016/j.ijhydene.2018.11.045.

[81] R. C. da S. Mazareli *et al.*, "Enzymatic routes to hydrogen and organic acids production from banana waste fermentation by autochthonous bacteria: Optimization of pH and temperature," *Int J Hydrogen Energy*, vol. 46, no. 12, pp. 8454–8468, Feb. 2021, doi: 10.1016/J.IJHYDENE.2020.12.063.

[82] N. Basak, A. K. Jana, D. Das, and D. Saikia, "Photofermentative molecular biohydrogen production by purple-non-sulfur (PNS) bacteria in various modes: The present progress and future perspective," *Int J Hydrogen Energy*, vol. 39, no. 13, pp. 6853–6871, Apr. 2014, doi: 10.1016/J.IJHYDENE.2014.02.093.

[83] "Special Issue: Agricultural Water Management in Arid and Semi-arid Regions | Emirates Journal of Food and Agriculture." Accessed: Oct. 24, 2023. [Online]. Available: https://www.ejfa.me/index.php/journal/announcement/view/10

[84] P. Carlozzi, M. Seggiani, P. Cinelli, N. Mallegni, and A. Lazzeri, "Photofermentative Poly-3-Hydroxybutyrate Production by Rhodopseudomonas sp. S16-VOGS3 in a Novel Outdoor 70-L Photobioreactor," *Sustainability 2018, Vol. 10, Page 3133*, vol. 10, no. 9, p. 3133, Sep. 2018, doi: 10.3390/SU10093133.

[85] D. D. Androga *et al.*, "Photofermentative Hydrogen Production in Outdoor Conditions," *Hydrogen Energy - Challenges and Perspectives*, Oct. 2012, doi: 10.5772/50390.

[86] B. Wang, C. Q. Lan, and M. Horsman, "Closed photobioreactors for production of microalgal biomasses," *Biotechnol Adv*, vol. 30, no. 4, pp. 904–912, Jul. 2012, doi: 10.1016/J.BIOTECHADV.2012.01.019.

[87] I. Akkerman, M. Janssen, J. Rocha, and R. H. Wijffels, "Photobiological hydrogen production: photochemical efficiency and bioreactor design," *Int J Hydrogen Energy*, vol. 27, no. 11–12, pp. 1195–1208, Nov. 2002, doi: 10.1016/S0360-3199(02)00071-X.

[88] D. T. Kysela, A. M. Randich, P. D. Caccamo, and Y. V. Brun, "Diversity Takes Shape: Understanding the Mechanistic and Adaptive Basis of Bacterial Morphology," *PLoS Biol*, vol. 14, no. 10, p. e1002565, Oct. 2016, doi: 10.1371/JOURNAL.PBIO.1002565.

[89] R. Ruhal and R. Kataria, "Biofilm patterns in gram-positive and gram-negative bacteria," *Microbiol Res*, vol. 251, p. 126829, Oct. 2021, doi: 10.1016/J.MICRES.2021.126829.

[90] G. A. O'Toole, "Classic Spotlight: How the Gram Stain Works," *J Bacteriol*, vol. 198, no. 23, pp. 3128–3128, 2016, doi: 10.1128/JB.00726-16.

[91] O. Sizar and C. G. Unakal, "Gram Positive Bacteria," *Management of Antimicrobials in Infectious Diseases*, pp. 29–41, Feb. 2022, doi: 10.1385/1-59259-036-5:29.

[92] Y. S. Do, T. M. Schmidt, J. A. Zahn, E. S. Boyd, A. De la Mora, and A. A. DiSpirito, "Role of Rhodobacter sp. strain PS9, a purple non-sulfur photosynthetic bacterium isolated from an anaerobic swine waste lagoon, in odor remediation," *Appl Environ Microbiol*, vol. 69, no. 3, pp. 1710–1720, Mar. 2003, doi: 10.1128/AEM.69.3.1710-1720.2003.

[93] I. A. M. Swinnen, K. Bernaerts, E. J. J. Dens, A. H. Geeraerd, and J. F. Van Impe, "Predictive modelling of the microbial lag phase: a review," *Int J Food Microbiol*, vol. 94, no. 2, pp. 137–159, Jul. 2004, doi: 10.1016/J.IJFOODMICRO.2004.01.006.

[94] D. V. Raju, A. Nagarajan, S. Pandit, M. Nag, D. Lahiri, and V. Upadhye, "Effect of bacterial quorum sensing and mechanism of antimicrobial resistance," *Biocatal Agric Biotechnol*, vol. 43, p. 102409, Aug. 2022, doi: 10.1016/J.BCAB.2022.102409.

[95] M. Urvoy, R. Lami, C. Dreanno, D. Delmas, S. L'Helguen, and C. Labry, "Quorum Sensing Regulates the Hydrolytic Enzyme Production and Community Composition of Heterotrophic Bacteria in Coastal Waters," *Front Microbiol*, vol. 12, p. 3831, Dec. 2021, doi: 10.3389/FMICB.2021.780759/BIBTEX.

[96] M. R. Barer, "Bacterial growth, physiology and death," *Medical Microbiology: Eighteenth Edition*, pp. 39–53, Jan. 2012, doi: 10.1016/B978-0-7020-4089-4.00019-6.

[97] L. Preiss, D. B. Hicks, S. Suzuki, T. Meier, and T. A. Krulwich, "Alkaliphilic bacteria with impact on industrial applications, concepts of early life forms, and bioenergetics of ATP synthesis," *Front Bioeng Biotechnol*, vol. 3, no. JUN, 2015, doi: 10.3389/FBIOE.2015.00075/FULL.

[98] T. Venkova, G. Wegrzyn, S. Brom, J. Nesvera, P. Srivastava, and J. Jaishankar, "Molecular Basis of Stationary Phase Survival and Applications," *Front. Microbiol*, vol. 8, 2017, doi: 10.3389/fmicb.2017.02000.

[99] S. Sood, R. Singhal, S. Bhat, and A. Kumar, "Inoculum Preparation," *Comprehensive Biotechnology, Second Edition*, vol. 2, pp. 152–164, Sep. 2011, doi: 10.1016/B978-0-08-088504-9.00090-8.

[100] M. Kamran, "Bioenergy," *Renewable Energy Conversion Systems*, pp. 243–264, Jan. 2021, doi: 10.1016/B978-0-12-823538-6.00002-6.

[101] Y. Jiao, "Waste to biohydrogen: potential and feasibility," *Waste to Renewable Biohydrogen: Volume 1: Advances in Theory and Experiments*, pp. 33–53, Jan. 2021, doi: 10.1016/B978-0-12-821659-0.00006-X.

[102] A. K. Chandel, G. Chandrasekhar, K. Radhika, R. Ravinder, and P. Ravindra, "Bioconversion of pentose sugars into ethanol: A review and future directions," *Biotechnology and Molecular Biology Review*, vol. 6, no. 1, pp. 8–020, 2011.

[103] S. R. Kim, S. J. Ha, N. Wei, E. J. Oh, and Y. S. Jin, "Simultaneous co-fermentation of mixed sugars: a promising strategy for producing cellulosic ethanol," *Trends Biotechnol*, vol. 30, no. 5, pp. 274–282, May 2012, doi: 10.1016/J.TIBTECH.2012.01.005.

[104] G. Yang and J. Wang, "Biohydrogen production by co-fermentation of sewage sludge and grass residue: Effect of various substrate concentrations," *Fuel*, vol. 237, pp. 1203–1208, Feb. 2019, doi: 10.1016/J.FUEL.2018.10.026.

[105] G. Luo, L. Zhang, T. Chen, W. Yuan, and Y. Geng, "Butyric acid fermentation in xylose and glucose by Clostridium tyrobutyricum," *Bioresources*, vol. 12, no. 2, pp. 2930–2940, May 2017, doi: 10.15376/BIORES.12.2.2930-2940.

[106] T. Jarunglumlert, C. Prommuak, N. Putmai, and P. Pavasant, "Scaling-up bio-hydrogen production from food waste: Feasibilities and challenges," *Int J Hydrogen Energy*, vol. 43, no. 2, pp. 634–648, Jan. 2018, doi: 10.1016/J.IJHYDENE.2017.10.013.

[107] T. Yuan, S. Bian, J. H. Ko, H. Wu, and Q. Xu, "Enhancement of hydrogen production using untreated inoculum in two-stage food waste digestion," *Bioresour Technol*, vol. 282, pp. 189–196, Jun. 2019, doi: 10.1016/J.BIORTECH.2019.03.020.

[108] O. García-Depraect, E. R. Rene, J. Gómez-Romero, A. López-López, and E. León-Becerril, "Enhanced biohydrogen production from the dark co-

fermentation of tequila vinasse and nixtamalization wastewater: Novel insights into ecological regulation by pH," *Fuel*, vol. 253, pp. 159–166, Oct. 2019, doi: 10.1016/J.FUEL.2019.04.147.

[109] P. C. Hallenbeck, "Photofermentative Biohydrogen Production," *Biohydrogen*, pp. 145–159, 2013, doi: 10.1016/B978-0-444-59555-3.00007-6.

[110] P. C. Hallenbeck and D. Ghosh, "Advances in fermentative biohydrogen production: the way forward?," *Trends Biotechnol*, vol. 27, no. 5, pp. 287–297, May 2009, doi: 10.1016/J.TIBTECH.2009.02.004.

[111] Y. Liu and P. C. Hallenbeck, "A kinetic study of hydrogen production by a Calvin-Benson-Bassham cycle mutant, PRK (phosphoribulose kinase), of the photosynthetic bacterium Rhodobacter capsulatus," *Int J Hydrogen Energy*, vol. 41, no. 26, pp. 11081–11089, Jul. 2016, doi: 10.1016/J.IJHYDENE.2016.03.203.

[112] H. Zhang, J. Li, Q. Zhang, S. Zhu, S. Yang, and Z. Zhang, "Effect of substrate concentration on photo-fermentation bio-hydrogen production process from starch-rich agricultural leftovers under oscillation," *Sustainability (Switzerland)*, vol. 12, no. 7, Apr. 2020, doi: 10.3390/SU12072700.

[113] H. Yang, J. Zhang, X. Wang, F. Jiangtao, W. Yan, and G. Liejin, "A newly isolated Rhodobacter sphaeroides HY01 with high hydrogen production performance," *Int J Hydrogen Energy*, vol. 39, no. 19, pp. 10051–10060, Jun. 2014, doi: 10.1016/J.IJHYDENE.2014.04.171.

[114] A. Pandey, S. Dolly, D. Semwal, and A. Pandey, "Effect of pH on optimization of photofermentative hydrogen production by co-culture of Rhodobacter sphaeroides-NMBL-02 and Bacillus firmus-NMBL-03," *Cell Mol Biol*, vol. 63, no. 6, pp. 68–72, 2017, doi: 10.14715/CMB/2017.63.6.14.

[115] L. D. Palmer and E. P. Skaar, "Transition Metals and Virulence in Bacteria," *Annu Rev Genet*, vol. 50, p. 67, Nov. 2016, doi: 10.1146/ANNUREV-GENET-120215-035146.

[116] H. Sun *et al.*, "Manganese ferrite nanoparticles enhanced biohydrogen production from mesophilic and thermophilic dark fermentation," *Energy Reports*, vol. 7, pp. 6234–6245, Nov. 2021, doi: 10.1016/J.EGYR.2021.09.070.

[117] J. Zhang, W. Zhao, J. Yang, Z. Li, J. Zhang, and L. Zang, "Comparison of mesophilic and thermophilic dark fermentation with nickel ferrite nanoparticles supplementation for biohydrogen production," *Bioresour Technol*, vol. 329, p. 124853, Jun. 2021, doi: 10.1016/J.BIORTECH.2021.124853.

[118] P. T. Sekoai and M. O. Daramola, "Effect of metal ions on dark fermentative biohydrogen production using suspended and immobilized cells of mixed bacteria," *Chem Eng Commun*, vol. 205, no. 8, pp. 1011–1022, Aug. 2018, doi: 10.1080/00986445.2018.1428958.

[119] L. Xiao, Z. Deng, K. Y. Fung, and K. M. Ng, "Biohydrogen generation from anaerobic digestion of food waste," *Int J Hydrogen Energy*, vol. 38, no. 32, pp. 13907–13913, Oct. 2013, doi: 10.1016/J.IJHYDENE.2013.08.072.

[120] M. Taherdanak, H. Zilouei, and K. Karimi, "Investigating the effects of iron and nickel nanoparticles on dark hydrogen fermentation from starch using central composite design," *Int J Hydrogen Energy*, vol. 40, no. 38, pp. 12956–12963, Oct. 2015, doi: 10.1016/J.IJHYDENE.2015.08.004.

[121] H. Zhang, Y. Li, L. Chen, and Q. Zhang, "Effect of zinc ion on photo-fermentative hydrogen production performance, kinetics and electronic distribution in biohydrogen production by HAU-M1," *Bioresour Technol*, vol. 324, p. 124680, Mar. 2021, doi: 10.1016/J.BIORTECH.2021.124680.

[122] H. H. Al-Mohammedawi and H. Znad, "Impact of metal ions and EDTA on photofermentative hydrogen production by Rhodobacter sphaeroides using a mixture of pre-treated brewery and restaurant effluents," *Biomass Bioenergy*, vol. 134, p. 105482, Mar. 2020, doi: 10.1016/J.BIOMBIOE.2020.105482.

[123] A. Tangprasittipap, P. Prasertsan, W. Choorit, and K. Sasaki, "Biosynthesis of intracellular 5-aminolevulinic acid by a newly identified halotolerant Rhodobacter sphaeroides," *Biotechnol Lett*, vol. 29, no. 5, pp. 773–778, May 2007, doi: 10.1007/S10529-006-9303-4/METRICS.

[124] C. Lu *et al.*, "Enhancing photo-fermentation biohydrogen production by strengthening the beneficial metabolic products with catalysts," *J Clean Prod*, vol. 317, p. 128437, Oct. 2021, doi: 10.1016/J.JCLEPRO.2021.128437.

[125] S. Liu, G. Zhang, J. Li, X. Li, and J. Zhang, "Effects of metal ions on biomass and 5-aminolevulinic acid production in Rhodopseudomonas palustris wastewater treatment," 2016, doi: 10.2166/wst.2015.479.

[126] S. T. Jaronski and M. A. Jackson, "Mass production of entomopathogenic Hypocreales," *Manual of Techniques in Invertebrate Pathology*, pp. 255–284, Jan. 2012, doi: 10.1016/B978-0-12-386899-2.00008-7.

[127] T. A. Ulhiza, N. I. M. Puad, and A. S. Azmi, "Preliminary optimization of process conditions for biohydrogen production from sago wastewater," *2017 IEEE 3rd International Conference on Engineering Technologies and Social Sciences, ICETSS 2017*, vol. 2018-January, pp. 1–4, Mar. 2018, doi: 10.1109/ICETSS.2017.8324203.

[128] S. K. Wardani, M. N. Cahyanto, Rahayu, and T. Utami, "The effect of inoculum size and incubation temperature on cell growth, acid production and curd formation during milk fermentation by Lactobacillus plantarum Dad 13," *Int Food Res J*, vol. 24, no. 3, pp. 921–926, 2017.

[129] P. S. Panesar, J. F. Kennedy, C. J. Knill, and M. Kosseva, "Production of L(+) lactic acid using Lactobacillus casei from whey," *Brazilian Archives of Biology and Technology*, vol. 53, no. 1, pp. 219–226, Jan. 2010, doi: 10.1590/S1516-89132010000100027.

[130] M. D. Ooms, C. T. Dinh, E. H. Sargent, and D. Sinton, "Photon management for augmented photosynthesis," *Nature Communications 2016 7:1*, vol. 7, no. 1, pp. 1–13, Sep. 2016, doi: 10.1038/ncomms12699.

[131] X. Shui *et al.*, "Effect of light perturbation on the photo-fermentative hydrogen production of biomass from giant reed," *J Clean Prod*, vol. 351, p. 131481, Jun. 2022, doi: 10.1016/J.JCLEPRO.2022.131481.

[132] N. Basak and D. Das, "Photofermentative hydrogen production using purple non-sulfur bacteria Rhodobacter sphaeroides O.U.001 in an annular photobioreactor: A case study," *Biomass Bioenergy*, vol. 33, no. 6–7, pp. 911–919, Jun. 2009, doi: 10.1016/J.BIOMBIOE.2009.02.007.

[133] C. Z. Lazaro, M. B. A. Varesche, and E. L. Silva, "Effect of inoculum concentration, pH, light intensity and lighting regime on hydrogen production by phototrophic microbial consortium," *Renew Energy*, vol. 75, pp. 1–7, Mar. 2015, doi: 10.1016/J.RENENE.2014.09.034.

[134] X. Zhang *et al.*, "Enhancement of the biohydrogen production performance from mixed substrate by photo-fermentation: Effects of initial pH and inoculation volume ratio," *Bioresour Technol*, vol. 319, p. 124153, Jan. 2021, doi: 10.1016/J.BIORTECH.2020.124153.

[135] A. Ghimire *et al.*, "A review on dark fermentative biohydrogen production from organic biomass: Process parameters and use of by-products," *Appl Energy*, vol. 144, pp. 73–95, Apr. 2015, doi: 10.1016/J.APENERGY.2015.01.045.

[136] X. Gómez, C. Fernández, J. Fierro, M. E. Sánchez, A. Escapa, and A. Morán, "Hydrogen production: Two stage processes for waste degradation," *Bioresour Technol*, vol. 102, no. 18, pp. 8621–8627, Sep. 2011, doi: 10.1016/J.BIORTECH.2011.03.055.

[137] L. Luo, N. C. H. Ng, J. Zhao, D. Li, Z. Shi, and M. Zhou, "Conversion of food waste to bioenergy and biochemicals via anaerobic digestion," *Biomass, Biofuels, Biochemicals: Microbial Fermentation of Biowastes*, pp. 25–44, Jan. 2022, doi: 10.1016/B978-0-323-90633-3.00008-0.

[138] P. K. Rai and S. P. Singh, "Integrated dark- and photo-fermentation: Recent advances and provisions for improvement," *Int J Hydrogen Energy*, vol. 41, no. 44, pp. 19957–19971, Nov. 2016, doi: 10.1016/J.IJHYDENE.2016.08.084.

[139] W. Zong, R. Yu, P. Zhang, M. Fan, and Z. Zhou, "Efficient hydrogen gas production from cassava and food waste by a two-step process of dark fermentation and photo-fermentation," *Biomass Bioenergy*, vol. 33, no. 10, pp. 1458–1463, Oct. 2009, doi: 10.1016/J.BIOMBIOE.2009.06.008.

[140] A. Ghimire *et al.*, "A review on dark fermentative biohydrogen production from organic biomass: Process parameters and use of by-products," *Appl Energy*, vol. 144, pp. 73–95, Apr. 2015, doi: 10.1016/J.APENERGY.2015.01.045.

[141] S. Ozmihci and F. Kargi, "Effects of starch loading rate on performance of combined fed-batch fermentation of ground wheat for bio-hydrogen production," *Int J Hydrogen Energy*, vol. 35, no. 3, pp. 1106–1111, Feb. 2010, doi: 10.1016/J.IJHYDENE.2009.11.048.

[142] Z. Y. Hitit, C. Z. Lazaro, and P. C. Hallenbeck, "Hydrogen production by co-cultures of Clostridium butyricum and Rhodospeudomonas palustris: Optimization of yield using response surface methodology," *Int J Hydrogen Energy*, vol. 42, no. 10, pp. 6578–6589, Mar. 2017, doi: 10.1016/J.IJHYDENE.2016.12.122.

[143] J. Zhang and N. fa Gao, "Application of response surface methodology in medium optimization for pyruvic acid production of Torulopsis glabrata TP19 in batch fermentation," *J Zhejiang Univ Sci B*, vol. 8, no. 2, p. 98, 2007, doi: 10.1631/JZUS.2007.B0098.

[144] H. Vardhan, S. Sasamal, and K. Mohanty, "Fermentation process optimisation based on ANN and RSM for xylitol production from areca nut husk followed by xylitol crystal characterisation," *Process Biochemistry*, vol. 122, pp. 146–159, Nov. 2022, doi: 10.1016/J.PROCBIO.2022.10.005.

[145] L. M. S. Pereira, T. M. Milan, and D. R. Tapia-Blácido, "Using Response Surface Methodology (RSM) to optimize 2G bioethanol production: A review," *Biomass Bioenergy*, vol. 151, p. 106166, Aug. 2021, doi: 10.1016/J.BIOMBIOE.2021.106166.

[146] X. Wang, K. Xia, X. Yang, and C. Tang, "Growth strategy of microbes on mixed carbon sources," *Nature Communications 2019 10:1*, vol. 10, no. 1, pp. 1–7, Mar. 2019, doi: 10.1038/s41467-019-09261-3.

[147] F. Kargi and S. Ozmihci, "Effects of dark/light bacteria ratio on bio-hydrogen production by combined fed-batch fermentation of ground wheat starch," *Biomass Bioenergy*, vol. 34, no. 6, pp. 869–874, Jun. 2010, doi: 10.1016/J.BIOMBIOE.2010.01.031.

[148] F. S. Moreira, M. S. Rodrigues, L. M. Sousa, F. R. X. Batista, J. S. Ferreira, and V. L. Cardoso, "Single-stage repeated batch cycles using co-culture of Enterobacter cloacae and purple non-sulfur bacteria for hydrogen production," *Energy*, vol. 239, p. 122465, Jan. 2022, doi: 10.1016/J.ENERGY.2021.122465.

[149] S. Al Azad, F. S. Chin, M. T. B. M. Lal, S. Al Azad, F. S. Chin, and M. T. B. M. Lal, "Efficacy of Purple Non Sulphur Bacterium Rhodobacter sphaeroides Strain UMSFW1 in the Utilization of Palm Oil Mill Effluent," *Journal of Geoscience and Environment Protection*, vol. 7, no. 10, pp. 1–12, Oct. 2019, doi: 10.4236/GEP.2019.710001.

[150] Y. Combet-Blanc, K. K. Kalamba, and P. Y. Kergoat, "Effect of pH on Bacillus thermoamylovorans Growth and Glucose Fermentation," *Appl Environ Microbiol*, vol. 61, no. 2, p. 656, 1995, doi: 10.1128/AEM.61.2.656-659.1995.

[151] J. Espinoza-Vergara *et al.*, "Effect of pH on the Electrochemical Behavior of Hydrogen Peroxide in the Presence of Pseudomonas aeruginosa," *Front Bioeng Biotechnol*, vol. 9, p. 1201, Dec. 2021, doi: 10.3389/FBIOE.2021.749057/BIBTEX.

[152] Y. Zhang and J. Shen, "Effect of temperature and iron concentration on the growth and hydrogen production of mixed bacteria," *Int J Hydrogen Energy*, vol. 31, no. 4, pp. 441–446, Mar. 2006, doi: 10.1016/J.IJHYDENE.2005.05.006.

[153] Y. Mu, X. J. Zheng, H. Q. Yu, and R. F. Zhu, "Biological hydrogen production by anaerobic sludge at various temperatures," *Int J Hydrogen Energy*, vol. 31, no. 6, pp. 780–785, May 2006, doi: 10.1016/J.IJHYDENE.2005.06.016.

[154] K. S. Lee, P. J. Lin, and J. S. Chang, "Temperature effects on biohydrogen production in a granular sludge bed induced by activated carbon carriers," *Int J Hydrogen Energy*, vol. 31, no. 4, pp. 465–472, Mar. 2006, doi: 10.1016/J.IJHYDENE.2005.04.024.

[155] M. Sakil Munna, J. Tahera, M. Mohibul Hassan Afrad, I. T. Nur, and R. Noor, "Survival of Bacillus spp. SUBB01 at high temperatures and a preliminary assessment of its ability to protect heat-stressed Escherichia coli cells," *BMC Res Notes*, vol. 8, no. 1, p. 637, Nov. 2015, doi: 10.1186/S13104-015-1631-9.

[156] K. Zhao *et al.*, "[Degradation of dichlorvos by Rhodobacter sphaeroides].," *Huan Jing Ke Xue*, vol. 30, no. 4, pp. 1199–1204, Apr. 2009.

[157] Z. Youcai and W. Ran, "Anaerobic fermentation process for biomethane production from vegetable waste," *Biomethane Production from Vegetable and Water Hyacinth Waste*, pp. 1–62, Jan. 2021, doi: 10.1016/B978-0-12-821763-4.00001-6.

[158] J. Ren, J. P. Cao, X. Y. Zhao, F. L. Yang, and X. Y. Wei, "Recent advances in syngas production from biomass catalytic gasification: A critical review on reactors, catalysts, catalytic mechanisms and mathematical models," *Renewable and Sustainable Energy Reviews*, vol. 116. Elsevier Ltd, p. 109426, Dec. 01, 2019. doi: 10.1016/j.rser.2019.109426.

[159] P. Chandrangsu, C. Rensing, and J. D. Helmann, "Metal Homeostasis and Resistance in Bacteria," *Nat Rev Microbiol*, vol. 15, no. 6, p. 338, Jun. 2017, doi: 10.1038/NRMICRO.2017.15.

[160] H. Zhang and X. Wang, "Modular co-culture engineering, a new approach for metabolic engineering," *Metab Eng*, vol. 37, pp. 114–121, Sep. 2016, doi: 10.1016/J.YMBEN.2016.05.007.

[161] H. Song, M. Z. Ding, X. Q. Jia, Q. Ma, and Y. J. Yuan, "Synthetic microbial consortia: from systematic analysis to construction and applications," *Chem Soc Rev*, vol. 43, no. 20, pp. 6954–6981, Sep. 2014, doi: 10.1039/C4CS00114A.

[162] Y. Xiao, X. Zhang, M. Zhu, and W. Tan, "Effect of the culture media optimization, pH and temperature on the biohydrogen production and the hydrogenase activities by Klebsiella pneumoniae ECU-15," *Bioresour Technol*, vol. 137, pp. 9–17, Jun. 2013, doi: 10.1016/J.BIORTECH.2013.03.109.

[163] J. M. Woo, K. M. Yang, S. U. Kim, L. M. Blank, and J. B. Park, "High temperature stimulates acetic acid accumulation and enhances the growth inhibition and ethanol production by Saccharomyces cerevisiae under fermenting conditions," *Appl Microbiol Biotechnol*, vol. 98, no. 13, pp. 6085–6094, 2014, doi: 10.1007/S00253-014-5691-X.

[164] S. Ghosh, R. Chowdhury, and P. Bhattacharya, "A review on single stage integrated dark-photo fermentative biohydrogen production: Insight into salient strategies and scopes," *Int J Hydrogen Energy*, vol. 43, no. 4, pp. 2091–2107, Jan. 2018, doi: 10.1016/J.IJHYDENE.2017.12.018.

[165] M. M. Arimi, J. Knodel, A. Kiprop, S. S. Namango, Y. Zhang, and S. U. Geißen, "Strategies for improvement of biohydrogen production from organic-rich wastewater: A review," *Biomass Bioenergy*, vol. 75, pp. 101–118, Apr. 2015, doi: 10.1016/J.BIOMBIOE.2015.02.011.

[166] X. Li, Z. Z. Dai, Y. H. Wang, and S. L. Zhang, "Enhancement of phototrophic hydrogen production by Rhodobacter sphaeroides ZX-5 using fed-batch operation based on ORP level," *Int J Hydrogen Energy*, vol. 36, no. 20, pp. 12794–12802, Oct. 2011, doi: 10.1016/J.IJHYDENE.2011.07.070.

[167] H. Arai, H. R. Jung, and S. Kaplan, "Transcriptome dynamics during the transition from anaerobic photosynthesis to aerobic respiration in Rhodobacter sphaeroides 2.4.1," *J Bacteriol*, vol. 190, no. 1, pp. 286–299, Jan. 2008, doi: 10.1128/JB.01375-07.

[168] S. M. Kotay and D. Das, "Microbial hydrogen production with Bacillus coagulans IIT-BT S1 isolated from anaerobic sewage sludge," *Bioresour Technol*, vol. 98, no. 6, pp. 1183–1190, Apr. 2007, doi: 10.1016/J.BIORTECH.2006.05.009.

[169] Y. Nakashimada, M. A. Rachman, T. Kakizono, and N. Nishio, "Hydrogen production of Enterobacter aerogenes altered by extracellular and intracellular redox states," *Int J Hydrogen Energy*, vol. 27, no. 11–12, pp. 1399–1405, Nov. 2002, doi: 10.1016/S0360-3199(02)00128-3.

[170] U. Rasche, "Bioreactors and Fermentors - Powerful Tools for Resolving Cultivation Bottlenecks".

[171] H. Janssen, Y. Wang, and H. P. Blaschek, "CLOSTRIDIUM | Clostridium acetobutylicum," *Encyclopedia of Food Microbiology: Second Edition*, pp. 449–457, Jan. 2014, doi: 10.1016/B978-0-12-384730-0.00070-7.

[172] X. Chen, Y. Lv, Y. Liu, R. Ren, and J. Zhao, "The hydrogen production characteristics of mixed photoheterotrophic culture," *Int J Hydrogen Energy*, vol. 42, no. 8, pp. 4840–4847, Feb. 2017, doi: 10.1016/J.IJHYDENE.2016.11.155.

[173] S. Im, M.-K. Lee, A. Mostafa, O. Prakash, K.-H. Lim, and D.-H. Kim, "Effect of Localized Temperature Difference on Hydrogen Fermentation," *Energies 2021, Vol. 14, Page 6885*, vol. 14, no. 21, p. 6885, Oct. 2021, doi: 10.3390/EN14216885.

[174] M. Sun, Y. Lv, and Y. Liu, "A New Hydrogen-Producing Strain and Its Characterization of Hydrogen Production," *Appl Biochem Biotechnol*, vol. 177, no. 8, pp. 1676–1689, Dec. 2015, doi: 10.1007/S12010-015-1845-2/METRICS.

[175] I. C. Clark, R. H. Zhang, and S. K. Upadhyaya, "The effect of low pressure and mixing on biological hydrogen production via anaerobic fermentation," *Int J Hydrogen Energy*, vol. 37, no. 15, pp. 11504–11513, Aug. 2012, doi: 10.1016/J.IJHYDENE.2012.03.154.

[176] E. L. Folador *et al.*, "Protein-Protein Interactions: An Overview," *Encyclopedia of Bioinformatics and Computational Biology: ABC of Bioinformatics*, vol. 1–3, pp. 821–833, Jan. 2019, doi: 10.1016/B978-0-12-809633-8.20292-6.

[177] V. Hatzimanikatis, C. Li, J. A. Ionita, C. S. Henry, M. D. Jankowski, and L. J. Broadbelt, "Exploring the diversity of complex metabolic networks," *Bioinformatics*, vol. 21, no. 8, pp. 1603–1609, Apr. 2005, doi: 10.1093/BIOINFORMATICS/BTI213.

[178] H. A. Shah, J. Liu, Z. Yang, X. Zhang, and J. Feng, "DeepRF: A deep learning method for predicting metabolic pathways in organisms based on annotated genomes," *Comput Biol Med*, vol. 147, p. 105756, Aug. 2022, doi: 10.1016/J.COMPBIOMED.2022.105756.

[179] H. Ma and I. Goryanin, "Human metabolic network reconstruction and its impact on drug discovery and development," *Drug Discov Today*, vol. 13, no. 9–10, pp. 402–408, May 2008, doi: 10.1016/J.DRUDIS.2008.02.002.

[180] Y. Matsuoka and K. Shimizu, "Importance of understanding the main metabolic regulation in response to the specific pathway mutation for metabolic engineering of Escherichia coli," *Comput Struct Biotechnol J*, vol. 3, no. 4, p. e201210018, 2012, doi: 10.5936/CSBJ.201210018.

[181] D. H. Vu, S. Wainaina, M. J. Taherzadeh, D. Åkesson, and J. A. Ferreira, "Production of polyhydroxyalkanoates (PHAs) by Bacillus megaterium using food waste acidogenic fermentation-derived volatile fatty acids," *Bioengineered*, vol. 12, no. 1, pp. 2480–2498, 2021, doi: 10.1080/21655979.2021.1935524.

[182] H. S. Shin, J. H. Youn, and S. H. Kim, "Hydrogen production from food waste in anaerobic mesophilic and thermophilic acidogenesis," *Int J Hydrogen Energy*, vol. 29, no. 13, pp. 1355–1363, Oct. 2004, doi: 10.1016/J.IJHYDENE.2003.09.011.

[183] S. Sittijunda, S. Baka, R. Jariyaboon, A. Reungsang, T. Imai, and P. Kongjan, "Integration of Dark Fermentation with Microbial Electrolysis Cells for Biohydrogen and Methane Production from Distillery Wastewater and Glycerol Waste Co-Digestion," *Fermentation 2022, Vol. 8, Page 537*, vol. 8, no. 10, p. 537, Oct. 2022, doi: 10.3390/FERMENTATION8100537.

[184] K. Szacherska, P. Oleskowicz-Popiel, S. Ciesielski, and J. Mozejko-Ciesielska, "Volatile Fatty Acids as Carbon Sources for Polyhydroxyalkanoates Production," *Polymers (Basel)*, vol. 13, no. 3, pp. 1–21, Feb. 2021, doi: 10.3390/POLYM13030321.

[185] H. Argun and F. Kargi, "Photo-fermentative hydrogen gas production from dark fermentation effluent of ground wheat solution: Effects of light source and light intensity," *Int J Hydrogen Energy*, vol. 35, no. 4, pp. 1595–1603, Feb. 2010, doi: 10.1016/J.IJHYDENE.2009.12.040.

[186] T. Rygus, A. Scheler, R. Allmansberger, and W. Hillen, "Molecular cloning, structure, promoters and regulatory elements for transcription of the Bacillus megaterium encoded regulon for xylose utilization," *Arch Microbiol*, vol. 155, no. 6, pp. 535–542, Jun. 1991, doi: 10.1007/BF00245346/METRICS.

[187] C. Li and H. H. P. Fang, "Fermentative hydrogen production from wastewater and solid wastes by mixed cultures," *Crit Rev Environ Sci Technol*, vol. 37, no. 1, pp. 1–39, Jan. 2007, doi: 10.1080/10643380600729071.

[188] E. Sagir and S. Alipour, "Photofermentative hydrogen production by immobilized photosynthetic bacteria: Current perspectives and challenges," *Renewable and Sustainable Energy Reviews*, vol. 141, p. 110796, May 2021, doi: 10.1016/J.RSER.2021.110796.

[189] J. M. van Dijl and M. Hecker, "Bacillus subtilis: from soil bacterium to super-secreting cell factory," *Microb Cell Fact*, vol. 12, no. 1, Jan. 2013, doi: 10.1186/1475-2859-12-3.

[190] C. Z. Lazaro and P. C. Hallenbeck, "Fundamentals of Biohydrogen Production," *Biohydrogen*, pp. 25–48, Jan. 2019, doi: 10.1016/B978-0-444-64203-5.00002-2.

[191] J. Lin *et al.*, "Computer Simulation of Bioprocess," *Computer Simulation*, Jun. 2017, doi: 10.5772/67732.

[192] K. Postawa, J. Szczygieł, and M. Kułażyński, "A comprehensive comparison of ODE solvers for biochemical problems," *Renew Energy*, vol. 156, pp. 624–633, Aug. 2020, doi: 10.1016/J.RENENE.2020.04.089.

[193] L. Fagbemi, D. Adamon, and E. K. Ekouedjen, "Modeling Carbon-to-Nitrogen Ratio Influence on Biogas Production by the 4th-order Runge–Kutta Method," *Energy & Fuels*, vol. 33, no. 9, pp. 8721–8726, Sep. 2019, doi: 10.1021/ACS.ENERGYFUELS.9B01721.

[194] D. Liu *et al.*, "Fermentation process modeling with Levenberg-Marquardt algorithm and Runge-Kutta method on ethanol production by saccharomyces cerevisiae," *Math Probl Eng*, vol. 2014, Apr. 2014, doi: 10.1155/2014/289492.

[195] G. Romeo, "Mathematics for dynamic economic models," *Elements of Numerical Mathematical Economics with Excel*, pp. 139–215, Jan. 2020, doi: 10.1016/B978-0-12-817648-1.00004-9.

[196] Y. K. Oh, S. H. Kim, M. S. Kim, and S. Park, "Thermophilic biohydrogen production from glucose with trickling biofilter," *Biotechnol Bioeng*, vol. 88, no. 6, pp. 690–698, Dec. 2004, doi: 10.1002/BIT.20269.

[197] F. Y. Chang and C. Y. Lin, "Biohydrogen production using an up-flow anaerobic sludge blanket reactor," *Int J Hydrogen Energy*, vol. 29, no. 1, pp. 33–39, Jan. 2004, doi: 10.1016/S0360-3199(03)00082-X.

[198] N. Azbar *et al.*, "Comparative Evaluation of Bio-Hydrogen Production From Cheese Whey Wastewater Under Thermophilic and Mesophilic Anaerobic Conditions," *http://dx.doi.org/10.1080/15435070902785027*, vol. 6, no. 2, pp. 192–200, 2009, doi: 10.1080/15435070902785027.

[199] G. L. Cao, L. Zhao, A. J. Wang, Z. Y. Wang, and N. Q. Ren, "Single-step bioconversion of lignocellulose to hydrogen using novel moderately thermophilic bacteria," *Biotechnol Biofuels*, vol. 7, no. 1, pp. 1–13, Jun. 2014, doi: 10.1186/1754-6834-7-82/TABLES/5.

[200] G. Ivanova, G. Rákhely, and K. L. Kovács, "Thermophilic biohydrogen production from energy plants by Caldicellulosiruptor saccharolyticus and comparison with related studies," *Int J Hydrogen Energy*, vol. 34, no. 9, pp. 3659–3670, May 2009, doi: 10.1016/J.IJHYDENE.2009.02.082.

[201] R. Zagrodnik and M. Łaniecki, "Hydrogen production from starch by co-culture of Clostridium acetobutylicum and Rhodobacter sphaeroides in one step hybrid dark- and photofermentation in repeated fed-batch reactor," *Bioresour Technol*, vol. 224, pp. 298–306, Jan. 2017, doi: 10.1016/j.biortech.2016.10.060.

[202] S. Z. Zhiznin, N. N. Shvets, V. M. Timokhov, and A. L. Gusev, "Economics of hydrogen energy of green transition in the world and Russia.Part I," *Int J Hydrogen Energy*, Mar. 2023, doi: 10.1016/J.IJHYDENE.2023.03.069.

[203] Y. Cao, H. Liu, W. Liu, J. Guo, and M. Xian, "Debottlenecking the biological hydrogen production pathway of dark fermentation: insight into the impact of strain improvement," *Microb Cell Fact*, vol. 21, no. 1, Dec. 2022, doi: 10.1186/S12934-022-01893-3.

Appendix 1: Growth curve study and simultaneous hydrogen production based on 1g/L inoculum concentration.

Time (hours)	Cereibacter sp.		Bacillus sp.	
	H₂ (PPM)	Cell No.	H₂ (PPM)	Cell No.
0	0	1.760×10^8	0	3.040×10^8
4	82	4.000×10^8	243	7.120×10^8
8	254	3.760×10^8	478	7.440×10^8
12	304	3.760×10^8	447	7.680×10^8
16	321	4.240×10^8	473	7.440×10^8
20	262	3.840×10^8	453	7.680×10^8
24	238	3.760×10^8	395	7.840×10^8
28	152	3.600×10^8	249	7.920×10^8
32	193	4.240×10^8	201	8.000×10^8
36	208	3.600×10^8	295	8.640×10^8
40	182	3.920×10^8	276	1.160×10^9
44	169	3.840×10^8	329	3.728×10^9
48	167	4.400×10^8	265	5.176×10^9
52	167	5.520×10^8	246	6.280×10^9
56	156	6.080×10^8	156	7.080×10^9
60	120	6.960×10^8	216	7.592×10^9
64	117	8.720×10^8	197	8.080×10^9
68	129	1.104×10^9	231	8.040×10^9
72	138	1.200×10^9	209	8.808×10^9
76	100	1.323×10^9	149	8.696×10^9
80	86	1.404×10^9	130	8.896×10^9
84	66	1.632×10^9	86	8.608×10^9
88	62	1.804×10^9	66	8.624×10^9
92	42	2.004×10^9	41	8.624×10^9
96	36	2.184×10^9	36	8.464×10^9

Appendix 2: Growth curve study and simultaneous hydrogen production based on 10g/L inoculum concentration.

Time (hours)	Cereibacter sp.		Bacillus sp.	
	H₂ (PPM)	Cell No.	H₂ (PPM)	Cell No.
0	0	1.376×10^9	0	1.304×10^9
4	21	1.368×10^9	56	1.320×10^9
8	39	1.368×10^9	85	1.408×10^9
12	42	1.512×10^9	134	1.496×10^9
16	100	2.216×10^9	261	1.376×10^9
20	137	2.520×10^9	360	1.304×10^9
24	216	2.912×10^9	340	1.816×10^9
28	180	3.272×10^9	294	2.544×10^9
32	153	3.296×10^9	262	3.016×10^9
36	148	3.472×10^9	244	3.072×10^9
40	138	3.648×10^9	226	3.280×10^9
44	130	3.856×10^9	202	3.360×10^9
48	125	4.208×10^9	140	3.440×10^9
52	128	4.520×10^9	154	3.576×10^9
56	99	4.536×10^9	141	3.400×10^9
60	95	4.768×10^9	151	3.416×10^9
64	80	5.120×10^9	144	3.432×10^9
68	96	5.200×10^9	170	3.496×10^9
72	98	5.272×10^9	173	3.408×10^9
76	107	5.536×10^9	170	3.608×10^9
80	94	5.584×10^9	174	3.648×10^9
84	75	5.640×10^9	180	3.664×10^9
88	80	5.600×10^9	184	3.672×10^9
92	83	5.616×10^9	175	3.616×10^9
96	100	5.584×10^9	165	3.728×10^9

Preliminary single strain dark or light fermentation

Parametric study of biological hydrogen production based on different xylose concentration

Appendix 3: Biological hydrogen production and pH changes after 24 hours (xylose)

Xylose Concentration	*Cereibacter sp.*		*Bacillus sp.*	
	H$_2$ (PPM)	pH	H$_2$ (PPM)	pH
0g/L	49	6.85	36	6.28
2.5g/L	70	6.81	72	5.99
5g/L	71	6.70	61	5.97
7.5g/L	61	6.81	157	5.96
10g/L	82	6.79	178	5.95
12.5g/L	83	6.78	180	5.88
15g/L	60	6.77	197	5.89
17.5g/L	76	6.77	233	5.87
20g/L	54	6.75	185	5.87

Appendix 4: Biological hydrogen production and pH changes after 48 hours (xylose)

Xylose Concentration	*Cereibacter sp.*		*Bacillus sp.*	
	H$_2$ (PPM)	pH	H$_2$ (PPM)	pH
0g/L	29	7.02	27	6.23
2.5g/L	26	6.90	44	5.97
5g/L	24	6.88	56	5.97
7.5g/L	37	6.88	78	5.97
10g/L	28	6.89	72	5.96
12.5g/L	31	6.85	82	5.86
15g/L	28	6.84	117	5.86
17.5g/L	34	6.83	134	5.85

20g/L	28	6.82	49	5.84

Appendix 5: Biological hydrogen production and pH changes after 72 hours (xylose)

Xylose Concentration	Cereibacter sp.		Bacillus sp.	
	H₂ (PPM)	pH	H₂ (PPM)	pH
0g/L	25	7.02	26	6.23
2.5g/L	24	6.88	45	5.98
5g/L	27	6.81	33	5.95
7.5g/L	28	6.82	44	5.93
10g/L	58	6.82	36	5.88
12.5g/L	30	6.81	40	5.85
15g/L	20	6.77	41	5.84
17.5g/L	30	6.75	48	5.83
20g/L	26	6.73	60	5.81

Parametric study of biological hydrogen production based on different glucose concentration

Appendix 6: Biological hydrogen production and pH changes after 24 hours (glucose)

Glucose Concentration	Cereibacter sp.		Bacillus sp.	
	H₂ (PPM)	pH	H₂ (PPM)	pH
0g/L	49	6.85	40	6.04
2.5g/L	71	6.81	135	4.76
5g/L	78	6.70	143	4.71
7.5g/L	64	6.81	193	4.69
10g/L	88	6.79	198	4.68
12.5g/L	67	6.78	173	4.68

	71	6.77	168	4.67
15g/L	71	6.77	168	4.67
17.5g/L	77	6.77	271	4.67
20g/L	63	6.75	191	4.67

Appendix 7: Biological hydrogen production and pH changes after 48 hours (glucose)

	Cereibacter sp.		Bacillus sp.	
Glucose Concentration	H$_2$ (PPM)	pH	H$_2$ (PPM)	pH
0g/L	43	7.02	27	6.06
2.5g/L	26	6.90	41	4.72
5g/L	25	6.88	57	4.69
7.5g/L	27	6.88	43	4.68
10g/L	24	6.89	41	4.66
12.5g/L	23	6.85	59	4.68
15g/L	24	6.84	57	4.66
17.5g/L	32	6.83	53	4.65
20g/L	34	6.82	58	4.65

Appendix 8: Biological hydrogen production and pH changes after 72 hours (glucose)

	Cereibacter sp.		Bacillus sp.	
Glucose Concentration	H$_2$ (PPM)	pH	H$_2$ (PPM)	pH
0g/L	33	7.05	22	6.01
2.5g/L	24	6.95	35	4.68
5g/L	27	6.89	45	4.69
7.5g/L	24	6.87	26	4.64

10g/L	27	6.87	31	4.69
12.5g/L	32	6.81	63	4.66
15g/L	28	6.79	51	4.68
17.5g/L	32	6.77	37	4.63
20g/L	26	6.77	56	4.62

Parametric study of biological hydrogen production based on different metal ions

Appendix 9: Biological hydrogen production and pH changes before fermentation (metal ions)

Metal Ions	*Cereibacter sp.*		*Bacillus sp.*	
	H$_2$ (PPM)	pH	H$_2$ (PPM)	pH
Fe	0	6.71	0	6.43
Cu	0	6.73	0	6.43
Mn	0	6.73	0	6.42
Zn	0	6.71	0	6.39
Co	0	6.75	0	6.42
Ni	0	6.75	0	6.43
Ca	0	6.77	0	6.44
Without ions	0	6.81	0	6.46

Appendix 10: Biological hydrogen production and pH changes after 24 hours (metal ions)

Metal Ions	*Cereibacter sp.*		*Bacillus sp.*	
	H$_2$ (PPM)	pH	H$_2$ (PPM)	pH
Fe	73	6.69	92	5.69
Cu	69	6.73	69	5.74

	112	6.74	71	5.68
Mn	112	6.74	71	5.68
Zn	74	6.73	98	5.46
Co	80	6.73	110	5.70
Ni	85	6.73	74	5.72
Ca	72	6.78	73	5.74
Without ions	54	6.78	68	5.87

Appendix 11: Biological hydrogen production and pH changes after 48 hours (metal ions)

Metal Ions	*Cereibacter sp.*		*Bacillus sp.*	
	H$_2$ (PPM)	pH	H$_2$ (PPM)	pH
Fe	48	6.69	44	5.68
Cu	44	6.70	41	5.70
Mn	22	6.72	39	5.68
Zn	27	6.73	44	5.53
Co	32	6.71	39	5.68
Ni	42	6.71	27	5.70
Ca	35	6.74	34	5.71
Without ions	24	6.74	23	5.85

Appendix 12: Biological hydrogen production and pH changes after 72 hours (metal ions)

Metal Ions	*Cereibacter sp.*		*Bacillus sp.*	
	H$_2$ (PPM)	pH	H$_2$ (PPM)	pH
Fe	20	6.67	40	5.68
Cu	31	6.65	41	5.70
Mn	25	6.68	36	5.72
Zn	24	6.70	32	5.54

Co	25	6.71	51	5.69
Ni	22	6.63	22	5.70
Ca	24	6.67	33	5.70
Without ions	10	6.72	20	5.83

Parametric study of biological hydrogen production based on different inoculum concentration

Appendix 13: Biological hydrogen production and pH changes before fermentation (inoculum concentration)

	Cereibacter sp.		*Bacillus sp.*	
g/L	H$_2$ (PPM)	pH	H$_2$ (PPM)	pH
2	0	6.59	0	6.57
4	0	6.67	0	6.55
6	0	6.71	0	6.53
8	0	6.77	0	6.51
10	0	6.81	0	6.46

Appendix 14: Biological hydrogen production and pH changes after 24 hours (inoculum concentration)

	Cereibacter sp.		*Bacillus sp.*	
g/L	H$_2$ (PPM)	pH	H$_2$ (PPM)	pH
2	60	6.58	95	6.38
4	92	6.65	89	6.23
6	91	6.70	84	6.03
8	70	6.74	89	5.85
10	54	6.78	68	5.58

Appendix 15: Biological hydrogen production and pH changes after 48 hours (inoculum concentration)

g/L	Cereibacter sp.		Bacillus sp.	
	H₂ (PPM)	pH	H₂ (PPM)	pH
2	21	6.55	33	6.32
4	30	6.60	25	6.13
6	25	6.63	21	5.98
8	26	6.69	22	5.78
10	24	6.74	23	5.55

Appendix 16: Biological hydrogen production and pH changes after 72 hours (inoculum concentration)

g/L	Cereibacter sp.		Bacillus sp.	
	H₂ (PPM)	pH	H₂ (PPM)	pH
2	17	6.50	30	6.29
4	25	6.57	27	6.14
6	16	6.58	23	5.98
8	14	6.64	17	5.79
10	10	6.66	20	5.56

Co-culture hybrid fermentation

Appendix 17: Biological hydrogen production and pH changes in various set of experimental runs (investigation of D/L ratio and substrate concentration)

Experiment Run	H₂ (24 hours)	H₂ (48 hours)	H₂ (72 hours)	pH (initial)	pH (24 hours)	pH (48 hours)	pH (72 hours)
1	196	49	55	6.43	6.48	6.53	6.55
2	152	105	99	6.42	6.42	6.46	6.42
3	194	155	132	6.46	6.53	6.50	6.54
4	135	106	81	6.47	6.45	6.46	6.44

5	158	128	77	6.46	6.47	6.54	6.54
6	134	108	78	6.43	6.44	6.46	6.41
7	222	173	124	6.48	6.57	6.52	6.49
8	222	173	124	6.49	6.46	6.47	6.44
9	135	96	62	6.47	6.50	6.54	6.51
10	282	211	200	6.48	6.44	6.47	6.43
11	135	96	62	6.46	6.43	6.41	6.40
12	174	135	125	6.50	6.47	6.47	6.49
13	95	75	51	6.49	6.49	6.48	6.50
14	121	67	121	6.47	6.45	6.44	6.43
15	196	147	143	6.48	6.46	6.47	6.46
16	188	145	136	6.49	6.50	6.47	6.48
17	199	144	145	6.49	6.52	6.48	6.48
18	190	147	138	6.50	6.52	6.47	6.48
19	189	145	138	6.49	6.50	6.46	6.48
20	195	146	142	6.50	6.51	6.48	6.48

Appendix 18: Biological hydrogen production and pH changes based on various initial pH

Initial pH with various substrate concentration	H_2 (24 hours)	H_2 (48 hours)	H_2 (72 hours)	pH (24 hours)	pH (48 hours)	pH (72 hours)
5 (15g/L xylose)	121	83	66	5.09	5.08	5.07
6 (15g/L xylose)	165	101	133	6.01	5.99	5.96
7 (15g/L xylose)	251	146	151	6.87	6.70	6.62
8 (15g/L xylose)	193	155	291	7.78	7.70	7.65
9 (15g/L xylose)	500	456	650	8.81	8.74	8.64
5 (17.5g/L xylose)	135	127	84	5.09	5.07	5.07
6 (17.5g/L xylose)	282	160	124	6.01	5.98	5.90
7 (17.5g/L xylose)	354	332	86	6.86	6.60	6.40
8 (17.5g/L xylose)	156	720	224	7.60	7.40	7.23
9 (17.5g/L xylose)	408	389	166	8.47	8.30	8.15
5 (20g/L xylose)	143	94	78	5.09	5.06	5.04
6 (20g/L xylose)	120	55	66	5.94	5.87	5.84

7 (20g/L xylose)	216	190	231	6.84	6.59	6.38
8 (20g/L xylose)	532	437	146	7.57	7.36	7.20
9 (20g/L xylose)	480	240	239	8.45	8.32	8.12

Appendix 19: Biological hydrogen production based on various temperature

Temperature	H_2 (24 hours)	H_2 (48 hours)	H_2 (72 hours)
30°C	267	205	134
35°C	183	118	321
40°C	428	281	187
45°C	560	413	241
50°C	469	622	239
55°C	538	406	220

Appendix 20: Biological hydrogen production and pH changes based on various metal ions

Metal Ions	H_2 (24 hours)	H_2 (48 hours)	H_2 (72 hours)
Co 0μM	355	115	139
Co 20μM	441	128	278
Co 40μM	346	218	172
Co 60μM	419	138	150
Co 80μM	312	175	151
Co 100μM	477	107	100
Mn 0μM	230	109	100
Mn 20μM	312	86	190
Mn 40μM	200	192	170
Mn 60μM	295	81	182
Mn 80μM	232	122	127
Mn 100μM	166	63	95

Appendix 21: Biological hydrogen production and pH changes in various set of experimental runs (investigation of D/L ratio and substrate concentration)

Experiment Run	H₂ (24 hours)	H₂ (48 hours)	H₂ (72 hours)	pH (initial)	pH (24 hours)	pH (48 hours)	pH (72 hours)
1	198	150	13	7	6.7	6.61	6.58
2	104	70	54	7	6.74	6.61	6.6
3	153	81	54	7	6.78	6.62	6.62
4	173	81	58	7	6.7	6.64	6.63
5	240	171	101	7	6.8	6.75	6.71
6	270	184	120	7	6.8	6.74	6.7
7	254	189	128	7	6.81	6.75	6.71
8	224	178	123	7	6.8	6.75	6.71
9	340	198	1152	9	7.97	7.64	7.55
10	840	223	610	9	7.92	7.84	7.77
11	250	120	197	9	7.91	7.62	7.56
12	270	368	173	9	7.87	7.71	7.64
13	384	335	242	9	8.05	7.81	7.67
14	1261	1425	1441	9	8.12	7.89	7.76
15	798	224	249	9	8.11	7.87	7.76
16	758	254	225	9	8.08	7.88	7.75
17	231	149	139	8	7.59	7.5	7.46
18	250	301	190	8	7.6	7.52	7.46
19	291	301	190	8	7.59	7.5	7.45
20	190	242	180	8	7.6	7.51	7.45
21	193	211	227	8	7.29	7.2	7.18
22	243	250	320	8	7.57	7.45	7.38
23	313	186	207	7	6.65	6.4	6.3
24	610	324	249	9	8.05	7.47	7.27
25	409	286	266	8	7.11	6.73	6.62
26	384	241	233	8	7.62	7.51	7.46
27	266	244	364	8	7.6	7.5	7.47
28	284	244	284	8	7.61	7.5	7.46
29	280	238	274	8	7.6	7.51	7.46
30	282	240	270	8	7.61	7.5	7.46

Appendix 22: Biological hydrogen production, pH changes, dissolved hydrogen, and redox potential in 200mL co-culture fermentation.

Time (hours)	H_2 (PPM)	pH	Dissolved H_2	Redox potential (mV)
0	0	9	0	0
4	187	8.09	80	-39
8	384	7.99	120	-61
12	648	7.95	122	-61
16	1129	7.91	78	-38
20	1635	7.95	96	-48
24	1632	7.87	74	-36
28	2091	7.85	90	-45
32	2662	7.82	84	-42
36	2631	7.73	70	-35
40	2160	7.65	84	-42
44	1635	7.73	102	-50
48	1575	7.78	40	-20
52	920	7.7	104	-52
56	1068	7.68	64	-32
60	1050	7.66	80	-40
64	887	7.68	56	-28
68	863	7.64	78	-39
72	1237	7.6	80	-40
76	1283	7.56	42	-21
80	1164	7.59	64	-32
84	1160	7.43	58	-27
88	1001	7.34	90	-45
92	970	7.36	130	-62
96	777	7.37	112	-57

Appendix 23: Biological hydrogen production and pH changes in 2L CSTR.

Time (hours)	H_2 (PPM)	pH	Time (hours)	H_2 (PPM)	pH
0	0	9	49th	18000	7.78
1st	21600	8.7	50th	21600	7.78
2nd	25200	8.68	51st	23400	7.78
3rd	39600	8.67	52nd	25200	7.78
4th	43200	8.65	53rd	27000	7.78
5th	46800	8.64	54th	28800	7.79
6th	48600	8.63	55th	30600	7.79
7th	50400	8.62	56th	32400	7.79
8th	57600	8.56	57th	34200	7.79
9th	57600	8.52	58th	36000	7.79
10th	54000	8.46	59th	37800	7.8
11th	57600	8.4	60th	38520	7.8
12th	61200	8.36	61st	39600	7.8
13th	64800	8.33	62nd	40680	7.8
14th	64800	8.29	63rd	42120	7.8
15th	57600	8.24	64th	43200	7.81
16th	54000	8.18	65th	45000	7.81
17th	54000	8.13	66th	46800	7.81

18th	50400	8.08	67th	50400	7.81
19th	50400	8.05	68th	54000	7.82
20th	50400	8.04	69th	57600	7.82
21st	50400	8.03	70th	61200	7.82
22nd	46800	8.01	71st	64800	7.82
23rd	43200	7.99	72nd	72000	7.82
24th	36000	7.99	73rd	79200	7.82
25th	25200	7.98	74th	90000	7.82
26th	25200	7.97	75th	93600	7.82
27th	21600	7.96	76th	95400	7.82
28th	21600	7.95	77th	97200	7.82
29th	18000	7.94	78th	93600	7.82
30th	14400	7.93	79th	91800	7.82
31st	14400	7.92	80th	90000	7.82
32nd	12600	7.91	81st	90000	7.82
33rd	12600	7.9	82nd	88200	7.82
34th	12600	7.89	83rd	86400	7.82
35th	12600	7.89	84th	84600	7.82
36th	10800	7.88	85th	82800	7.82
37th	10800	7.88	86th	81000	7.82
38th	10800	7.87	87th	79200	7.82
39th	7200	7.86	88th	77400	7.82
40th	7200	7.85	89th	75600	7.82
41st	7200	7.84	90th	73800	7.82
42nd	3600	7.83	91st	72000	7.82
43rd	3600	7.82	92nd	61200	7.82
44th	3600	7.82	93rd	50400	7.83
45th	1800	7.8	94th	43200	7.83
46th	1800	7.79	95th	39600	7.84
47th	3600	7.78	96th	36000	7.84
48th	7200	7.78			